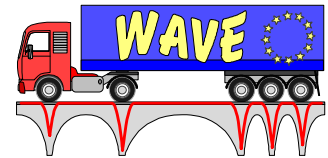




European Commission
DG VII - Transport
**4th Framework Programme
Transport**



Weighing-in-motion of
Axles and
Vehicles for
Europe

RTD project, RO-96-SC, 403

WEIGHING-IN-MOTION OF AXLES AND VEHICLES FOR EUROPE (WAVE)

Report of Work Package 1.2

Bridge WIM systems (B-WIM)



University College Dublin

June 2001

CIP – Kataložni zapis o publikaciji
Narodna in univerzitetna knjižnica, Ljubljana, Slovenia

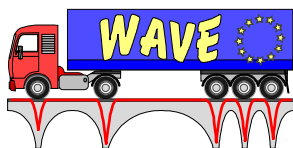
624.04
624.2/.8(4)

WEIGHING-in-motion of Axles and Vehicles for Europe (WAVE).
Report of work package 1.2. Bridge WIM Systems (B-WIM) / editors
Eugene O'Brien, Aleš Žnidarič. – Ljubljana : Zavod za gradbeništvo
Slovenije, 2001

ISBN 961-90366-1-1
1. O'Brien, Eugene
114000640

A great deal of additional information about the WAVE project is available on <http://wim.zag.si/>.

Printed in Slovenia



THE PROJECT

'WAVE' (Weighing-in-motion of Axles and Vehicles for Europe) is a research and development project of the fourth Framework Programme (Transport). Concerned with the weighing in motion of road vehicles, the project ended in June 1999 after two and a half years of steady work. Thanks to an integrated programme with a fruitful collaboration between the partners, and complementary contributions from the participating organisations, significant scientific and technical progress was made and very many results were achieved.

1. Origin of the project

During the COST 323 action (WIM-LOAD, 1993-98), part of the activities of COST Transport, it emerged that further research on WIM was necessary to address the latest requirements of road managers and decision makers. In 1994, the 4th Framework Programme of the European Commission was presented, with a specific "Road Transport" programme. Part of the latter was entitled "Road infrastructure" and a task of this was "Monitoring of factors affecting pavements and structures to support existing and future harmonisation legislation in respect of axle and vehicle weights" (task 7-4/27).

To address this task, a proposal for a large research project, 'WAVE' (Weighing-in-motion of Axles and Vehicles for Europe) was submitted to the Commission by a consortium of 11 partners from 10 countries, following the first call in March 1995. A majority of the partners were already participants in the COST 323 action. After a positive review by the experts and a negotiation phase in Autumn 1995, the project began in September 1996, after a 6 month delay for administrative reasons.

2. Objectives

The objective of the 'WAVE' project was to effect a significant step forward for those responsible for road networks, through the following actions:

- 1.1. Improve the capacity of conventional WIM systems to accurately estimate static loads from measurements of dynamic impact forces applied by axles, through use of arrays of sensors whose combined results can allow for the dynamic interaction between vehicle and pavement.
- 1.2. Develop and improve the functioning and accuracy of bridge-based WIM systems through more sophisticated vehicle/bridge interaction modelling and data processing.
2. Develop common data structures, formats and quality assurance procedures to facilitate the exchange and comparison of WIM data throughout Europe, to increase confidence in such data and to provide reliable management information to decision makers.
- 3.1 Perform tests of WIM systems to assess their durability and performance in various climatic conditions, particularly in cold regions where pavements deform and are weaker during the thaw and sensors are susceptible to studded tyres and de-icing salt.
- 3.2. Develop standardised calibration methods and procedures by improving existing methods and extending their applicability to all European climates and types of WIM system.

-
4. Develop and implement a new WIM technology, based on an innovative fibre optic sensor which has considerable potential in terms of quality and the extent of information provided and its insensitivity to harsh climatic conditions.

This project constituted a strategic policy initiative to confirm the Europe's leadership in WIM. It led to the development of new technologies such as advanced multiple sensor and bridge WIM systems, a quality assurance procedure to be implemented in a pan-European database, data about the behaviour of WIM systems in harsh environments, an improvement in calibration procedures and the development of a new European optic-fibre WIM technology. That will help road and transport decision makers.

3. Project organisation and means

The consortium involved 6 Contractors and 5 Associate Contractors:

Coordinator: Laboratoire Central des Ponts et Chaussées - LCPC - France

Contractors: Cambridge University Engineering Department - CUED - United Kingdom
Trinity College Dublin - TCD – Ireland
Road and Hydraulic Engineering Division - DWW - The Netherlands
Alcatel Contracting - ALCO (9/96-5/98) / Alcatel CIT Saintes (6/98-6/99) - France
Swedish National Road Administration - SNRA - Sweden

Associated Contractors:

Belgian Road Research Centre - BRRC – Belgium
Technische Universität München - TUM - Germany
Technical Research Centre of Finland - VTT - Finland
Swiss Federal Institute of Technology - ETH - Switzerland
Slovenian National Building and Civil Engineering Institute - ZAG - Slovenia

All together, more than 15 senior scientists and engineers, 25 Ph.D. students, post-doctoral or young engineers or researchers, and many technicians were involved in WAVE. Some subcontractors were SME (Small or Medium Enterprises), manufacturers and/or vendors of WIM systems or services; they were therefore self-motivated and interested in the output and deliverables of the project.

The project was planned for 24 months, from September 1996. A 9 month extension was subsequently accepted by DGVII, which lead to a project completion date of June 1999.

The complete project was organised in 4 main research areas, each of which was divided into two or three parts to give a total of nine work packages (WPs). The WPs were sub-divided into tasks. Each task consisted of work with a specific deliverable or output to be used in another task. Each specific WP covered one of the main objectives of the project and a basic need in Europe. The four main research areas were consistent areas, but had relationships between them. Each WP worked towards providing more efficient and accurate WIM systems and more reliable traffic load data.

The detailed organisation of the WPs is described below:

WP1. Accurate estimation of static weights using WIM systems

WP1.1. Multiple Sensor WIM (MS-WIM) - *leader: CUED / co-leader: LROP/LCPC*

- a. New and improved theories

- b. Validation using experimental data
- c. Tests of MS-WIM systems
- d. Specifications and legal issues

WP 1.2. Bridge WIM systems (B-WIM) - *leader: TCD*

- a. Increased Accuracy for Typical Bridges
- b. Extension of B-WIM to Orthotropic Decks
- c. Extension of B-WIM to Other Bridges
- d. Dynamic Analysis for Typical Bridges
- e. Calibration

WP2. Quality, management and exchange of WIM data - leader: DWW

WP2.1. WIM data quality assurance

- a. Analysis of existing quality systems
- b. Site quality
- c. System quality
- d. Calibration procedures
- e. Data quality

WP2.2. WIM data format and database structures

- a. Submitted data format
- b. Harmonisation procedure
- c. Description of two database levels
- d. Database management and maintenance

WP3. Consistency of Accuracy and Durability

WP3.1. Durability of WIM systems in cold climates - *leader: SNRA*

- 0. Preparatory work in advance of the project start
- a. Reporting previous experience on the subject matter
- b. Inviting WIM manufacturers to the test
- c. Final decision on test site localisation
- d. Site preparation
- e. WIM installation
- f. First summer test
- g. Winter test
- h. Second summer test
- i. Random traffic test
- j. Final report

WP3.2. Calibration of WIM systems - *leader: VTT*

- a. State of the art report
- b. Test of calibration devices and procedures
- c. Specification of the calibration procedures

WP4. Optical fibre WIM systems, technology for the future - leader: LCPC

WP4.1. Sensor Design

- a. Feasibility
- b. Characterisation and testing
- c. Calibration
- d. Mathematical model (1)

WP4.2. Optoelectronic Head

- a. Design
- b. Multiple sensor head
- c. Long-term performance
- d. Prototype improvements

WP4.3. Data Acquisition and Processing Unit

- a. Data acquisition and treatment
- b. Mathematical model (2)
- c. Validation and Report

A total budget of 1.5 million Euros was allocated to the WAVE project, of which 0.75 million Euros was provided by the European Commission. The total time spent on the project was nearly 30,000 man-hours, i.e. 20 man-years. The personnel cost represents 69% of the total budget. A mid-term seminar was organised in September 1997 in Delft, The Netherlands (WAVE, 1997) and a Final Symposium in Paris (May 1999), in order to widely disseminate the results of the project. In addition, much of the results were presented at the Second European Conference on WIM organised through the COST 323 action. A Web site was initially built by LCPC and is now merged with the European WIM web site built by the COST 323 action and hosted by ZAG (<http://wim.zag.si/>). A CD-ROM was prepared (edited by the BRRC) to present all the reports and output of the project.

Several large testing facilities or bridge and road test sites were used in the project. Two road sections were instrumented with multiple-sensor arrays, in the UK and France, for testing MS-WIM systems. For the calibration of these arrays, instrumented lorries and pre-weighted lorries were used. Several bridges of different type were instrumented in France, Germany, Sweden, Slovenia and Ireland to develop and test B-WIM systems. For WP3.1 in Sweden, a road section of 0.5 km was instrumented with five WIM systems, and a static weighing area with a large weigh-bridge was used.

4. Project output

New theories, models, algorithms, and procedures have been generated, prototypes built, and field tests performed. New prospects have been opened up for weighing using multiple sensors and instrumented bridges, an innovative technology has been developed using optical fibres and optronics, and there have been significant advances in the calibration of the systems and in the quality and management of weigh-in-motion data. Experiments on roads fitted with sensors and on instrumented bridges have yielded highly valuable quantitative information on the durability, performance, and precision of many types of weigh-in-motion system.

As happens in most active and innovative research projects, many questions have been answered and others asked, opening up new prospects. The scope of weigh-in-motion has been expanded to encompass new needs in the checking of vehicle weights, thanks to a substantial improvement of the levels of precision, and in the design and management of road infrastructure, thanks to new approaches to the instrumentation of roads and bridges.

In addition to performing the research and attaining the project's objectives, the consortium has attached special importance to dissemination of the knowledge and results acquired, both within the scientific community and to the users and industrial builders of the systems. The fallout from such a project is almost as much a matter of "making known" as of "know-how".

Overall results of the project are presented in the General Project Report, published by the LCPC. Detailed results of each WP are presented in each WP's report, which are published by the WP leader's organisations.

Report on the WP 2.1

This report was drafted by the Work package 1.2 members of the WAVE project and was edited by Prof. Eugene O'Brien and Aleš Žnidarič.

The main contributors are:

- Eugene O'Brien, UCD Dublin, Ireland
- Aleš Žnidarič, ZAG Ljubljana, Slovenia
- Werner Baumgärtner, TUM München, Germany

- Tony Dempsey, LCPC Paris, France
- Arturo Gonzales, UCD Dublin, Ireland
- Jan Kalin, ZAG Ljubljana, Slovenia
- Igor Lavrič, ZAG Ljubljana, Slovenia
- Stefan Lutzenberger, TUM München, Germany
- Peter Mc Nulty, UCD Dublin, Ireland

TABLE OF CONTENTS

1. INTRODUCTION TO BRIDGE WIM.....	1
1.1 Strain measurements and axle detection	2
1.2 Where to use Bridge WIM Systems.....	2
1.3 Accuracy of bridge WIM systems.....	3
1.4 Bridge WIM calibration.....	6
2. OBJECTIVES OF WORKPACKAGE WP1.2	7
2.1 Understanding the Dynamics of the Lorry Crossing Event.....	7
2.2 Development of a Prototype B-WIM System	7
2.3 New Approaches and Algorithms	7
2.4 Durability: Free of Axle Detector Systems	8
2.5 Testing the Accuracy of B-WIM Systems	8
3. ORGANISATION OF WP 1.2.....	9
4. THE DYNAMICS OF THE LORRY CROSSING EVENT	12
4.1 VTT Lorry Crossing Belleville bridge.....	12
4.2 Description of VTT truck and Belleville bridge, roughness profile.....	12
4.3 Measured wheel forces (VTT) and bridge strains	13
4.4 Simulation of Bridge-Truck Interaction.....	16
4.5 Discussion of Belleville Experiment.....	18
5. DEVELOPMENT OF A PROTOTYPE B-WIM SYSTEM.....	20
5.1 General principles and system requirements.....	20
5.2 SiWIM components	22
5.2.1 Data acquisition	22
5.2.2 Gathering data, filtering and monitoring.....	22
5.2.3 Vehicle detection.....	22
5.2.4 Weighing.....	23
5.3 Data exchange with external algorithm.....	23
5.3.1 Interaction with the external algorithm.....	23
5.3.2 SiWIM data for external algorithm.....	24
5.3.3 External algorithm data for SiWIM	25
6. NEW APPROACHES AND ALGORITHMS.....	27
6.1 Optimisation Algorithms Developed for the Orthotropic B-WIM System.....	27
6.1.1 Choice of Optimisation Procedure.....	28
6.1.2 Determination of Constraints for Optimisation.....	28
6.1.3 Calculation of the Hessian Matrix	29
6.1.4 Determination of Constraints for Optimisation.....	30
6.1.5 Guidelines for Control of Optimisation Parameters.....	35
6.1.6 Identification Algorithm	37
6.1.7 Optimisation Algorithm for 2-Dimensional Bridge Model.....	38
6.1.8 Conclusion on Orthotropic B-WIM Optimisation Algorithms	41
6.2 Multiple-Sensor Static B-WIM Algorithm	41

6.2.1	Introduction to Multiple-Sensor Static B-WIM	41
6.2.2	Theory of Multiple-Equation B-WIM Systems.....	42
6.2.3	Preliminary Experimental Verification	45
6.2.4	Conclusions on Multiple-Sensor Static B-WIM.....	47
6.3	Combined B-WIM and Pavement WIM System.....	47
6.3.1	Robustness.....	47
6.3.2	The Basis of a Combined Algorithm.....	49
6.4	The Development of a Dynamic Bridge WIM Algorithm.....	51
6.4.1	Theoretical Testing.....	53
6.4.2	Spectral Algorithm	54
6.4.3	Dynamic Multi-sensor Bridge WIM Algorithm (González et al. 1999)	56
6.4.4	Dynamic Bridge WIM Algorithm based on one sensor location.....	61
7.	DURABILITY: FREE OF AXLE DETECTOR SYSTEMS.....	66
7.1	Review of Bridge WIM Instrumentation - Strain Measurements and Axle Detection	66
7.2	Bridges Appropriate for FAD B-WIM Instrumentation.....	66
7.3	Calculation of velocity and axle spacings.....	70
7.3.1	Orthotropic FAD identification algorithm.....	70
7.4	Upgrade of the SiWIM Software for FAD	74
8.	TESTING THE ACCURACY OF B-WIM SYSTEMS	76
8.1	Orthotropic Bridge Weigh-in-Motion	76
8.1.1	Instrumentation and Experimentation	76
8.1.2	Results and Accuracy Classes	78
8.2	Tests in Lulea, Sweden.....	80
8.2.1	TCD/UCD Results (DuWIM)	81
8.2.2	ZAG Results (SiWIM)	87
8.2.3	Integral slab bridge.....	88
8.3	Slab bridges	88
8.3.1	Two-span integral slab bridges, skewed 7° and 26°	92
8.3.2	Integral slab bridge with a span of 8 m and a bump.....	94
8.3.3	Culvert-type bridge.....	95
8.3.4	Conclusion for Slab Bridges.....	95
9.	CONCLUSIONS, RECOMMENDATIONS AND FUTURE NEEDS.....	97
10.	REFERENCES AND BIBLIOGRAPHY	98

List of figures

Figure 1:	Bridge WIM instrumentation	1
Figure 2:	Pneumatic axle detectors on a bridge and strain transducers screwed on a bridge deck	2
Figure 3:	Two types of bridges instrumented for B-WIM.....	4
Figure 4:	Measured strain responses of an 8-m long slab bridge (left) and a 32-m long beam bridge (right) due to crossings of a five axle semi-trailer.....	4
Figure 5:	Influence lines for simply and fixed supported (integral) single-span bridge	5
Figure 6:	Relationship between Tasks of Workpackage and Structure of Report	11
Figure 7:	VTT Lorry crossing Belleville bridge.....	13
Figure 8:	Belleville Bridge	13
Figure 9:	Measured Wheel Forces (provided by VTT). Lines at 10 m mark the beginning of the bridge, lines at 64.9 m the pier and lines at 116.6 the end of the bridge.....	14
Figure 10:	Strain Record at Bottom of Box Girder	15
Figure 11:	Strain record, concrete deck plate, transverse direction	15
Figure 12:	Strain Record, concrete deck plate, longitudinal direction.....	16
Figure 13:	FE model of the Belleville bridge	17
Figure 14:	Strains at Belleville Bridge	18
Figure 15:	SiWIM Data Flow Diagram.....	21
Figure 16:	Contour map of objective function for variations in axle spacing and velocity (2-axle truck)	31
Figure 17:	Objective function versus axle weights.....	31
Figure 18:	Variation of objective function with first axle weight and axle spacing (2-axle truck).....	32
Figure 19:	Variation of objective function with various parameters (5-axle truck).....	32
Figure 20:	Theoretical study to evaluate the upper and lower limits on axle spacing	34
Figure 21:	Upper and Lower Bounds on Axle Spacing Optimisation Parameter.....	34
Figure 22:	Evaluation of the objective function for variations in velocity and alignment parameters	35
Figure 23:	Sensitivity of truck parameters to misalignment of theoretical and modelled bridge responses	36
Figure 24:	Flowchart for Identification Algorithm.....	38
Figure 25:	FEM mesh for the central span of the Autreville bridge.....	39
Figure 26:	FEM mesh for one instrumented section of the Autreville bridge	40
Figure 27:	Effect of lorry transverse position on calculated stresses: (a) stress on the soffit of the longitudinal stiffeners for positions 1 and 29 of the front axle of the truck; (b) transverse influence line for one longitudinal stiffener	40
Figure 28:	Longitudinal sensor locations and corresponding influence lines.....	44
Figure 29:	Dependency of Influence Functions.....	44
Figure 30:	Belleville bridge and strain gauge locations.....	45
Figure 31:	Errors in calculated gross vehicle weight versus distance.....	46
Figure 32:	Comparison of results from multiple-equation (M-E) B-WIM and conventional B-WIM algorithms.....	46
Figure 33:	Comparison of determinates for various bridge span lengths and axle spacings	49

Figure 34:	Errors in GVW for Combined Bridge Weigh-In-Motion System	51
Figure 35:	Individual Axle Errors for Combined WIM System	52
Figure 36:	Theoretical Bridge-Truck Dynamic Interaction Models.....	54
Figure 37:	Influence line versus Dynamic unit response at midspan.....	57
Figure 38:	Strain induced by a 2-axle vehicle and adjustment by static and DB-WIM algorithms.....	57
Figure 39:	Values of determinant $ \epsilon_i $ for each vehicle position.....	58
Figure 40:	Applied axle load calculated by 2 different multi-sensor approaches using a least squares fitting technique at each instant	59
Figure 41:	Effect on accuracy of the change of vehicle mechanics	60
Figure 42:	Existing B-WIM axle detection.....	67
Figure 43:	Existing B-WIM strain measurements	67
Figure 44:	Influence lines for simply and fixed supported (integral) single-span bridge and for a 2-span bridge	68
Figure 45:	Influence of the superstructure thickness on the peak of the influence line	68
Figure 46:	Definition of factor f_i	69
Figure 47:	Responses of two bridge spans with 3 different superstructure thicknesses, expressed in percentage of the span length, to the passage of a tandem with axle spacing equal to 15% of the span length	69
Figure 48:	FAD installation on a short slab bridge (left) and instrumented section of the orthotropic deck bridge in Autreville (right).....	70
Figure 49:	Schematic of (a) orthotropic deck and (b) short span slab bridge and response to passage of a 2-axle truck.....	71
Figure 50:	Response of the sum of the gauges in the 2 instrumented sections due to the passage of a 3-axle truck.....	72
Figure 51:	Response of one stiffener to the passage of a 5-axle truck	73
Figure 52:	Axle peak identification algorithm for orthotropic deck B-WIM.....	73
Figure 53:	Values of P_t , P_{t-1} and P_{t+1} evaluated from the strain signal	74
Figure 54:	Flowchart outlining the FAD modulus in SiWIM software	74
Figure 55:	FAD implementation in the SiWIM software	75
Figure 56:	Autreville bridge in eastern France.....	77
Figure 57:	Schematic of instrumented sections 2 and 3.....	77
Figure 58:	Details of transverse cross beams supporting the longitudinal stiffeners and instrumentation.....	77
Figure 59:	Results from optimisation and identification algorithm	79
Figure 60:	Comparison of accuracy for gross vehicle weights calculated from optimisation algorithms.....	79
Figure 61:	Point by point process	83
Figure 62:	Graphs of WIM versus Static Weights for the 1 st Summer Test; (a) Gross Vehicle Weights, (b) Axle Groups, (c) Single Axles.....	84
Figure 63:	Graphs of WIM versus Static Weights for Winter Test; (a) Gross Vehicle Weights, (b) Axle groups, (c) Single axles.....	85
Figure 64:	WIM versus static weight for 2 nd Summer test; (a) Gross vehicle weight, (b) Group of axle weights, (c) Single axle weights.....	86
Figure 65:	Side elevation of an integral slab bridge.....	88
Figure 66:	SiWIM results for Luleå – 1 st Summer Test.....	89
Figure 67:	SiWIM results for Luleå – Winter Test.....	90

Figure 68:	SiWIM results for Luleå – 2 nd Summer Test.....	91
Figure 69:	Results of Type V analysis of the full reproducibility test on the slab bridge.....	93
Figure 70:	Two span integral slab bridge with a skew of 26°.....	93
Figure 71:	Culvert-type bridge	95

List of tables

Table 1:	Task Descriptions for WP1.2.....	9
Table 2:	SWD File Fields.....	24
Table 3:	Planned SWX file fields.....	24
Table 4:	EAD file fields	25
Table 5:	EAX file fields	26
Table 6:	Accuracy Classification	61
Table 7:	Accuracy results for different bridge finite element models	64
Table 8:	Experimental Programme on Autreville Bridge.....	78
Table 9:	Accuracy classification according to COST 323 specification	80
Table 10:	Accuracy classification according to COST 323 specification (optimisation algorithm based on 2-D bridge model	80
Table 11:	Results of the first Summer Test.....	83
Table 12:	Results of the Winter Test.....	83
Table 13:	Accuracy classification for 2 nd Summer Test.....	87
Table 14:	Accuracy of the CET bridge WIM measurements from 1 st Summer Test	87
Table 15:	Accuracy of the CET bridge WIM measurements from Winter Test (with and without temperature compensation)	87
Table 16:	Accuracy of the CET bridge WIM measurements from June 1998, (I).....	88
Table 17:	Accuracy results from the integral slab bridge obtained by the SiWIM system, (R2, I).....	92
Table 18:	Accuracy results of traffic on skewed and straight 2-span slab bridges (R2, I)	94
Table 19:	Accuracy results on an 8 m integral span slab bridge with a bump, (r2, I, k=0.8).....	94
Table 20:	Accuracy results of the culvert-type bridge, (r2, I, k=0,8)	95

1. INTRODUCTION TO BRIDGE WIM

Weigh-in-motion (WIM) techniques have been traditionally used to collect truck and axle data for statistical purposes and also for the design of new and assessment of existing pavements and bridges, for traffic studies, bridge code calibration, bridge monitoring etc.. Most of the WIM systems at present are based on weighing detectors which are embedded into the pavement and measure wheel or axle pressures on it as the vehicle passes over them. As an alternative to pavement WIM systems, Moses and others (1979) developed the concept of using bridges as scales to weigh trucks in motion. In Australia a similar system appeared a few years later but was soon replaced by another that uses culverts (Peters, 1986). There are currently around 150 such systems in operation. In the nineties, new Bridge WIM (B-WIM) systems were developed independently in Ireland (Dempsey et al., 1995) and in Slovenia (Žnidarič et al., 1991).

Despite many advantages, B-WIM systems have not been widely used and are at present known only in a few countries around the world. Following the experience and results from the COST 323 action “Weigh-in-Motion of Road Vehicles” and research done in the WAVE project, this should change in the future.

Regardless of the system used, all B-WIM systems deal with an *existing instrumented bridge or culvert from the road network* as illustrated in Figure 1. Certain members of the structure are instrumented and strains are measured to provide information about its behaviour under the moving vehicle. Most of the existing systems require axle or vehicle detectors on the pavement close to the bridge to provide vehicle type, velocity and axle spacings. Strains are recorded during the whole vehicle pass over the structure and such redundant data provides useful information when the influence of dynamic effects due to vehicle-bridge interaction has to be accounted for. This is an undeniable advantage over pavement WIM systems where measurements of an axle last only a few milliseconds.

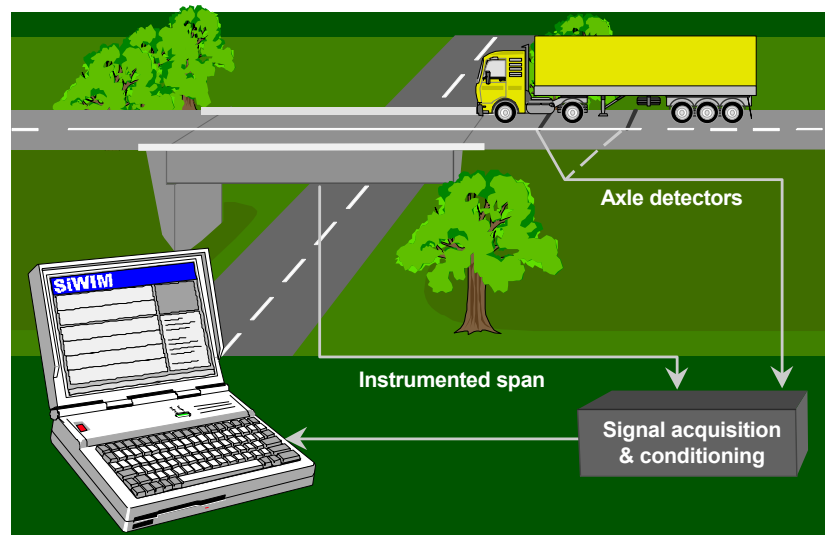


Figure 1: Bridge WIM instrumentation

1.1 Strain measurements and axle detection

Strains are measured either by strain gauges or reusable strain transducers which are attached to the main structural elements (see Figure 2, right). The midspans have been traditionally used as they generally provide the highest strain values but other locations can be instrumented to provide adequate or even improved information about structural behaviour under traffic.

Most of the existing bridge WIM systems use *axle detectors*, which can be either *removable*, such as tape switches, road hoses or similar pneumatic sensors (Figure 2), or *permanent* like piezoceramic or other similar built-in pavement sensors. Two detectors in each lane provide velocity of each axle and thus the dimensions, velocity and type of the vehicle. Depending on the data processing, they are placed before or on the bridge. First steps have been made in the WAVE project to replace axle detectors with appropriate strain recordings. This would completely eliminate all installation and maintenance activity on the pavement and would hence reduce the cost of installation and inconvenience to road users. It would also increase the durability of the systems, particularly in harsh climates. Considerable progress has been made for orthotropic decks (see Chapter 6) and for short concrete slab bridges (Chapter 7).

1.2 Where to use Bridge WIM Systems

There are two basic concepts for weighing vehicles in motion using existing instrumented bridges. Traditionally, a bridge WIM system was recommended for bridges with spans between 8 and 25 m (Snyder, 1992) or, like the Australian CULWAY system, on culverts. The first one weighs vehicles or many axles simultaneously while the second one weighs axles or axle groups individually.

Developments in computers in recent years have enabled extensive further improvements and modifications of B-WIM systems and algorithms. Several studies have been carried out in the WAVE project to increase their accuracy and to extend their applicability to other types of bridge, such as short slabs and long span bridges.

As the conventional B-WIM approach cannot be successfully applied on longer-span bridges, measurements are generally taken on parts of the spans between structural elements in the lateral direction, such as stiffeners. Typical such structures are steel box girders or steel orthotropic deck bridges. The most important new features of the orthotropic B-WIM systems are:



Figure 2: Pneumatic axle detectors on a bridge and strain transducers screwed on a bridge deck

- There are no axle detectors placed on the road surface which makes the system completely undetectable and facilitates its installation without the need to divert traffic.
- As the secondary spans are rather short, sharp peaks in the strain responses are recorded when an axle crosses it. These signals can be used for axle detection.
- As orthotropic decks are very sensitive in the lateral direction, more strain detectors are needed in the transverse direction. This makes it possible to calculate other truck parameters not normally calculated by conventional WIM systems, i.e., transverse position of trucks in lanes, width of truck wheel-base and possibly tyre type (single, dual or super-single).
- The strain measurements can be used for fatigue calculation.

The approach has been tested successfully and further experiments are planned to improve the algorithm and the system.

Similar attempts have been made on a steel box girder bridge, which is composed of two spans of about 54 m and 52 m. Girders are stiffened at 7 m intervals by a diaphragm which again provides 'substructures' similar to the orthotropic deck bridge. As bending strains from under the deck plate give clear signals for the axles, two longitudinally spaced sensors will be used to calculate the velocity and axle spacings of a crossing truck. Three strain sensors have been installed in the transverse direction to determine the lateral position of the vehicle.

Short slab bridges were in the past treated as only conditionally acceptable for B-WIM instrumentation. However, in many countries they are the prevailing type of bridge which, unlike longer bridges composed of beams, can be found on practically any road section. To obtain information about the suitability of short slab bridges for B-WIM, several of them were instrumented (Chapter 8). One of the most important findings of the analyses performed in WAVE is that, when applying an appropriate bridge instrumentation and B-WIM algorithm and provided the road surface is relatively smooth and without settlement prior to the bridge, *short slab bridges do not have any real disadvantages over longer beam-type bridges* (Žnidarič et al., 1998). Being short and slender, they even enable more accurate calculation of single axles and axles of a group which in most cases increases the overall accuracy class of the measurements.

1.3 Accuracy of bridge WIM systems

The fact that the whole length of the span or sub-span (in the case of long-span bridges) is used for weighing should in theory provide accurate results – Figure 3. This can indeed be the case if sufficient attention is paid to the selection of the structure and its influence line, measurement of vehicle velocity, optimisation of results, vehicle-bridge dynamics and calibration.

Although there is no theoretical limit to the number of axles (vehicles), which can be on the bridge during the measurements, the density of traffic limits the length of the instrumented span which can be efficiently used for weighing. The higher the number of axles on the bridge, the lower the accuracy of the calculated weights. In addition, the contributions of individual, closely spaced axles are more difficult to distinguish on longer bridges which can further affect the quality of the measurements. This phenomenon is evident in the example of Figure 4.

When the approach to the bridge was smooth, the best measured results were obtained on spans of around 10 m in length. Generally such bridges are also easy to instrument and calibrate. If the density of heavy traffic is low, if the axle weights are less important than the gross weights and if the

required accuracy of results is not very high, spans over 30 meters can provide satisfactory results. It should be kept in mind that longer spans and dense traffic increase the probability of having more vehicles on the bridge simultaneously which has unfavourable effects on the accuracy of weighing results for existing systems. The type of the bridge (steel girders, prestressed concrete girders, reinforced concrete girders or concrete slab) and skew of up to 30° should have only a minor influence on the accuracy. Nevertheless, in doubtful situations, it is recommended to perform some simple preliminary site measurements and to make the final decision when the calibration results are available.

Influence lines, which are used in practically all B-WIM systems, describe the bridge behaviour under the moving load. For this application they are defined as the bending moments at the points of measurement due to a unit axle load moving along the bridge. The true influence line of a bridge lies between the ideal simply supported and completely fixed curves (Figure 5). Furthermore, in some cases the influence line can be extended beyond the ends of the supports (Figure 5, dotted lines). A similar situation occurs with multi-span bridges.

The greater the difference between the assumed and the true influence lines, the higher the error of the results. Very often the error of the gross vehicle weights remains within acceptable limits even with poorly matched influence lines, but the axle weights can be severely redistributed (Žnidarič et al., 1998). Therefore, it is strongly recommended to apply as accurate an influence line as possible, preferably by processing the measured strains at the site. If an appropriate procedure or software is



Figure 3: Two types of bridges instrumented for B-WIM

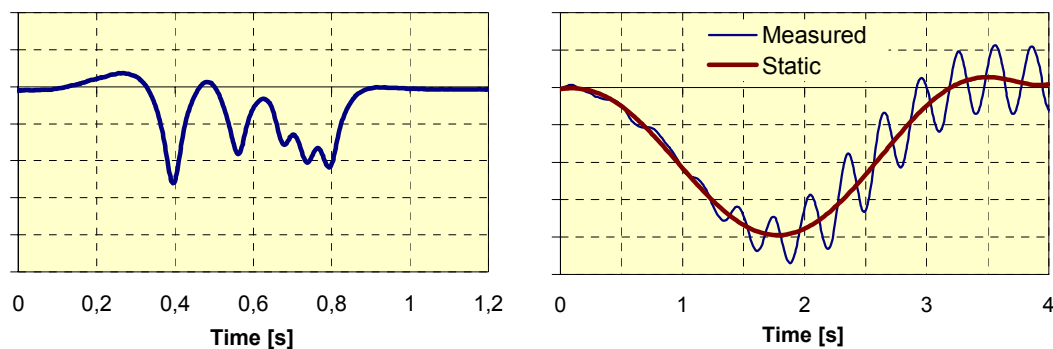


Figure 4: Measured strain responses of an 8-m long slab bridge (left) and a 32-m long beam bridge (right) due to crossings of a five axle semi-trailer

available, this can be easily done as a part of the calibration procedure and requires no knowledge of the detailed dimensions or structural make-up of the bridge.

Accurate evaluation of the vehicle velocity is another extremely important parameter for accurate B-WIM measurements (Moses 1979, Žnidarič 1998). The required precision of speed measurements can however be greatly reduced if the weighing results are optimised. This is usually done by applying optimisation routines to find the precise velocity and axle spacings which minimise the difference between the measured and simulated responses of the bridge under vehicle load. This method was first introduced by Dempsey (1998) who showed that the optimisation algorithm needs a good approximation of the initial values. While Dempsey (1998) uses some pre-set axle loads and an identification algorithm to obtain initial estimates of axle spacings and velocity on orthotropic deck bridges, the SiWIM[®] software, a B-WIM system developed in Slovenia (Žnidarič et al., 1998), takes the values from the results of an initial application of the conventional B-WIM algorithm.

When there is no major unevenness or bump on or just before the bridge and if the bridge WIM algorithm is able to process data throughout the period of passing of the vehicle, the effect of dynamics is considerably less for bridge WIM than for pavement WIM systems. However, if a bump is present, vehicles can jump on or even over the bridge. This mostly happens to light vehicles and unloaded trucks on very short bridges or culverts. International roughness index (IRI), which is a very important parameter for accurate pavement WIM measurements, is of little help for B-WIM as it does not account for such local situations. Also, it has been found that if the first natural period of the bridge is greater than the time taken for the truck to cross the bridge, significant errors can result in the calculation of axle weights.

Low-pass filtering of the strain records can considerably reduce the influence of dynamics. However, it was found in WAVE that, even for bridges with high first natural frequencies, filtering had the effect of blurring the distinction between the effects of successive closely-spaced axles. Thus, filtering of the strain signals is not recommended except at high frequencies.

To minimise errors due to dynamics, it is recommended to choose:

- sites with a smooth approach and no bump or major unevenness just before the bridge and
- bridges with higher eigen-frequencies (shorter spans, stiffer superstructure or structural elements) that interfere as little as possible with vehicle frequencies of bouncing and suspension.

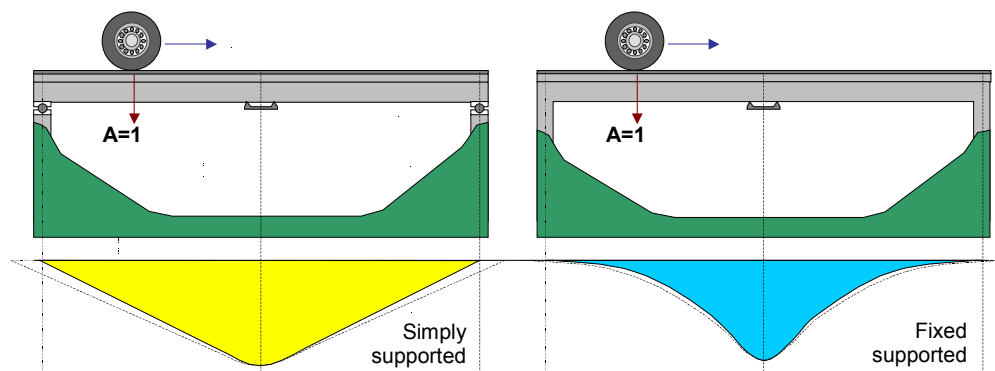


Figure 5: Influence lines for simply and fixed supported (integral) single-span bridge

For complex or unusual bridge structures it is very helpful to perform numerical interaction studies before the installation, e.g., using Finite Element models (Baumgärtner, 1998). Optimised locations for sensors can be identified with respect to the shape of their strain responses and to what degree the records are affected by dynamics.

1.4 Bridge WIM calibration

Trucks of known weight are used to calibrate all bridge WIM systems. Test plan 2.1 from the European specification for WIM (COST 323, 1997), where 2 trucks, one 2 or 3-axle rigid and one 4 to 5 axle trailer or semi-trailer are driven 10 times in each lane with 3 different speeds, is highly recommended. Loading close to the expected mean gross weight should be used. Several additional runs with unloaded or half-loaded vehicles can be useful to verify measuring parameters that were input to the system. Calibration results should not exhibit any nonlinearity depending on loading or speed of the vehicle. If this occurs, influence lines and speed acquisition have to be checked or correction functions have to be applied (Peters 1986). If test plan 2.1 cannot be provided, at least test plan 1.1 (10 runs of one truck with 2 or 3 different speeds) should be used in each lane. A shorter, 2 or 3-axle rigid truck is recommended, which often indicates possible dynamic problems. Compared to the longer non-rigid vehicles, they are also more sensitive to uneven pavement and bumps before the bridge, thus providing a conservative upper-bound indication of the accuracy of WIM results.

If the B-WIM software supports it, higher methods of calibrations can further improve the accuracy of the results (COST 323, 1997). In addition to Method I, which defines a calibration factor based on gross weights of all test vehicles, Method II treats vehicles differently according to their type (rigid, trailers, semi-trailers etc.) and Method III according to the type of axle (single, member of tandem/tridem) and its position.

With appropriate strain measurements, which can compensate for temperature changes, the influence of weather on bridge WIM results should be small. Only in some extreme cases the temperature changes influence the bridge behaviour and consequently the weighing results. In such cases, it is recommended to repeat the calibration in different extremes of temperature (during two summer and winter days or at least, on a sunny day, at dawn and mid-afternoon).

2. OBJECTIVES OF WORKPACKAGE WP1.2

The objectives of Workpackage WP1.2 of WAVE are given in the following sections.

2.1 Understanding the Dynamics of the Lorry Crossing Event

In the short number of seconds that a lorry crosses a bridge, a complex interplay of forces takes place. Trucks consist of masses joined together with suspension elements and, at a particular point in time, are undergoing bouncing and rocking motions. When a truck arrives on a bridge, it induces vibration in it in addition to the static effect. There is a dynamic interaction between these lorry and bridge motions which may or may not be significant.

The objective of Bridge WIM (B-WIM) is to determine the static axle forces of a lorry by monitoring the strains induced in a bridge. Clearly the dynamic component of the force applied by each axle, if significant, can be a major source of inaccuracy in any B-WIM system. For this reason, it has been a major objective of WP1.2 to develop an improved understanding of the forces generated as a lorry crosses a bridge. This is achieved through both theoretical modelling and experimentation.

2.2 Development of a Prototype B-WIM System

There are two major elements in the software of any B-WIM system, namely, data acquisition and the calculation of the weights of the lorry's axles. Data acquisition is relatively routine but needs to be customised for the particular requirements of B-WIM systems. For example, there must be facilities for calibration based on repeated runs of pre-weighed lorries, real time calculation of axle weights and, as an alternative, storage of strain data for subsequent processing. The second element of a B-WIM system is the so-called B-WIM algorithm, the software which uses the recorded strain and axle location data to calculate the axle weights. A number of developments to Bridge WIM algorithms were effected as part of WP1.2 and there is potential for future development in this area.

While there were, at the outset of the WAVE project, only three Bridge/Culvert WIM systems available in the world, two further systems have been developed as part of the WAVE project. Given the increasing number of algorithms available, an objective of WP1.2 has been the development of an open-architecture prototype commercial B-WIM system. This consists of the two components, data acquisition and the calculation of the axle weights. However, the interface between the two is clearly defined and publicly available. This facilitates the use of the basic data acquisition system with any of the three existing European algorithms for the calculation of axle weights. Further, it promotes the standardisation of the interface for future developments in either of the component parts. The prototype system facilitates an improved interaction between industry and academic researchers as it provides a user-friendly data acquisition environment for academic developers of weight calculation algorithms.

2.3 New Approaches and Algorithms

It is an objective of WP1.2 to develop improved accuracy in B-WIM systems and to extend B-WIM to bridge types for which it was previously considered unsuitable or less appropriate. This has led

to developments in the B-WIM algorithms, the software that is used to calculate axle weights from the measured data. For Orthotropic bridges where axle detectors are not feasible but where the spans between supports are quite short, it has been possible to determine vehicle speed and axle spacing using optimisation routines which minimise differences between strain responses in different spans. Other algorithms are intended to improve accuracy. There has been considerable development in algorithms which allow for the dynamic interaction between the lorry and the bridge. Other work has considered whether accuracy can be improved by combining results from bridge and pavement WIM systems.

2.4 Durability: Free of Axle Detector Systems

Durability is a great potential advantage of Bridge WIM over the alternative pavement-based technologies as a B-WIM system consists almost completely of sensors that are not exposed to traffic. The exception to this is the axle detection devices in current B-WIM systems. It was therefore an objective of WP1.2 to investigate the possibility of B-WIM systems that would be **Free of Axle Detectors (FAD)**. The concept of a FAD system is that strain gauges attached to the underside of the bridge would be used to determine the vehicle location, speed and axle spacing. This is possible but is less accurate than a sensor placed on the road surface. The research consisted of seeking sensor locations and orientations that would improve the accuracy of detection and developing B-WIM algorithms that would compensate for inaccuracies in the axle detection results.

2.5 Testing the Accuracy of B-WIM Systems

A number of field trials were carried out as part of WP1.2 to assess the accuracy of B-WIM systems. This is the first time that such trials were carried out on such a large scale to a consistent format (the COST 323 specification) which allows the results to be compared to other WIM systems. A wide range of bridge types was used to demonstrate the consistency of B-WIM and its insensitivity to bridge type. Different B-WIM algorithms were compared to each other using the same data set. In other cases, different variations on the basic B-WIM algorithm and different approaches to calibration were assessed in the trials.

3. ORGANISATION OF WP 1.2

Workpackage WP 1.2 was divided into tasks as described in Table 1. The correspondence between these tasks and the sections of this report are illustrated in Figure 6.

Table 1: Task Descriptions for WP1.2

<i>Task No.</i>	<i>Description</i>	<i>Partners Involved</i>
<i>Increased Accuracy for Typical Bridges</i>		
a1	Experiment: Field trials in NE France will be carried out using pre-weighed lorries and an instrumented vehicle. Other tests will be carried out in Slovenia and Sweden.	TCD TUM LCPC ZAG
a2	More Analysis: Development of improved B-WIM software through more sophisticated algorithms incorporating the effects of dynamics, etc..	TCD TUM
a3	Combined System: Development of concept of combining bridge and pavement WIM measurements to generate a more accurate algorithm.	TCD
<i>Extension of B-WIM to Orthotropic Decks</i>		
b1	Instrumentation & Data Collection: The orthotropic Autreville Bridge in NE France was instrumented for use as a B-WIM test site.	LCPC
b2	Computer Model: An elaborate Finite Element model of the Autreville bridge was developed for use in simulations.	LCPC
b3	Software Design: The Irish B-WIM software was developed and altered to make it applicable to orthotropic bridges	LCPC TCD
b4	Validation on a Large Scale Test: Field trials were carried out to test the new B-WIM algorithm on an orthotropic bridge.	LCPC TCD
b5	Operational Prototype: A full operational prototype Orthotropic Bridge WIM (OB-WIM) system was developed.	LCPC
<i>Extension of B-WIM to Other Bridges</i>		
c1	Concrete Slab Bridges: Concrete has a lower elastic modulus than steel and slab bridges have much higher load sharing transversely than beam/girder bridges.	ZAG
c2	Box Culverts: Box culverts are important because of their frequency and the potential of the surrounding soil to damp down the dynamic impact effects. They are different from other bridges as they are short relative to the lorry length.	TCD ZAG
c3	Influence of Surface Roughness on Accuracy: Increased road surface roughness is an important factor in the dynamic bouncing and rocking of lorries and therefore has a great influence on accuracy.	ZAG TUM

<i>Task No.</i>	<i>Description</i>	<i>Partners Involved</i>
<i>Dynamic Analysis for Typical Bridges</i>		
d1	Finite Element Model: FE models were developed for the Belleville bridge in NE France and the K38/1 bridge in Germany.	TUM
d2	Software Development: Software was developed for the estimation of some parameters of a simple 2-axle lorry moving along a simple 2-Dimensional bridge model (isotropic plate).	LCPC
d3	Experimental Test: Tests were carried out (a) for random traffic and (b) for an instrumented lorry at the Belleville bridge in NE France. In addition, the K38/1 bridge was instrumented and monitored in Germany.	TCD TUM
<i>Calibration</i>		
e1	Different Lorry Configuration: Different types of calibration lorry will be considered to determine its influence on the accuracy of the B-WIM system.	ZAG TCD
e2	Characterisation of Bridge: Methods of determining the bridge <i>Influence Line</i> , the curve which characterises the bridge behaviour, will be developed.	ZAG

Workpackage WP1.2 is closely related to WP3.1 in that a major part of the latter work package consisted of a field trial of WIM systems. A Bridge WIM system was tested alongside pavement WIM systems in this trial. The details of the Bridge WIM test are presented in the report for WP3.1 and a summary of results is given here in Chapter 8.

Tests for WP1.2 were also carried out near the test site for the Continental Motorway Test and test runs by the instrumented lorry carried out for WP3.2 were extended so that readings could be taken while the lorry crossed an instrumented bridge.

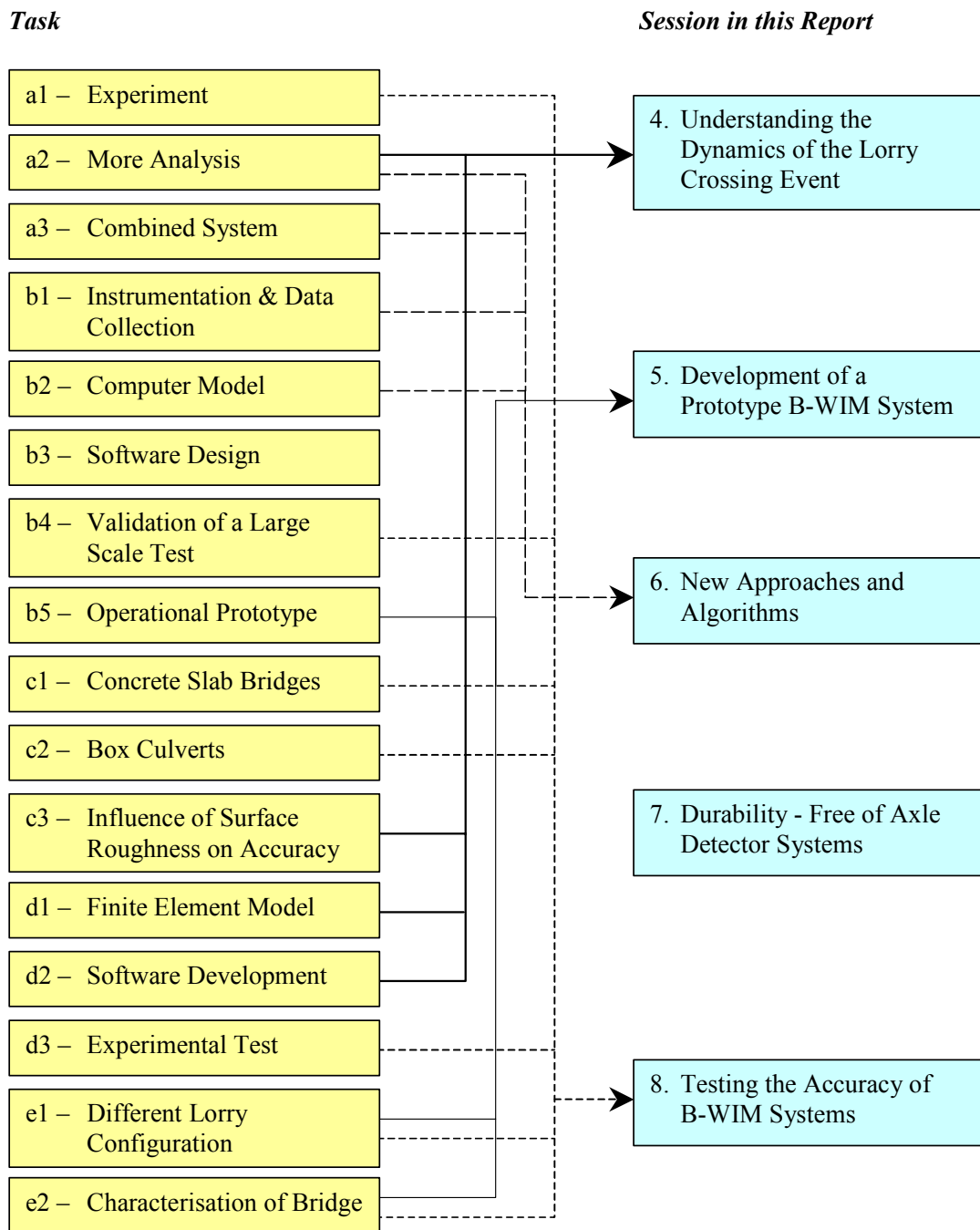


Figure 6: Relationship between Tasks of Workpackage and Structure of Report
 (Note: Chapter 7, *Durability*, describes work not originally planned)

4. THE DYNAMICS OF THE LORRY CROSSING EVENT

4.1 VTT Lorry Crossing Belleville bridge

The goal of TUM within the WAVE project was to study bridge dynamics and the interaction of the combined truck-bridge system. These measurements are mainly influenced by the static reaction of the bridge itself. Although the dynamic proportion can be reduced by low-pass filters or by averaging the calculated axle weights at every recorded time step, there are several reasons to consider further the dynamic effects and the interaction between the vehicle and the bridge:

- In many cases dynamic effects influence the accuracy of B-WIM systems. Very high accuracy B-WIM systems can not be realised on some bridges without considering the dynamic reaction of the bridge.
- Free of axle detector systems require an axle identification on the basis of the measurement records alone. The peaks in the measurement records due to the single axles of tandem and tridem axles are sensitive to bridge dynamics. Furthermore low-pass filtering is not possible for this task. Therefore it is desirable to look at the dynamic effects in sensitive bridges before the installation of sensors. This can be done by calculating the interaction of the truck crossing the bridge with a realistic road profile. However, such a simulation requires a very detailed knowledge of the bridge behaviour which is typically not possible without detailed calibration.
- Different locations of the bridge show different reactions due to the crossing of a truck. Some measurement locations show a rather global reaction, some show a rather local reaction and some show a combined global and local reaction. While the measurement points with the global reaction provide major strains, those with the local reaction are generally more appropriate for axle detection. Due to a proposal of TUM it has been shown that certain measurement points, even for large bridges with a concrete deck plate, are suitable for axle- and axle-group detection. The reaction (global/local/combined) of a measurement point can be studied in advance with the TUM interaction program.
- The simulation of a truck crossing a bridge allows parameter studies to be carried out, e.g., to evaluate the sensitivity of recorded strains to different parameters such as the lateral position of the truck, the vehicle speed or the axle configuration. It is also possible to test alternative WIM algorithms easily.
- The observation of the interaction facilitates bridge monitoring. As shown at the Fischerdorf bridge it is possible to evaluate the stresses under traffic, to record the change in the stresses with time and to monitor the fatigue of the bridge on the basis of real-time measurements (Baumgärtner 1998).

4.2 Description of VTT truck and Belleville bridge, roughness profile

Within the scope of the project, tests were performed in NE France with an instrumented lorry crossing a bridge.

The instrumented lorry is a three axle lorry owned by the technical research centre of Finland (VTT) – see Figure 7. The vehicle has traditional steel springs. The axle spacings are 4.20 m between the first and the second axle and 1.20 m between the second and the third axle. Due to a mechanical connection of the tandem axle the axle forces are partitioned to 55% for the second axle and 45% for the third axle. It is possible to lift up the third axle. The tandem axle is equipped with dual tyres. All tyres have a diameter of 1.05 m.

The Belleville bridge itself (Figure 8) is situated at the autoroute A31 in France between Metz and Nancy. Research work was carried out on the first two (Northern-most) spans only which act independently of the rest of the bridge. The spans are 54.9 m and 51.7 m in length with a depth of 2.02 m. The bridge is a steel box girder with a concrete deck slab with an average thickness of 30

cm. Based on measurements of strains and accelerations, the main frequencies of the bridge were found to be 1.35 Hz (1st bending), 2.0 Hz (2nd bending) and 4.4 Hz (1st torsion).

In most cases the road roughness is the cause of strong dynamic effects. For both tracks of the right lane of Belleville bridge, the measured roughness profile was provided by LCPC. The measurement started about 50 m prior to the bridge, in particular to get information of the dynamic excitation of an approaching truck. Long waves in the measured profile do not affect the dynamics of truck and bridge. Frequencies less than 2 Hz were filtered out to derive an effective profile. It has been noted that:

- the amplitudes of the roughness ahead of the bridge are much higher than on the bridge (typical for road surfaces ahead of bridges),
- there is a very high and sharp jump at the beginning of the bridge near the joint.

4.3 Measured wheel forces (VTT) and bridge strains

The measurement records of all six wheel forces were provided by the Finnish colleagues of VTT. The measurements started 10 m ahead of the bridge. Five runs were performed on Belleville bridge with velocities of about 83 km/h. The main effects were very similar in all runs. In Figure 9, the records of the right wheels are given. For an easier comparison with the roughness profile the wheel force records are related to length.

The right wheel of the first axle with a measured static force of 30.8 kN has a maximum dynamic amplification at the joint of about 50%. While crossing the bridge, the dynamic amplification is about 20% mainly with a body frequency of 2.2 Hz. The main dynamic amplifications of the



Figure 7: VTT Lorry crossing Belleville bridge



Figure 8: Belleville Bridge

wheels of the second and third axle (static force 42.3 kN and 39.4 kN) of nearly 100%, meaning a loss of contact, work with a frequency of about 8.5 Hz corresponding to the vibration of the axles. The frequency of 3.2 Hz belonging to a body vibration can be seen while crossing the second span, when the axle vibration is damped out.

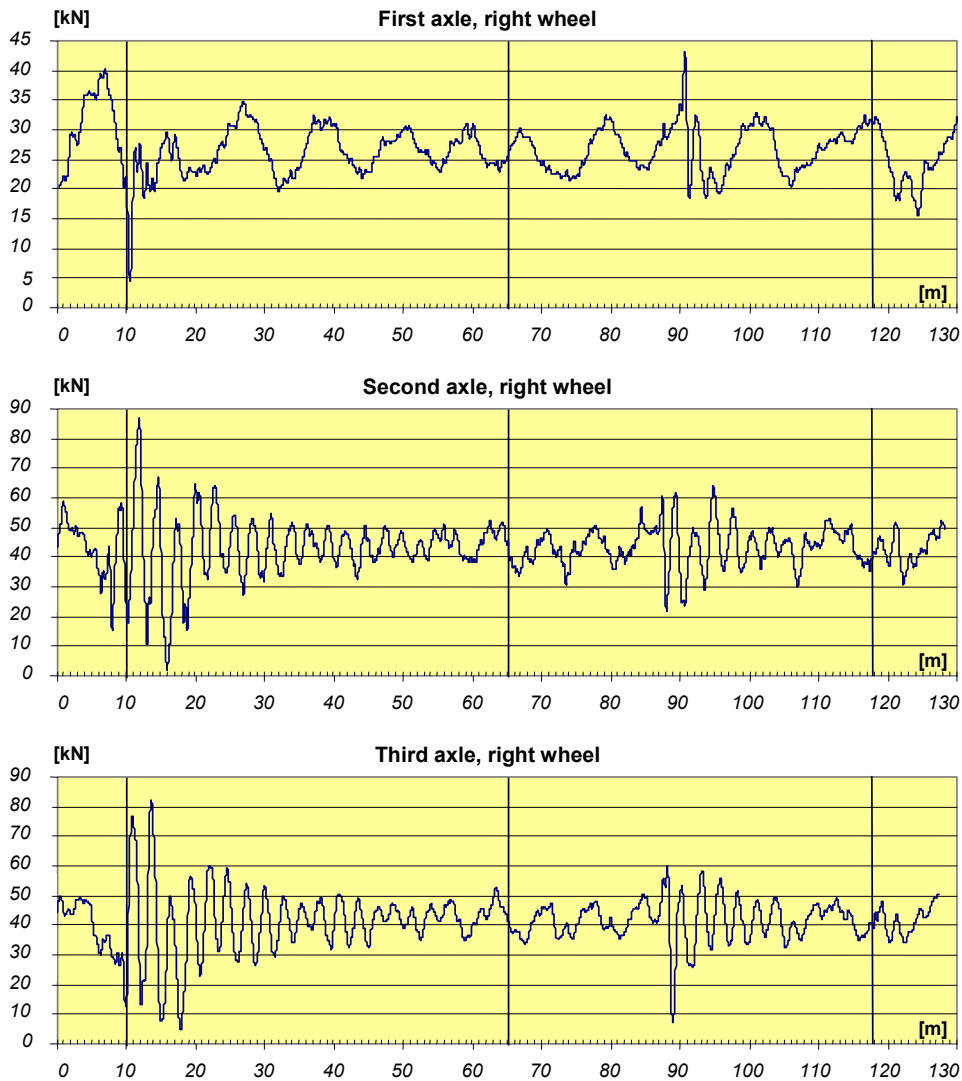


Figure 9: Measured Wheel Forces (provided by VTT). Lines at 10 m mark the beginning of the bridge, lines at 64.9 m the pier and lines at 116.6 the end of the bridge

While analysing Fourier spectra of the axle force records, a frequency was detected which changed with the velocity of the truck, e.g. 7.1 Hz for a speed of 84 km/h. An inverse transform of this frequency to time revealed that the amplitudes were nearly constant within the whole record, with

about 10 % of the static wheel force (third axle). This influence on vibration is caused by deficiencies of the roundness of the wheels, as the frequencies correspond to a wheel diameter of 1.05 m.

In the second span of the bridge a jump in the axle forces can be seen, which cannot be explained by the measured roughness profile. This local effect is caused by a mounted portable weigh scales which was used during the WAVE experiment by our colleagues from BRRC (Belgium).

It can be concluded that the dynamic amplification is mainly caused by the jump at the joint at the beginning of the bridge and the relatively high roughness amplitudes ahead of the bridge. The use of an average roughness on the bridge, represented by a power density function or an IRI index, is not sufficient to evaluate wheel dynamics.

Different locations at the bridge were instrumented with strain gauges by TUM to study the bridge reaction as an influence on B-WIM. Traditionally strains recording the longitudinal bending are used for WIM algorithms. The influence lines for these locations are related to both spans (global influence lines) and are not very much influenced by the lane where the truck is running. They provide very good information to evaluate the total weight of a crossing truck. However, for longer bridges such as Belleville, a separation to different axles is hardly possible. Figure 10 presents a record of a strain gauge located at the bottom of the steel box.

A local response can be obtained for sensors measuring the bending of the deck plate in the transverse direction. Three of these sensors were installed in the same cross section to detect the lane where the truck was running by combining the measurements in accordance with their influence lines. The influence of all three axles can be seen in the record given in Figure 11.

Two sensors measuring local characteristics at a known longitudinal location can be used to accurately determine the velocity of the crossing truck as the time delay between the sharp peaks of the measured strains.

A measurement point mounted under the concrete deck plate in the longitudinal direction shows a superposition of local and global responses. To study the possibility of using this sensor for B-WIM the two portions are separated by frequency filtering in Figure 12. The local reaction is due to longitudinal bending of the concrete plate when the axle crosses the location. The global reaction is not as clear as the strains in concrete are small for a single truck and as the point is near to the neutral axis.

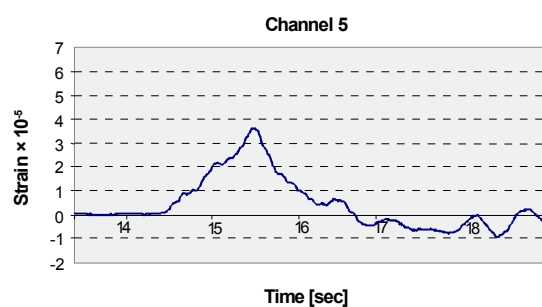


Figure 10: Strain Record at Bottom of Box Girder

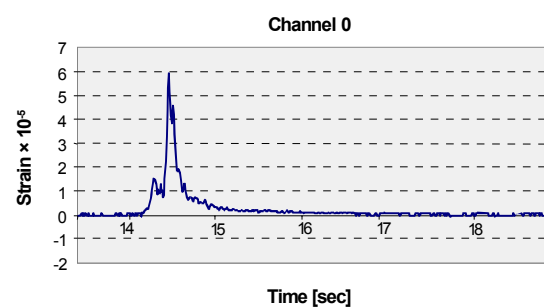


Figure 11: Strain record, concrete deck plate, transverse direction

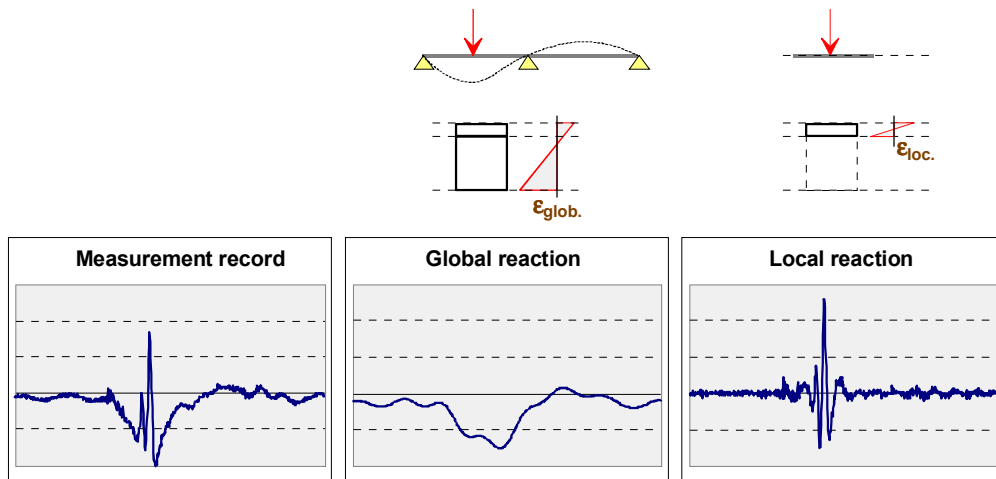


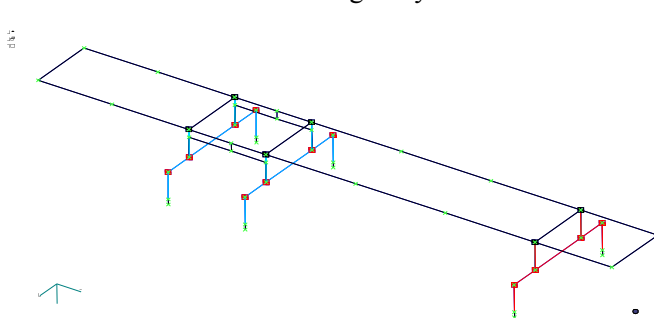
Figure 12: Strain Record, concrete deck plate, longitudinal direction

Compared to the very high dynamic axle forces due to the rather old axle-suspension configuration of the VTT truck, the corresponding strain records show moderate dynamic amplifications, which provides a good input for WIM algorithms. Common trucks, e.g., with air suspensions, react with even less dynamics in their axle forces. Therefore long bridges like Belleville bridge are suitable for B-WIM.

4.4 Simulation of Bridge-Truck Interaction

Since 1993 a method was under development at the TU München to calculate the interaction of two structures (Lutzenberger et al 1998). The basic concept is to create separate FE models with a commercial program that is widely available. Both models can be tested and verified separately, e.g., by different institutions. The program PRISIM allows to allow the calculation to be carried out with both structures moving relative to each other. The surface roughness is included in the equation which describes the contact condition. The results of the calculation can be displayed with a commercial graphical postprocessor, e.g. as an animation, or analysed using the TUM KONVERTER program and data analysis software.

A first truck model was created as a part of a TUM diploma work at VTT. A spatial model was established with beam elements describing the body and the axles and spring and damper elements for the suspensions and the tyres. In addition, the truck was modelled under full load so that a static calculation of the truck under gravity results in the same axle loads as the static weighing. Friction



elements, which are very important for the dynamic reaction of the truck will be included in future. The truck model was developed with few known structural data of the truck. Measured wheel forces at the test site in France were analysed and an experimental modal analysis was performed for the verification of the FE model.

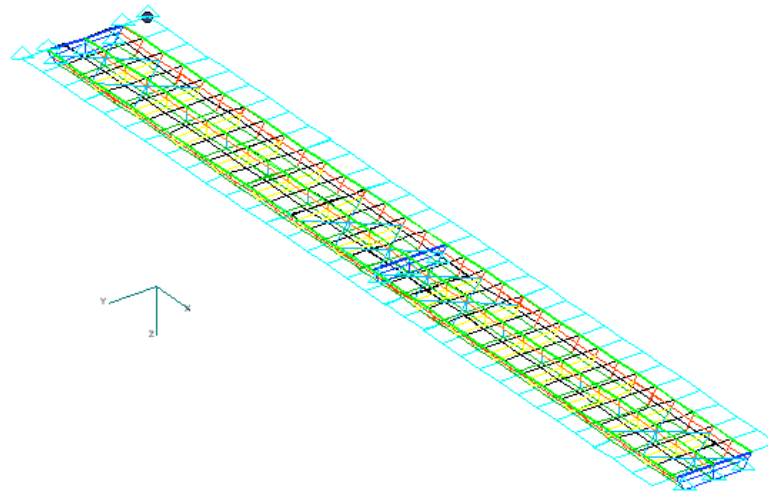


Figure 13: FE model of the Belleville bridge

The FE model of Belleville bridge (Figure 13) was mainly developed, calibrated and tested as a part of the diploma work of Penka (1997). It consists of about 500 nodes, plate elements for the concrete plate and the steel box and beam elements for the steel girder and the stiffening elements. Although the mesh is detailed enough to determine the dynamic wheel force for the simulation and global effects as the eigenmodes, it has still to be refined locally to get good results for calculated strains at the measurement points.

Measurements of strains and accelerations under traffic were performed and analysed to determine the eigenfrequencies and to estimate the eigenforms of the bridge. These measurements were also used to adapt and verify the FE bridge model.

As described above, the unevenness of the pavement is extremely important for the dynamic reaction of the truck and the bridge. Local effects in the reaction can only be determined if the road profile is known. Therefore to calculate a realistic response of the bridge and the truck, a road profile that encloses all wavelengths responsible for the main dynamic reactions, was included in the calculation.

A comparison of calculated and measured strains of the bridge is given in Figure 14. The calculated ones represent the mean strain of an element of the side wall of the box girder, whereas the measured ones were recorded at the bottom of the box girder. The difference of the amplitudes corresponds to the linear distribution of the strains over the height of the girder. The eigenfrequencies of the bridge model are in accordance with the bridge. The damping of the bridge is not yet included in the model, so that the vibration does not decrease with time as in the measured record.

A video of vibrating bridge and truck models (AVI format) can be provided (as presented at the WAVE Final Seminar in Paris).

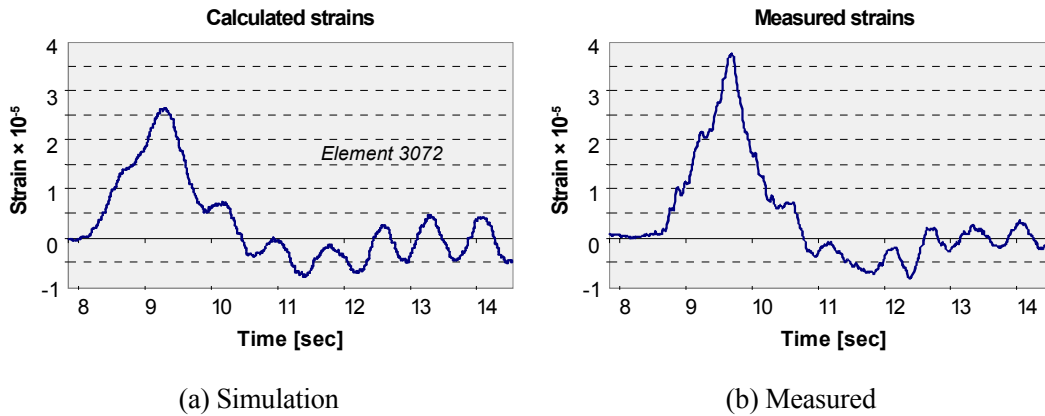


Figure 14: Strains at Belleville Bridge

4.5 Discussion of Belleville Experiment

The deficiencies of the roundness of the wheels results in a periodic dynamic axle load whereas the phase shift is dependent on the starting position of the wheels. This effect therefore influences the spatial repeatability.

Different measurement points show different reactions. Therefore, for long span bridges it is important to study the structural behaviour and to choose the best locations for each task.

Sensors under the concrete plate show a local reaction and are appropriate for axle detection and axle load evaluation.

The bridge itself acts as a transducing element between the dynamic wheel loads as an input and the strains as the output. This means that, for some locations, the bridge is less sensitive to disturbing influences and information about axles and axle groups diminishes. These locations seem to be appropriate for gross load evaluation. Furthermore, sensors at different longitudinal positions can be used to evaluate the speed of the vehicle.

Sensors measuring the transverse strains help to detect the lateral position of the truck which is important for high accuracy B-WIM systems.

As sensors under the deck plate are easy and cheap to install, a combination of several sensors should be used for axle information similar to multi-sensor WIM systems on road surfaces.

The road profile is the main influence for the truck dynamics. The best sensor locations are therefore those with the smoothest road in advance. Following a bump at the joint, changes in the dynamic wheel load can be up to 100% and strongly militate against axle identification. Due to this great influence on the measurement recordings, the use of a standard road profile is not sufficient for interaction simulations. Especially for the calculation of the dynamic wheel loads and the dynamic amplification factor, a realistic road profile is required.

It is planned to refine the FE-models of the VTT truck and the Belleville bridge. As construction plans of the axle configuration were not available, this part was modelled in a preliminary way. A better model will be designed and friction elements, which are important for the dynamic reaction

of this truck, will be included. To improve the calculated response of the bridge, it is planned to locally refine the FE model of the Belleville bridge in the region of the measurement locations.

Parameter studies will be performed to study the implications of different pavement roughnesses on the dynamic wheel loads. In another study it is planned to determine the influence of bridge dynamics on the dynamic wheel loads.

5. DEVELOPMENT OF A PROTOTYPE B-WIM SYSTEM

SiWIM is a new Weigh-in-Motion program that was developed at ZAG Ljubljana within the framework of WAVE, when it became clear that the old B-WIM system would not be sufficient to accomplish the planned work. This chapter describes the features of the program. The flow of the data is described from the point where it is acquired to the point where the final results (i.e., vehicle weights) are obtained.

The main features of the current version of SiWIM are:

- Sampling rate for data acquisition is variable between 32 and 2048 samples per second.
- Data is buffered between any two stages in the algorithm, so that any eventual delay in later stages of processing does not cause data loss.
- Data can be saved at various stages of processing to enable off-line processing. Currently SiWIM can write and read:
 - filtered signals in binary ACQ format compatible with other data acquisition software in use at ZAG Ljubljana,
 - processed strain signals in capture files with extension CAP, containing vehicle axle distances and speeds and strain transducer signals and compatible with the BWS (Bridge Weighing Systems Inc.) system,
 - FHWA (US Federal Highway Administration) CD7 files, containing vehicle by vehicle information on time of weighing, vehicle category, axle spacings, axle and gross weights etc.
- Signals can be filtered in real time. Filters include moving average, high-pass, low-pass and other FFT-based filters.
- Signals, raw or filtered, can be monitored in real time, as can power spectra of signals.
- After using Moses' algorithm for obtaining axle weights, SiWIM can pass the results to an optimisation algorithm (see Chapter 6) which can in some cases significantly increase the accuracy of results.
- In addition to using the internal algorithm, SiWIM can be used as a front-end to an external weighing algorithm via a standardised file-based interface.

SiWIM is being rewritten to include knowledge acquired while testing the prototype. Major changes include a complete overhaul of the internal data handling to improve performance, reduced memory requirements and increased program reliability. Significant changes to the user interface are also planned, including internationalisation, easier adjustment of parameters, flexible selection of data acquisition settings and influence line generation and less cluttered view of the signal monitor window.

5.1 General principles and system requirements

SiWIM is a multi-threaded (i.e., running several processes at the same time) program running in any of the 32-bit Microsoft Windows environments. It has been developed on a Windows NT 4.0

platform and has also been tested on a Windows 95/98 platform. Even for traffic with AADT of more than 30,000 vehicles/day, the program is capable of processing up to 16 input channels with real-time filtering and processing when run on a 300-MHz Pentium II computer with 64MB of RAM.

The data flow diagram can be seen in Figure 15. The data is acquired and processed in 1-second blocks, up to the vehicle detection, where it is gathered into larger blocks, whose length depends on the amount of time the vehicles are on the bridge.

A queue is set up between each pair of threads. This enables each thread to take as much time as needed for data processing, without leading to loss of data. It is nevertheless necessary that the total throughput is high enough to cope with the inflow of raw data.

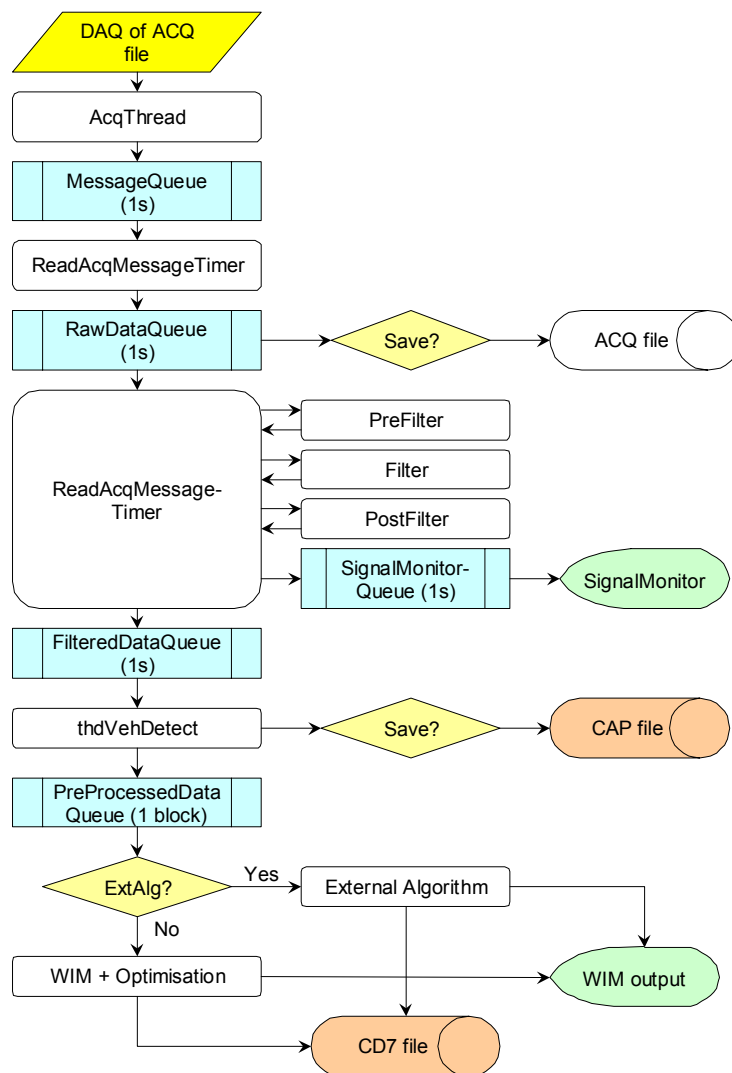


Figure 15: SiWIM Data Flow Diagram

5.2 SiWIM components

5.2.1 Data acquisition

The first step is the data acquisition. SiWIM is designed to work with National Instruments data acquisition products. Currently it supports two PCMCIA devices, but can easily be extended to other similar National Instruments cards.

When the acquisition is started, a data acquisition thread is created and one of two things happens, depending on the input source selection:

- either the data acquisition device is initialised or
- an ACQ file is opened for input.

The format of the data output by the acquisition thread is the same in both cases, so the rest of the program does not have to care where the data comes from.

Each second a block of data from the device or the file is pushed into an internal queue and the main program is notified that new data is available.

5.2.2 Gathering data, filtering and monitoring

When the main program receives the message from the acquisition thread, the following happens:

- First the data is picked from the acquisition thread queue. If selected, this raw data is saved into an ACQ file.
- Afterwards, the data can be filtered with one of several filters available.
- Depending on the user selection, the filtered or unfiltered data or power spectrum is then pushed into a signal monitor queue, from where it is read by the signal monitor thread and displayed on the screen.
- Finally the data is pushed into a filtered data queue, ready to be read by the vehicle detection thread.

5.2.3 Vehicle detection

The filtered data is read from the queue by the vehicle detection thread, which operates in one of two modes. If an internal algorithm is used, the data is first analysed to see if there are any vehicles on the bridge. This can be done either based on signals from the axle detectors mounted on the road surface or, in the case of FAD (Free of Axle Detector) B-WIM, from the strain sensors attached under the bridge. With activities on the bridge, an internal queue is set up and the data is collected until the last axle leaves the bridge. Otherwise the data is discarded. Once the activity on the bridge is finished, the data is packaged, together with the information on detected vehicles (i.e., speeds, axle distances, categories, ...), and fed to the pre-processed data queue. If the user wishes, this data is also written to a CAP file for later processing.

If an external algorithm is used, the vehicle detection thread actually does no vehicle detection. In this case it simply checks if data in a selected input channel is above a user-defined threshold, starts gathering data and when a certain amount of time (typically 10 seconds) has passed after the last such event, pushes this data into the pre-processed data queue. No CAP file can be written in this case.

5.2.4 Weighing

Weighing itself can be done with either an internal or external algorithm. In the latter case, the pre-processed data is written into a file and a predefined executable file is called to calculate the axle spacings and weights. Once the processing is done, the weights are read from a file, displayed on the screen and, optionally, written to a CD7 file. The data exchange files between SiWIM and the external algorithm contain all the information needed to weigh vehicles. Thus, any weighing algorithm can be tested and used independently of the SiWIM program itself, as long as the program doing the weighing adheres to the standards set for the data exchange files.

If the internal algorithm is used, the pre-processed data is first processed with Moses' algorithm. The results are then used as initial parameters for the optimisation algorithm, which is based on Powell's multidimensional minimisation. Once the results are obtained, they are displayed on the screen and, optionally, written to a CD7 file.

5.3 Data exchange with external algorithm

The data exchange protocol was developed with the orthotropic deck B-WIM algorithm in mind, but the general principles will allow other external algorithms to be used.

5.3.1 Interaction with the external algorithm

The external algorithm must be provided in the form of a compiled stand-alone console application (i.e., no graphical output) and must be able to read parameters from the command line and read and write ASCII files. Assuming the path to the external algorithm is **C:\directory\extalg.exe**, the whole interaction can be divided into following steps:

1. Select unique input and output file names for the external algorithm, **C:\directory\Xchn000.SWD** and **C:\directory\Xchn000.EAD**, where **000** is a zero-padded three-digit serial number, which is increased by one for each invocation of the external algorithm. This means that up to 1000 instances of the external algorithm can be active at the same time (even though this is unrealistic).
2. Write captured data and parameters in ASCII format (see subsection 5.3.2 for details) to **C:\directory\Xchn000.SWD**
3. Call the external algorithm using the command line:
"C:\directory\extalg.exe C:\directory\Xchn000.SWD C:\directory\Xchn000.EAD"
4. Wait 1 second
5. If the external algorithm has been running for more than a specified amount of time (typically 5 minutes), assume it has crashed or gone into a loop. In this case delete files **C:\directory\Xchn000.SWD** and **C:\directory\Xchn000.EAD** if they exist and go to step 8
6. If file **C:\directory\Xchn000.SWD** exists, external algorithm is still running; go to step 4. If not, assume it has finished
7. If file **C:\directory\Xchn000.EAD** exists (see subsection 5.3.3 for details), read vehicle data from it and delete it
8. Exit

The external algorithm must follow the prescribed set of steps *in this order* to enable it to cooperate with SiWIM:

1. Read data from file **C:\directory\Xchng000.SWD**
2. Process data and calculate vehicle weights
3. Write vehicle data to file **C:\directory\Xchng000.EAD**
4. Delete file **C:\directory\Xchng000.SWD**

5.3.2 SiWIM data for external algorithm

Files used for data exchange are tab-delimited ASCII files. Currently the extension for files written by SiWIM is SWD, but is planned to be later change to SWX. As noted before, the format was designed for use with the orthotropic deck B-WIM algorithm, so the number of parameters, as well as the number of data channels written to the file is fixed. Data fields are shown in Table 2 and Table 3. Each line represents one line in the file and the fields (columns) are separated with tabs.

Table 2: SWD File Fields

sampling rate			
number of spans			
span length			
distance between section 2 and section 3			
software gain for Ch.1	software gain for Ch.2	...	software gain for Ch.16
sample 0, Ch.1	sample 0, Ch2	...	sample 0, Ch.16
sample 1, Ch.1	sample 1, Ch2	...	sample 1, Ch.16
...
sample M, Ch.1	sample M, Ch2	...	sample M, Ch.16

If necessary, in the later SiWIM versions it may be possible to specify and set an arbitrary number of parameters (in addition to the required parameters, such as the sampling rate). The user will also be able to name these parameters for easier input and they will be checked against the name of the external algorithm, so as not to mix parameters if more than one external algorithm is used:

Table 3: Planned SWX file fields

sampling rate			
number of channels, N			
number of extra parameters, P			
extra parameter 1			
...			
extra parameter P			
software gain for Ch.1	software gain for Ch.2	...	software gain for Ch.N
sample 0, Ch.1	sample 0, Ch.2	...	sample 0, Ch.N
sample 1, Ch.1	sample 1, Ch.2	...	sample 1, Ch.N
...
sample M, Ch.1	sample M, Ch.2	...	sample M, Ch.N

Another important improvement in the SWX format will be the format of data samples. Currently the data is written as raw integers directly from the data acquisition card. This poses a problem when a 16-bit data acquisition card with a range of ± 32768 (as opposed to 12-bit with a range of ± 2048) is used. In SWX format, the acquisition data will always be written as a floating-point value with a range of ± 1 , which will dispense with the problem.

5.3.3 External algorithm data for SiWIM

Similarly, the external algorithm must supply its data in an ASCII file. The file extension is EAD. The data is viewed as blocks of data, one block for each weighed vehicle. Data fields for M vehicles are defined in Table 4.

Later SiWIM will extend the file format to include overall and vehicle status information (Table 5). The first line of the file will be the overall status and each vehicle block will be preceded with status information for that vehicle. Each status line must begin with one of the keywords **OK**, **WARNING** or **ERROR**, followed by an optional message in case of warnings and errors. The message will be displayed in the SiWIM program and written to log file. Vehicles whose status is **ERROR** will not be displayed among the weighed vehicles. Examples: "**OK**", "**WARNING Low average speed (5km/h)**", "**ERROR Division by zero in routine calculate**".

Table 4: EAD file fields

Data for vehicle 1	lane
	class
	average speed
	GVW
	number of axles, N
	axle 1 weight
	...
	axle N weight
	spacing between axles 1 and 2
	...
spacing between axles N-1 and N	
Data for vehicle M	lane
	class
	average speed
	GVW
	number of axles, N
	axle 1 weight
	...
	axle N weight
	spacing between axles 1 and 2
	...
spacing between axles N-1 and N	

Table 5: EAX file fields

	overall status
Data for vehicle 1	status for vehicle 1
	lane
	class
	average speed
	GVW
	number of axles, N
	axle 1 weight
	...
	axle N weight
	spacing between axles 1 and 2
	...
	spacing between axles N-1 and N
	...
Data for vehicle M	status for vehicle M
	lane
	class
	average speed
	GVW
	number of axles, N
	axle 1 weight
	...
	axle N weight
	spacing between axles 1 and 2
	...
	spacing between axles N-1 and N

6. NEW APPROACHES AND ALGORITHMS

6.1 Optimisation Algorithms Developed for the Orthotropic B-WIM System

Most of the existing B-WIM algorithms prior to the WAVE project required precise estimates of the velocity and axle spacings in order to calculate axle and gross vehicle weights accurately (Moses, 1979; Dempsey, 1997). Most of the currently available systems use axle detectors placed on the road surface to acquire this information. However, for many reasons, which are outlined in Section 7, placing axle detectors on the road surface on orthotropic decks was not a viable option. Hence, a Free of Axle Detector (FAD) algorithm was developed (refer section 7) whereby the velocity, number of axles and axle spacings were all determined from the strain gauges underneath the bridge. At the time of development of these FAD algorithms, the authors recognised that the accuracy of the calculated axle spacings and velocity would not be as high as the more traditional methods, i.e., axle detectors on the road surface. In order, to allow for these errors in axle spacings and velocities, new algorithms were developed to calculate axle and gross vehicle weights, which was not sensitive to errors in velocities and axle spacings. These algorithms were based on optimisation techniques and are described below. Optimisation algorithms can be applied to conventional as well as FAD B-WIM systems to improve the accuracy of calculated weights. However, in this section, they will be discussed only in the context of a FAD system on an orthotropic bridge.

In any optimisation problem, initial values of the optimisation parameters must be obtained prior to commencing the optimisation process. For the Orthotropic B-WIM optimisation problem, initial values for the velocity, axle numbers and spacings and position of the axles were determined from the FAD algorithm, i.e., from the strain gauge data. Initial values for the axle weights must also be chosen. The identification problem can be defined as the optimisation of an objective function, which is the sum of squares of differences between the measured bending moments and the expected (modelled) bending moments, in order to determine the trucks parameters. To facilitate real time running of the algorithm on an orthotropic bridge, the trucks were assumed to travel in the centre of the lane and the longitudinal stiffeners are modelled as a continuous beam spanning between the transverse crossbeams. The following truck parameters were included in the optimisation: number of axles, velocity, axle spacing, axle weights and a parameter which aligns the measured response with the modelled response. Hence, the optimisation problem can be defined as:

Minimise

$$O(y) = \sum_{i=1}^K [M(x_i) - M^M(x_i)]^2 \quad (1)$$

to find

$$\{y\} = \{v, L_1, L_2, \dots, L_{n-1}, z, A_1, A_2, \dots, A_n\} \quad (2)$$

where $O(y)$ is the objective function, i is the scan number, x_i is the distance of the first axle from some specified reference position on the bridge (x_i is discretised by virtue of the scanning frequency of the data acquisition system), K is the number of recorded strains during the passage of

the truck, $M(x_i)$ is the calculated moment (obtained from the model) at an instrumented section when the first axle of the truck is at position x_i , $M^M(x_i)$ is the measured moment at an instrumented section when the first axle of the truck is at position x_i , v is the velocity of the vehicle, L_1 , L_2 , and L_{n-1} are the axle spacings between the first and second, second and third and $(n-1)^{\text{th}}$ and n^{th} axles respectively, z is a distance parameter which relates the position of the measured and theoretical response of the truck to each other and A_1 , A_2 and A_n are the weights of the first, second and n^{th} axle respectively. The number of axles, n , is determined from the FAD algorithm described in section 7.

6.1.1 Choice of Optimisation Procedure

Optimisation methods known as gradient methods, which require the calculation of first and second derivatives, were considered as they are generally computationally more efficient than those which only use the evaluation of the function. However, although there is a decrease in computation time with gradient methods; this time saving does not always compensate for the additional time required to calculate the derivatives. More importantly, it is not always possible to calculate the first and second derivatives of the objective function as the function is not everywhere continuous and there are numerical problems that can arise when the objective function is non-convex. Therefore, it was decided to use a method that only evaluated the objective function. Of all these methods, 'direction set' methods, of which Powell's is the prototype, are the most efficient in finding the correct minima of an objective function. This is due to the fact that, unlike other methods such as the *downhill simplex* method, which just crawls in a straightforward fashion downhill, direction set methods take into account the shape and form of the objective function. One of the principle advantages of these methods is that they are extremely robust.

The idea of all direction set methods is that, as the algorithm proceeds, it updates the directions in which to search, attempting to develop a set of directions which includes some very good ones that take into account the shape of the objective function. Some direction set methods generate directions which include a number of "non-interfering" directions with the special property that minimisation along one direction is not spoiled by subsequent minimisations along another. Methods such as this are generally called *conjugate directions methods*, and Powell was the first to use them (Press et al. 1992). Therefore, Powell's method was chosen as the optimisation routine for the OB-WIM algorithm.

6.1.2 Determination of Constraints for Optimisation

The FAD algorithm identifies the number of axles of the truck and therefore only one objective function has to be optimised per truck event in order to determine all of the truck parameters. The velocity and axle spacings calculated from the FAD algorithm are used as input parameters for the optimisation algorithm, as the speed of the optimisation process is greatly increased if the initial values of the parameters are close to the actual (optimal) values. However, it was unknown if these initial values would result in the correct minimum being found. Furthermore, if the axle weights are considered, there were no initial values to assign at the start of the optimisation. Also, it was unknown what effect these values would have on the entire optimisation process. Therefore, in order to determine a suitable controlled optimisation procedure to accurately calculate the truck parameters, the shape and nature of the objective function had to be examined. This was used to decide if constraints were needed for any of the optimisation parameters and what initial values should be adopted for the axle weights. In order to achieve this, the Hessian matrix was calculated for the ob-

jective function and studies were conducted to analyse the shape of the objective function with respect to the truck parameters.

6.1.3 Calculation of the Hessian Matrix

The Hessian matrix of a function is often used as a tool to examine the convexity of that function. A function $f(x)$, is said to be convex if the Hessian matrix:

$$H(x) = \frac{\partial^2 f(x)}{\partial x_i \partial x_j} \quad i, j = 1 \dots \text{number of parameters} \quad (3)$$

of that function is positive semi-definite (Rao, 1984). If an objective function is convex, this means that Powell's optimisation procedure will find the correct values of the optimisation parameters regardless of their initial values. If the Hessian matrix is not convex, this means that there are multiple or infinite solutions for the optimisation parameters.

For this study, two objective functions were considered, one which modelled a 2-axle rigid truck on a simply supported beam and the second, the same rigid 2-axle truck on a continuously supported beam. The continuously supported beam closely models the behaviour of the longitudinal stiffener on the orthotropic deck. Initially, only the axle spacings and axle weights were considered as parameters of the objective function. The objective function for the 2-axle rigid truck on the simply supported beam is described as:

$$O(A_1, A_2, L) = \sum_{i=1}^K [M(x_i) - M^M(x_i)]^2 \quad (4)$$

The Hessian matrix of this function is described as:

$$\begin{bmatrix} \frac{\partial^2 O}{\partial A_1^2} & \frac{\partial^2 O}{\partial A_1 \partial A_2} & \frac{\partial^2 O}{\partial A_1 \partial L} \\ \frac{\partial^2 O}{\partial A_2 \partial A_1} & \frac{\partial^2 O}{\partial A_2^2} & \frac{\partial^2 O}{\partial A_2 \partial L} \\ \frac{\partial^2 O}{\partial L \partial A_1} & \frac{\partial^2 O}{\partial L \partial A_2} & \frac{\partial^2 O}{\partial L^2} \end{bmatrix} = \begin{bmatrix} 2 \sum_{i=1}^K I^2(x_i) & 2 \sum_{i=1}^K I(x_i)I(x_i - L) & \sum_{i=1}^K -A_2 I(x_i) \\ 2 \sum_{i=1}^K I(x_i)I(x_i - L) & 2 \sum_{i=1}^K I^2(x_i - L) & \sum_{i=1}^K -A_1 I(x_i) - 2A_2 I(x_i - L) \\ \sum_{i=1}^K -A_2 I(x_i) & \sum_{i=1}^K -A_1 I(x_i) + A_2(L - x_i) & \sum_{i=1}^K \frac{A_2^2}{2} \end{bmatrix} \quad (5)$$

where $I(x_i)$ is the mid-span bending moment influence line for a simply supported beam and is defined as:

$$I(x) = x / 2 \quad 0 \leq x \leq L / 2 \quad (6)$$

$$I(x) = (L - x) / 2 \quad L / 2 \leq x \leq L \quad (7)$$

Evaluating this Hessian matrix for a particular 2-axle truck (front axle weight = 50 kN, second axle weight = 100 kN, axle spacing = 5 m) travelling at 20 m/s on a 20 m span bridge, it was found that the Hessian matrix was positive semi-definite. The same analysis was then conducted for the 2-axle truck travelling on a continuously supported bridge. The only parameter which changes in the above system of equations, is the influence line, which for moment at the centre of a 5-span continuously supported beam, can be defined as:

$$\begin{aligned}
I(x) &= 2.5IR_{11} + 1.5IR_{21} + 0.5IR_{31} - (2.5L - b) & 0 \leq x \leq L \\
I(x) &= 2.5IR_{12} + 1.5IR_{22} + 0.5IR_{32} - (2.5L - b) & L \leq x \leq 2L \\
I(x) &= 2.5IR_{13} + 1.5IR_{23} + 0.5IR_{33} - (2.5L - b) & 2 \leq x \leq 2.5L \\
I(x) &= 2.5IR_{13} + 1.5IR_{23} + 0.5IR_{33} & 2.5 \leq x \leq 3L \\
I(x) &= 2.5IR_{14} + 1.5IR_{24} + 0.5IR_{34} & 3L \leq x \leq 4L \\
I(x) &= 2.5IR_{15} + 1.5IR_{25} + 0.5IR_{35} & 4L \leq x \leq 5L
\end{aligned} \tag{8}$$

where L (in this case) represents the distance between two successive supports on the continuously supported beam, R_{ij} is the reaction in the i^{th} support due to a load in the j^{th} span. The reactions, R_{ij} , can be calculated by solving the system of equations (for the load in each span):

$$[R] = \{f\}^{-1}[-D] \tag{9}$$

where

$[R]$ is the matrix of reactions in the supports of the continuous beams,

$\{f\}$ is the flexibility matrix,

$[D]$ is a matrix which represents the deformation inconsistencies of the structure when using the force method of analysis.

Once again, the Hessian matrix was evaluated for the same 2-axle truck (front axle weight = 50 kN, second axle weight = 100 kN, axle spacing = 5 m) travelling at 20 m/s for this continuously supported beam (spans = 4.62 m). However, this time the Hessian matrix was found to be negative semi-definite. Therefore, it was evident that there is only one minimum for the objective function for the simply supported beam (the objective function is perfectly convex) and multiple minima for the continuous beam objective function. Therefore, for the continuously supported case (which idealises the mid-span response of the longitudinal stiffener, which is supported every 4.62 m by transverse crossbeams) the value of the parameters at the minimum, which are found by the optimisation algorithm, are dependent on the initial values of those parameters. This means that the optimisation process has to be controlled or constrained, i.e., the optimisation process is only allowed to search for solutions in user-defined regions. It has to be stressed that only three of the optimisation parameters, the two axle weights and the axle spacing, showed that the objective function was non-convex for a continuously supported beam. This in fact illustrates the complexity of the optimisation problem, as the objective function is non-convex even when many other of the optimisation parameters were not included in the analysis.

6.1.4 Determination of Constraints for Optimisation

Velocity

The objective of this study was to determine which if any of the optimisation parameters had to be constrained. At the outset of this study, the authors felt that one of the most important parameters in the optimisation process was considered to be the velocity. Therefore, theoretical studies were conducted to determine the influence on the objective function of variations in velocity and other optimisation parameters. Figure 16 shows a contour map of the objective function of a 2-axle truck on a continuously supported beam for variations in velocity and axle spacing. It is evident from the contour map that if these two parameters are allowed to vary without constraints in the optimisation process, there are multiple minima for the objective function. However, it is observed that if the ve-

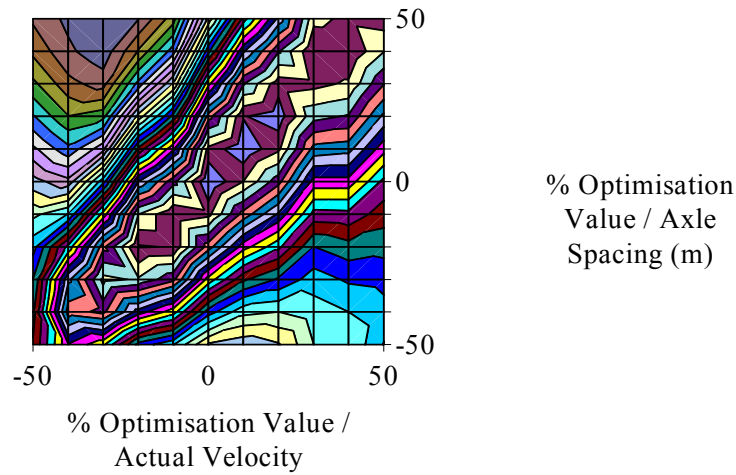


Figure 16: Contour map of objective function for variations in axle spacing and velocity (2-axle truck)

velocity parameter is constrained from varying by $\pm 5\%$ then the true minimum will be found. The same result was found for other truck objective functions.

Axle Weights

Two different objective functions were used in this theoretical study. The first represented a 2-axle truck crossing the instrumented section of the bridge (which was modelled statically as a 1-dimensional continuous beam). The second objective function represented a 5-axle semi-trailer crossing the instrumented section. Initially, the sensitivity of the axle weights for the 2-axle objective function was examined. Figure 17(a) illustrates the shape of the objective function for variations in these two axles. It is evident from the graph that the function is convex and therefore, if all the other parameters are known, the correct values of the axle weights will be calculated. This is, in fact, Moses' original B-WIM algorithm. Figure 17(b) shows the shape of the 5-axle objective function for variations in the first and fifth axle weight.

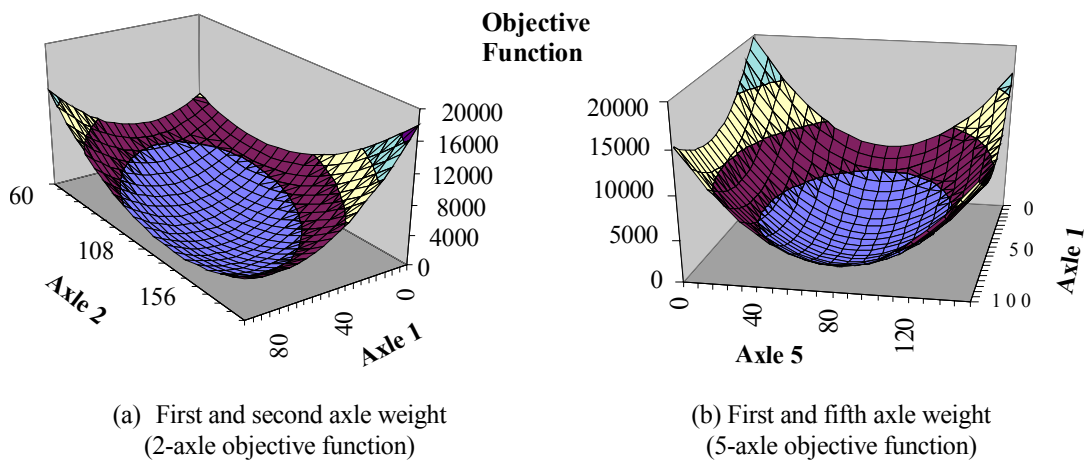


Figure 17: Objective function versus axle weights

It is evident from these graphs that the correct values of the axle weights for the five-axle truck will also be found if all the other truck parameters are approximately known. Therefore, there is numerically no need to place any constraints on the axle weights. The optimisation procedure can and does search in areas where the axle weights are negative and still finds the correct solution.

Axle Spacings

Once again the two different objective functions were examined. In Figure 18, all of the truck parameters for the 2-axle rigid truck were frozen except for the weight of the first axle and the axle spacing. The objective function was then evaluated for different values of these two parameters. In Figure 19 (a) and (b), the objective function for the 5-axle truck was evaluated for variations in the first and second axle spacing and first axle spacing and second axle weight. The presence of multiple minima is clearly evident from these two graphs, indicating that finding the correct minimum and therefore, the correct truck parameters, depends on the region in which the optimisation process starts. If there is a good initial estimation of the truck axle spacings, then the correct axle spacings and other truck parameters will be found. In order to determine *how good this initial estimate* should be, it was necessary to find the upper and lower limits of the axle spacing parameters, between which the correct value of the axle spacing would be found.

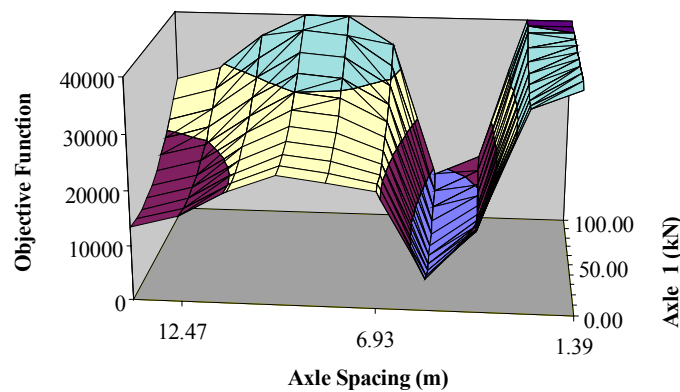


Figure 18: Variation of objective function with first axle weight and axle spacing (2-axle truck)

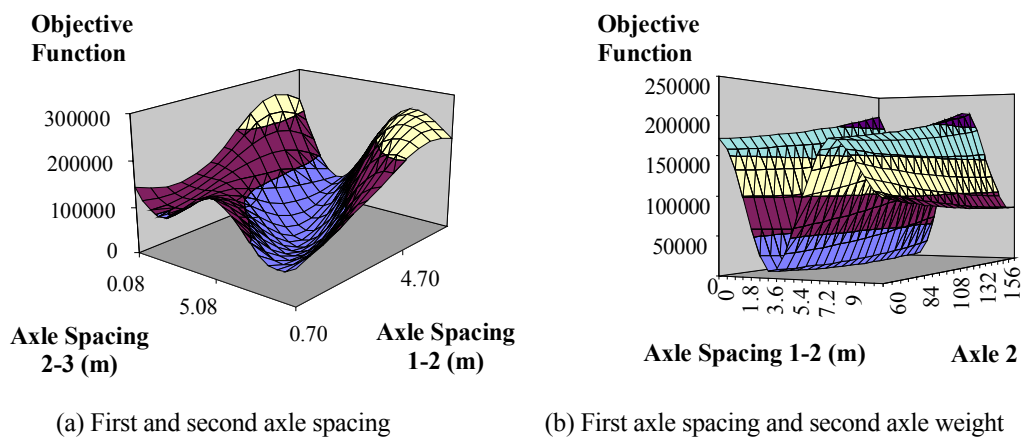


Figure 19: Variation of objective function with various parameters (5-axle truck)

Theoretical Study to Determine the Upper and Lower Limits for the Axle Spacing Parameter

A series of two-axle trucks (front axle weight = 50 kN, second axle weight = 100 kN) were used in this study. The axle spacing varied from 0.8 m to 9.6 m. The bending moment response of the bridge was calculated for each of the trucks. Figure 20(a) shows the static bridge response to five of these trucks with axle spacings ranging from 5.6 m to 9.6 m. Other bridge responses for the other axle spacings were calculated but are not shown here. The next step for each of the trucks was to evaluate the objective function for a range of axle spacings. This is illustrated in Figure 20(b). It is clear to see that, for example, considering the 5.6 m axle spacing truck objective function, the absolute minimum occurs when the correct axle spacing is input into the objective function. The objective function is also evaluated for other values of axle spacings, which are incorrect, in order to determine the shape of the objective function and the upper and lower limits of the axle spacing which will find the correct minimum in the optimisation process. If the initial value of the axle spacing in the optimisation process is between these two limits, the correct axle spacing will be determined. It is evident from the graph that the lower and upper bound values for the 5.6 m axle spacing truck objective function are 0.98 m and 10.22 m respectively. These are the values of the axle spacings, which correspond to the two maxima shown on the 5.6 m curve. The same process is repeated for all of the other trucks, so that the upper and lower bounds for a range of axle spacings can be determined.

From the evaluation of these objective functions, it was evident that the distance between the upper and lower bounds for each of the trucks was approximately the same, i.e., in optimisation terms, the width of the valley is the same for all of the trucks. Upon further analysis, it was determined that this distance was approximately equal to twice the distance between two successive cross beams. This is quite a relevant finding as it means that the width of the optimisation valley is governed by the type of orthotropic bridge deck construction and not by the truck configuration. This is important, as the bridge remains the same, but the truck configurations which cross it, are different. Once the upper and lower limits of the axle spacing optimisation parameters had been determined for each axle spacing, a graph was constructed to show the regions, for a variety of different axle spacings, in which an axle spacing optimisation parameter will find the correct value. This is illustrated in Figure 21. The three upper curves represent the upper bound limit values for the initial values of the axle spacings. One represents the upper bound curve, if there is no velocity error, while the other two represent the curve, if there are errors of $\pm 5\%$ in the velocity. Similarly, the three lower curves on the graph represent the lower bound values for initial estimates of the axle spacings. Therefore, if an initial estimate of axle spacing is above or below these limit curves, the optimisation procedure will not find the correct value of the axle spacing. It is interesting to note on the graph the axle spacings, as calculated by the FAD algorithm (see Section 7). All of these initial estimates lie between the upper and lower limit curves.

This was quite an important finding as it meant that the initial estimation of axle spacing was accurate enough and therefore there was no need for any constraints to be placed on the axle spacing optimisation parameters.

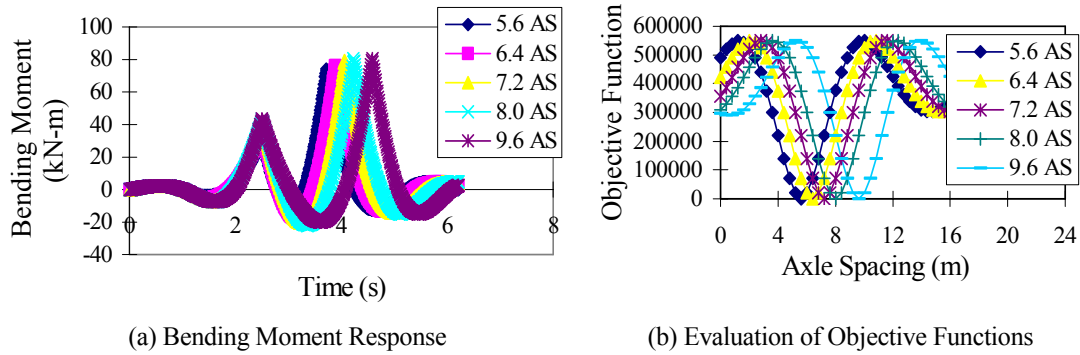


Figure 20: Theoretical study to evaluate the upper and lower limits on axle spacing

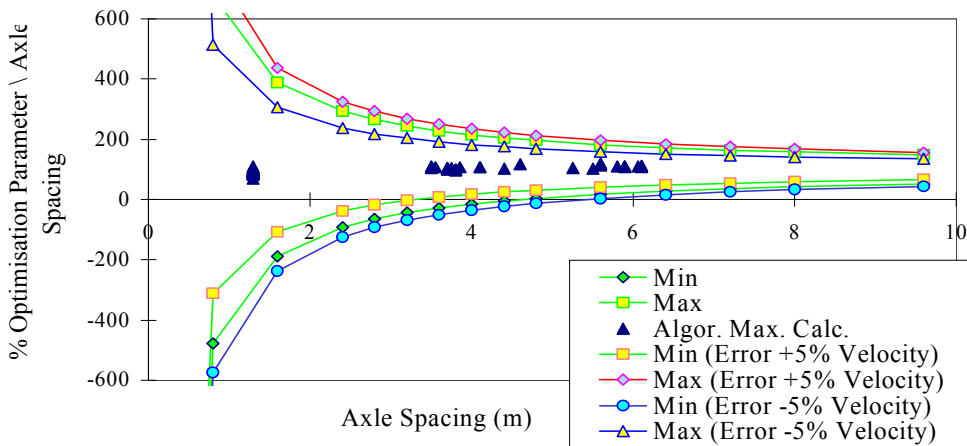


Figure 21: Upper and Lower Bounds on Axle Spacing Optimisation Parameter

Alignment

The next parameter to be examined was the z -parameter, which is an alignment parameter between the measured and theoretical bridge responses. However, after initial studies, it was determined that if the three variables, the velocity, axle spacing and the alignment of the measured and modelled response, were all allowed to vary, there were an infinite number of solutions, even within a relatively localised region. As an example of this, Figure 22 shows the shape of the objective function for variations of velocity and this alignment parameter. It is clear to see that there are multiple minima for this case. If the axle spacings were also allowed to vary in this analysis, although this cannot be visualised graphically, the number of solutions increases dramatically.

As a result, it was decided not to allow the alignment parameter to vary in the optimisation procedure. Therefore, before the start of the optimisation process, the measured and modelled response of the bridge was aligned by ensuring that the first peaks of both responses occurred at the same

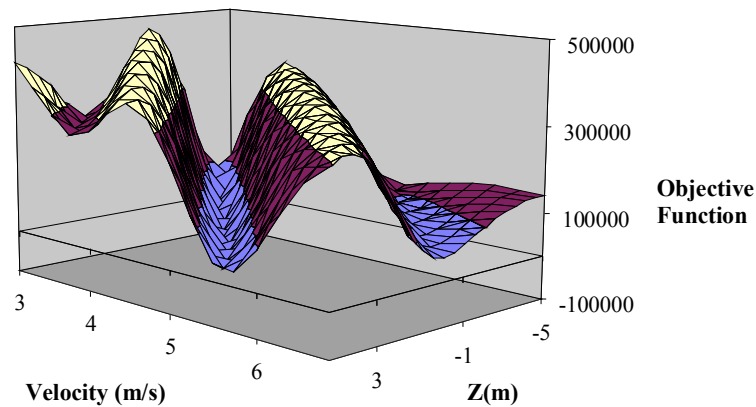


Figure 22: Evaluation of the objective function for variations in velocity and alignment parameters

longitudinal location. However, in practice, it would not always be certain that the correct alignment of the two peaks would be obtained. In this case, there would be small errors in the alignment. In order to determine the sensitivity of the truck parameters to errors in alignment, the following analysis was conducted: a two-axle truck was modelled crossing the bridge and the static response of the bridge was calculated and deemed to be the ‘measured’ data. In this analysis, both the ‘measured’ and the modelled responses were the same. Therefore, when the correct alignment was used in the analysis, no errors were found in the truck parameters. The alignment parameter z , was then varied by ± 0.2 m in steps (i.e., the alignment of the measured and theoretical bridge response was varied) and the optimisation was performed for each step. In fact it was determined that for a truck travelling at 20 m/s and a recording rate of 200 Hz, the absolute maximum error of the alignment parameter would be 0.1 m.

The conclusion of this study was that, for the maximum likely misalignment of the theoretical and measured responses, i.e., 0.1 m, the errors in axle weights, velocity and axle spacings are not significant (less than 0.5%, 1% and 1% respectively, Figure 23). It was important that the resulting error in velocity was less than the 5% constraint on the velocity calculation.

6.1.5 Guidelines for Control of Optimisation Parameters

Having completed these studies, the following guidelines were proposed for the optimisation algorithm for Orthotropic Bridges:

- The number of axles was calculated from the FAD algorithm and this determined the number of parameters for the optimisation process, i.e., the objective function formula is determined.
- The initial values for the optimisation process were generated: the velocity was determined from the Separate Velocity Optimisation Procedure (SVOP) to an accuracy of within $\pm 5\%$.
- The initial values for the axle spacings were calculated for the FAD algorithm and the calculated velocity.
- The initial weight of the axles has been shown not to be critical. The initial value for each axle weight is chosen to be 30 kN.

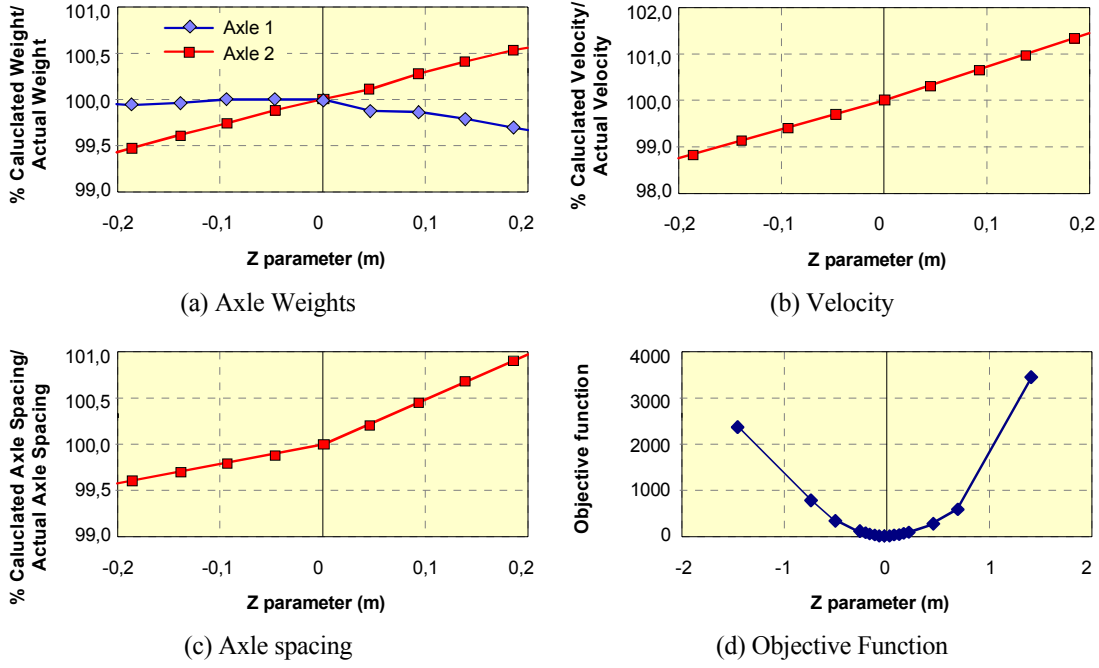


Figure 23: Sensitivity of truck parameters to misalignment of theoretical and modelled bridge responses

- The only constraints that are used in the optimisation are that the velocity is not allowed to vary greater than $\pm 5\%$ from the initial value. If the velocity exceeds these limits then a penalty function is applied to the objective function, which dramatically increases the value of the objective function and thus prevents the optimisation process from searching further in this area.

The optimisation procedure can now be defined as:

With initial parameters estimates:

$$y = \{v^*, L_1^*, L_2^*, \dots, L_n^*, A_1^*, A_2^*, \dots, A_n^*\}$$

Minimise:

$$O(y) = \sum_{i=1}^K [M(x_i) - M^M(x_i)]^2$$

to find:

$$y = \{v, L_1, L_2, \dots, L_n, A_1, A_2, \dots, A_n\}$$

where n is known.

If $0.95(v^*) < v < 1.05(v^*)$ then

Minimise:

$$O(y) = \sum_{i=1}^K [M(x_i) - M^M(x_i)]^2 + k(v - v^*)^2$$

where:

k is a constant defined by the user,

y^* indicates the initial estimate of parameter y at the start of optimisation.

6.1.6 Identification Algorithm

Once the requirements for the optimisation procedure had been determined, the identification algorithm was developed. It is summarised briefly in this section and illustrated in Figure 24:

- The FAD algorithm identifies the presence of a vehicle by monitoring the strain gauge in the first instrumented section. Once the strain exceeds a certain threshold limit, a vehicle occurrence is identified, and the recording of strain in the other two instrumented sections is initiated.
- Using the recorded strains from sections 2 and 3 and the Separate Velocity Optimisation Procedure (SVOP), the truck velocity is determined.
- The FAD algorithm then identifies the number of axles and axle spacings. If the FAD algorithm fails to identify a truck event, even though the strain in the first instrumented section is greater than the threshold value, the recorded strains are then stored in a file for post-processing.
- The number of axles determined the number of parameters in the optimisation procedure and the values calculated from the FAD algorithm for axle spacings are used as the initial values in the optimisation process. Likewise, the velocity calculated by the SVOP is used as the initial value for velocity in the optimisation process. The initial values of the axle weights, as stated earlier, are not critical and have been chosen at 30 kN.
- The theoretical and measured responses of the truck are aligned prior to any optimisation by ensuring that the first peaks of the measured and the modelled response curves occur at the same longitudinal location.
- The optimisation procedure then calculates the truck parameters as described in section 6.1.5.
- After each iteration of Powell's method, the alignment of the theoretical and measured responses are checked and if necessary, they are realigned.

The optimisation procedure finishes when, for one iteration, the change in the values of the parameters is less than a specified tolerance. In some cases, the peak algorithm fails to clearly identify the number of axles of a truck or there is some doubt as to the axle configuration determined by the FAD algorithm (i.e., the configuration does not fall into some well accepted vehicle classification (COST 323 1997)). It has been found by analysing experimental data that the FAD algorithm has problems in identifying closely spaced unloaded axles. In such a case, a 6-axle truck objective function is applied to determine the truck parameters. The assumption in this is that, if there are in reality fewer than 6 axles, the optimisation will assign zero weight to the non-existent axles.

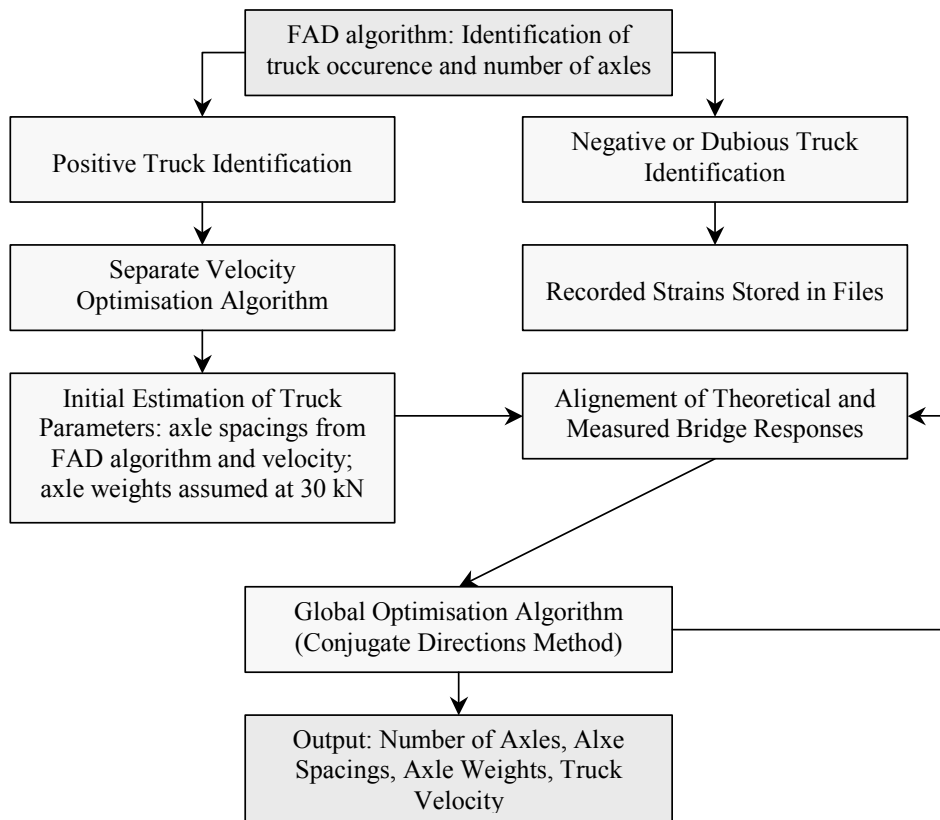


Figure 24: Flowchart for Identification Algorithm

6.1.7 Optimisation Algorithm for 2-Dimensional Bridge Model

One of the experiments conducted on the Autreville bridge involved calculating the influence lines for different longitudinal stiffeners. These measurements can be used to determine the influence that different transverse locations of truck can have on the response of the bridge. In the Autreville bridge, the stiffened steel plate spans longitudinally onto transverse cross beams. These in turn are supported by two large longitudinal main beams, one on each side (Figure 25). In the measurements it was observed that the amplitude of the response on the soffit of the longitudinal stiffeners depended on the position of the truck relative to the main longitudinal beams. The stiffeners close to the main beam were less strained than those which were further away from it; clearly some load was being taken directly by this beam. Therefore, it was evident that, if there were variations in the transverse positions of trucks, the accuracy of the calculated axle weights would be affected. The extent of the final inaccuracy is quantified in section 8.1.2.

In order to overcome this problem, an optimisation algorithm based on a two-dimensional bridge model was developed.

Finite Element Model of the Autreville Bridge

The Orthotropic B-WIM algorithms were tested on a typical bridge of this type in NE France, the Autreville Bridge. In order to simulate wheel loads on a small portion of the Autreville bridge, i.e.,

the two instrumented sections, it was necessary to create a finite element model (FEM) of the whole bridge. The first step in modelling the bridge was to calculate the properties (area, reduced area, second moment of area, torsional inertia etc.) for each part. There are essentially four main parts of the bridge, the main longitudinal beams, longitudinal stiffeners, transverse cross beams and the orthotropic plate (Figure 25). The entire three spans of the bridge were modelled using a FEM package, CESAR (Humbert, 1989). The central span of the bridge was then modelled more accurately. The boundary conditions (at the two supports) for this model were obtained from the model of the whole bridge. Figure 25 illustrates the FEM of the central span. The same truck load, which was applied in the first analysis, was applied and the differences in the stresses of both models were found to be small. The model was further refined so that only 6 sections of the central span were represented. The boundary conditions were determined from the central span model. Figure 26 shows the detailed mesh for one of the instrumented sections in the model.

The first analysis, which was conducted on this FEM of the six central sections of the bridge, was to calculate the transverse influence line for each of the longitudinal stiffeners, using a two-axle deflectograph truck. A very fine mesh was constructed so that the weight of the truck could be simulated as tyre loads. The lateral position of the truck was varied across the width of the slow lane (in steps of 5 cm and for 29 positions in total). The stress at the bottom of each longitudinal stiffener was calculated for each of the 29 positions, so that the transverse influence line could be constructed for each stiffener. An analysis was also conducted to determine the effect of varying the transverse location of the load on the boundary condition values, which were applied to the model. The results of this analysis indicated that there were no significant changes in these values. Therefore, the stress in each of the longitudinal stiffeners for each different truck position and the transverse influence line for the stress in each stiffener was obtained. Figure 27(a) shows the transverse stress distribution at the instrumented section of the bridge for the two extremes of truck position (transversely). Figure 27(b) shows a transverse influence line for one longitudinal stiffener.

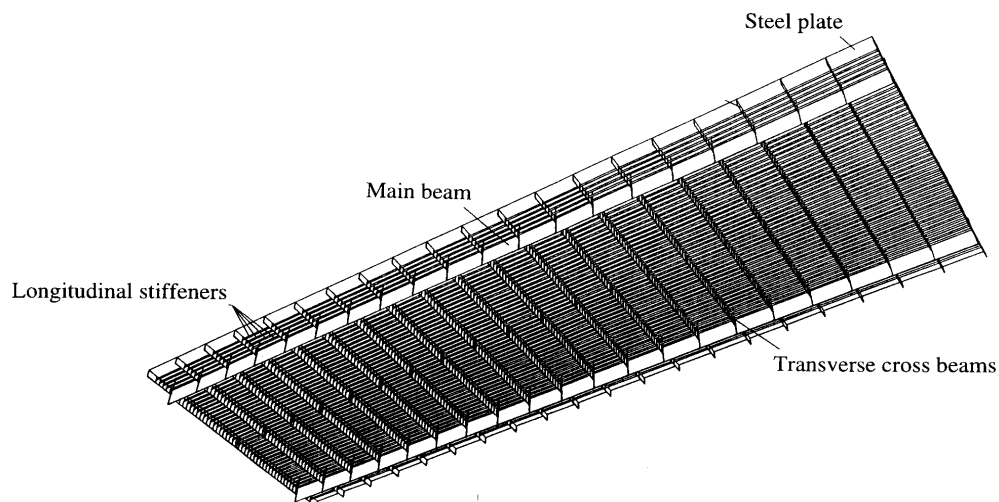


Figure 25: FEM mesh for the central span of the Autreville bridge

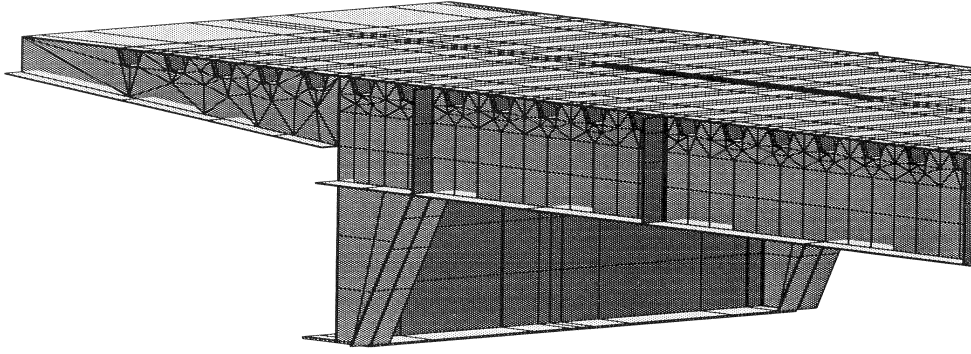


Figure 26: FEM mesh for one instrumented section of the Autreville bridge

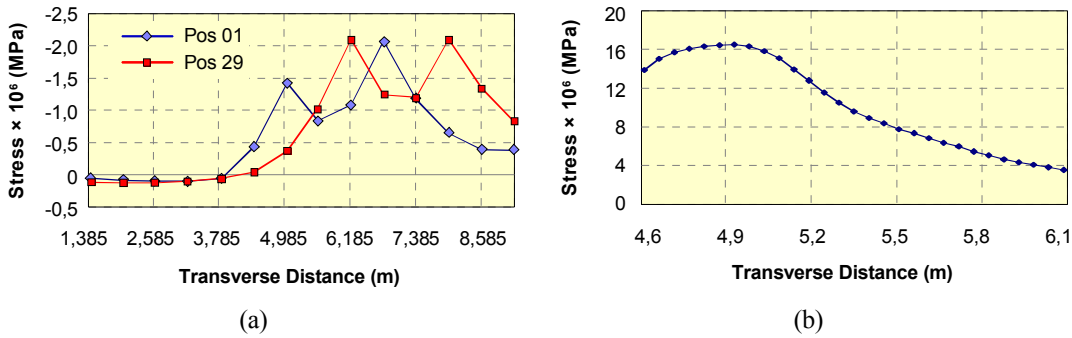


Figure 27: Effect of lorry transverse position on calculated stresses: (a) stress on the soffit of the longitudinal stiffeners for positions 1 and 29 of the front axle of the truck; (b) transverse influence line for one longitudinal stiffener

In extending the optimisation algorithm from a one-dimensional bridge model to a two-dimensional bridge model, instead of requiring one influence line for the complete bridge, an influence line for each of the longitudinal stiffeners is required. These influence lines were determined from a combination of the experimental work conducted for constructing influence lines and from the FEM just described. Spline interpolation was used to determine the transverse influence line ordinates for points which were not located at the discrete points. The optimisation algorithm was also extended to incorporate a 2-dimensional bridge model. This model was based on the fact that each longitudinal stiffener has an influence surface, which can be compared to the measured response. The optimisation problem can thus be defined as follows:

Minimise

$$O_{CDM-2D}(y) = \sum_{j=1}^S \sum_{i=1}^K [M_j(x_i) - M_j^M(x_i)]^2 + k|y - y_o|^2$$

to find

$$\{y\} = \{v, L_1, L_2, \dots, L_m, A_1, A_2, \dots, A_n, t\}$$

where S is the number of instrumented stiffeners, k is a constant, t is the transverse location of the truck and y_0 represents the initial values of the optimisation parameters. The improvement in the accuracy of the calculated axle weight is reported in section 7.

6.1.8 Conclusion on Orthotropic B-WIM Optimisation Algorithms

The *WAVE* research described in this section is important for two reasons, the Orthotropic B-WIM application and the optimisation approach. Orthotropic Bridges are an important application area for WIM. As it is made from steel, this bridge type is prone to fatigue damage and there are indeed a number of examples across Europe of orthotropic bridges where repair and monitoring costs are very high. The development of a B-WIM system that can be used to assess loading on this type of bridge is of great benefit to the industry and has considerable commercial potential. In addition, there is considerable potential for Orthotropic B-WIM systems to be used as general WIM systems. The fact that the system is completely free of axle detectors (FAD) is of great significance as its installation and maintenance requires no road closures with consequent improvements in safety and traffic disruption.

The second major significance of the research described in this section is that it demonstrates a means by which optimisation can be used to determine better fits between measured and modelled strains. This same principle is likely to be incorporated into all B-WIM systems in the future as it has the potential to,

- reduce the required accuracy of or completely remove the need for axle detection,
- improve the accuracy of B-WIM systems,
- allow for automatic calibration of B-WIM systems using pre-weighed lorries without any requirement for an understanding of bridge behaviour.

A first Free of Axle Detector B-WIM system has been described in this section for orthotropic bridges; the precursor to work described in Section 7. Further, the use of full 2-dimensional bridge models is developed; another feature that is likely to be incorporated into general B-WIM systems in the near future.

6.2 Multiple-Sensor Static B-WIM Algorithm

Another theoretical approach to B-WIM that was developed in WP1.2 was to use multiple sensors longitudinally on the bridge, modelled using a static algorithm. This approach was developed theoretically and a number of experimental tests were carried out. Instantaneous calculation of axle and gross weights is shown to be theoretically possible provided the equations relating strains to weights are not dependent. This is shown to be possible for two-axle trucks in single-span bridges and for three-axle trucks in two-span bridges. The experimental trial demonstrates some of the features of the system and is a useful indicator of where further research is needed.

6.2.1 Introduction to Multiple-Sensor Static B-WIM

The concept of B-WIM has considerable potential for accuracy as it makes possible the measurement of impact forces over more than one eigenperiod of lorry and axle vibration. As bridges are large, a great number of sensor readings can be recorded during the time it takes for a lorry to cross. Full exploitation of this data can be used to gain information on the dynamic behaviour of the truck

whose axle weights are being sought. This in turn can be used to obtain a more accurate estimate of the static axle weights.

6.2.2 Theory of Multiple-Equation B-WIM Systems

A method is developed for improving the accuracy of B-WIM systems through the measurement of strain (proportional to moment) at more than one location longitudinally along the bridge in order to obtain more equations relating strains to axle weights. Conventional B-WIM systems involve the recording of strain at one longitudinal location only. The theoretical strain at such a location, ϵ_A , is a function of the influence line and the axle weights:

$$\epsilon_A(x) = A_1 I_A(x) + A_2 I_A(x-L_1) + A_3 I_A(x-L_2) + \dots + A_n I_A(x-L_{n-1}) \quad (10)$$

where:

$\epsilon_A(x)$ = theoretical strain at A when the first axle is at a distance x from the start of the bridge,

A_1, A_2, \dots, A_n = axle weights,

n = number of axles,

$I_A(x)$ = influence function (strain at A due to unit load at a distance x from the start of the bridge) and,

L_1, L_2, \dots, L_{n-1} = distances of axle numbers 2, 3, n respectively from axle No. 1.

Strain is recorded at high frequency as a truck crosses the bridge and several equations of the form of equation (10) can be written. As there are generally more equations than unknown axle weights, the best-fit solution is generally chosen, i.e., the axle weights which minimise:

$$O = \sum_{i=1}^K \{\epsilon_A^M(x_i) - \epsilon_A(x_i)\}^2 \quad (11)$$

O = objective function

K = number of measurements

$\epsilon_A^M(x_i)$ = measured strain when the first axle is at a distance x_i from the start of the bridge

Individual axle weights are summed to determine the gross vehicle weight. A major source of inaccuracy in B-WIM systems results from truck bouncing and rocking motions. Different forces are applied by an axle to the bridge when it is at different points along it. This affects the measured strains and is not accounted for in equation (10).

The problem of axle bouncing and rocking motions is addressed in this approach through the use of measured strains at a number of different longitudinal locations along a bridge. If strain were measured at n different longitudinal locations and n independent equations of the form of equation (10) could be applied, then all n axle weights can be calculated for each value of x_i , i.e., an instantaneous calculation of axle weights would be possible. This would solve the problem of varying axle forces by providing a complete history of such forces as the truck crossed the bridge. Unfortunately, while it is possible to measure strain at many different longitudinal bridge locations, the resulting equations are not always independent.

Single-Span Bridge

A single-span simply supported bridge is considered first with two longitudinal sensor locations. The influence function for strain at a distance a from the start of such a bridge is given by:

$$I(x) = \begin{cases} \frac{a(l-x)}{EZl} & \text{for } a \leq x \\ \frac{x(l-a)}{EZl} & \text{for } a > x \end{cases} \quad (12)$$

where:

- a = distance of strain gauge location from start of bridge,
- l = span of bridge,
- x = distance of unit load from start of bridge,
- E = modulus of elasticity,
- Z = section modulus (relating moment to stress).

If there are two longitudinal sensor locations, there will be two equations of the form of equation (10). For a two-axle truck, an instantaneous calculation can be carried out by substituting the measured strains for the theoretical to give:

$$\begin{aligned} \varepsilon_A^M(x) &= A_1 I_A(x) + A_2 I_A(x-L_1) \\ \varepsilon_B^M(x) &= A_1 I_B(x) + A_2 I_B(x-L_1) \end{aligned}$$

These can be expressed in matrix form as:

$$\begin{Bmatrix} \varepsilon_A^M \\ \varepsilon_B^M \end{Bmatrix} = \begin{bmatrix} I_A(x) & I_A(x-L_1) \\ I_B(x) & I_B(x-L_1) \end{bmatrix} \begin{Bmatrix} A_1 \\ A_2 \end{Bmatrix} \quad (13)$$

Equations (13) can be solved for A_1 and A_2 if and only if the determinant of the matrix is non-zero, i.e., if $D \neq 0$ where:

$$D = I_A(x)I_B(x-L_1) - I_B(x)I_A(x-L_1) \quad (14)$$

When both axles are before the first sensor location or after the second sensor location, substitution of equation (12) into equations (14) gives a determinant of zero. Thus, the equations are dependent and an instantaneous calculation of axle weights is not possible. However, when both axles are between the sensors, equation (14) reduces to:

$$D = ll_1$$

where l is the bridge span length and l_1 is the length between the axles. This is clearly non-zero and an instantaneous calculation is indeed possible.

A simply supported bridge with three longitudinal sensor locations was also investigated. It was found that, for all possible truck locations, two of the equations were dependent. Thus, for a simply supported bridge, only two independent equations are possible and simultaneous calculation of axle weights is only possible for 2-axle trucks.

Two-span bridge

A two-span bridge with two equal spans was also investigated. Five possible longitudinal sensor locations were considered in total as illustrated in Figure 28. The five corresponding influence lines are also illustrated in the figure.

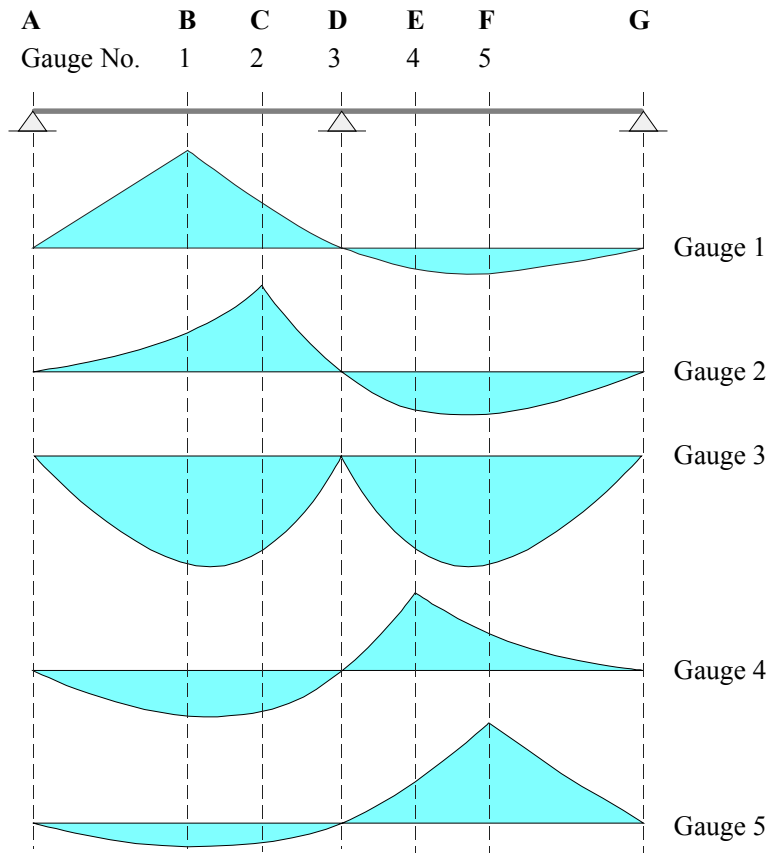


Figure 28: Longitudinal sensor locations and corresponding influence lines

Region	AB	BC	CD	DE	EF	FG
	(1	1	(1	(1	(1	(1
	2	2	2	2	2	2
	3	(3	(3	3	3	3
	(4	(4	(4	4	4	4
	5	5	5	(5	5	(5

Figure 29: Dependency of Influence Functions

Different combinations of the influence functions were found to be dependent in different parts of the bridge. This is illustrated schematically in Figure 29. The curves in this figure indicate the dependencies between influence functions. For example, for an axle in part AB of the bridge, the influence functions for sensor numbers 1 and 2 are dependent and those for sensor numbers 3, 4 and 5 are dependent. This leaves only two independent equations for this part of the bridge. Fortunately, there are two parts of the bridge, BC and EF, where three independent equations exist. In these parts, an instantaneous calculation of axle weights is possible for trucks with up to three axles. If it is assumed that individual axles within tandems or tridems are of equal weight, then three independent equations is enough to make instantaneous calculations possible for most truck types. For a particular example, the determinant of the matrix of three equations was calculated for a range of positions between B and C. It was found that, if a small error existed in the calculated vehicle speed or axle spacing, the determinant varied significantly and approached zero at one point within the region. However through most of the region, the determinant was non-zero and the equations were independent.

6.2.3 Preliminary Experimental Verification

A preliminary test was completed of a multiple-equation B-WIM system using the Belleville Bridge on the A31 motorway in NE France (Figure 8).

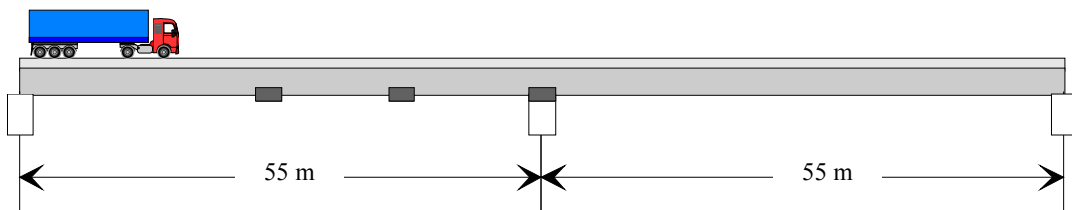


Figure 30: Belleville bridge and strain gauge locations

As illustrated in Figure 30, strain gauges were installed at three longitudinal locations corresponding to sensor numbers 1, 2 and 3 in Figure 28. Instantaneous calculation of axle weights were carried out when trucks were between mid-way and $\frac{3}{4}$ -way across the left span (part BC in Figure 28). At each longitudinal sensor location, active electrical resistance strain gauges were attached to longitudinal stiffeners at two points transversely on the bottom surface on the inside of the box.

Axle detectors are used in conventional B-WIM systems to identify the location of the truck, its speed and the numbers and spacing of axles. Low grade piezo-electric bars were installed at the end of the Belleville bridge for axle detection purposes. However, at the time of the trials, they were malfunctioning. As a result, axle spacings were measured manually on the stationary trucks while they were being weighed statically and the speed of each truck on the bridge was determined using a hand-held laser device. The synchronisation of the measured strain records with the theoretical calculation requires a knowledge of the time that the truck reaches the start of the bridge. This was estimated from a video record of the traffic. As a result, a high level of accuracy could not be expected from this study.

Pre-weighed data for six vehicles was collected. One of these was selected at random as a calibration vehicle and the remaining five used to carry out the preliminary test. One run of one truck is

clearly inadequate for normal calibration purposes but was considered sufficient for the purposes of a preliminary trial.

A typical result from the preliminary trial for gross vehicle weight is illustrated in Figure 31. In the region between 33 m and 37 m from the start of the bridge, the determinant of the matrix of equations was small and the calculated gross vehicle weights approached infinity. Outside of this region, it can be seen that the errors vary considerably, particularly in the left portion of the graph. It is unlikely that this variation is due to the dynamic movements of the truck although this would be expected to be a contributory factor. It is more likely that there are substantial errors due to inaccuracies in the synchronisation of measured with theoretical results. This and a relatively low resolution in the strain readings would lead to errors which would be exasperated by a near-zero determinant. The relatively low variation in results on the right hand side of the graph may be due to larger values of the determinant. It is not clear why there is an apparent bias which is different in the different parts of the graph. Despite the great deviation in calculated gross weights from the static value, the calculated mean gross weight from all the instantaneous values is relatively accurate.

Figure 32 provides a comparison of the result for the multiple equation B-WIM system with results calculated using the conventional B-WIM algorithm. Gross weights were calculated separately us-

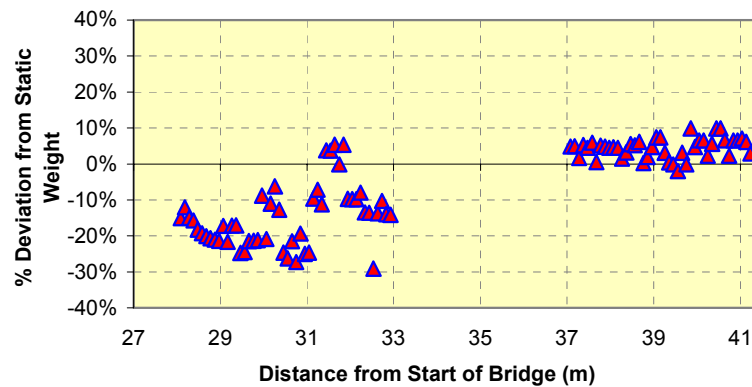


Figure 31: Errors in calculated gross vehicle weight versus distance

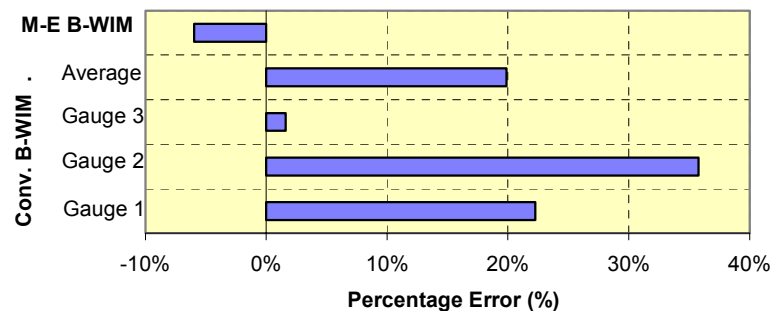


Figure 32: Comparison of results from multiple-equation (M-E) B-WIM and conventional B-WIM algorithms

ing data from each of the three longitudinal sensor locations. In addition, the mean of the three is presented. It can be seen that, except for strain gauge No. 3 (near central support), the multiple equation B-WIM system is more accurate than the conventional B-WIM system. This result is typical of the five trucks for which data was available. The reason for the high accuracy of results from gauge No. 3 is not clear although it is significant that the strain resolution at this location was the highest for all locations. The gross weight calculated using gauge No. 3 was higher than the multiple equation system in three cases, similar in one and less high in one other.

6.2.4 Conclusions on Multiple-Sensor Static B-WIM

The multiple equation B-WIM system is shown to be theoretically possible for two-axle trucks on single-span bridges. For two-span bridges the parts of the bridge for which instantaneous calculations are possible for three-axle trucks are identified. A preliminary test gives some indication of the type of results that can be expected. It is anticipated that significant improvements could be achieved. However the Belleville bridge is excessively long for a high-accuracy system as will be shown in section 6.3. Further, all bridges will be affected by the reduced resolution that is possible at points away from mid-span and over central supports. The potential benefit of getting an instantaneous applied dynamic force was not realised due to the high scatter of results. This might be much improved through the use of a shorter bridge.

6.3 Combined B-WIM and Pavement WIM System

6.3.1 Robustness

One potential advantage of a combined Bridge and Pavement WIM system is 'robustness', i.e., insensitivity of the results to minor errors in the input data. Robustness is best considered in the first instance for a regular B-WIM system. A theoretical study is presented here which examines the robustness of such a system. There are several factors which affect the robustness of the algorithm. These include strain gauge resolution, sampling frequency, the span length to axle spacing ratio, etc.. This theoretical study examines this ratio. The robustness of the algorithm is examined using two different bridge span lengths being traversed by a two axle truck of two different axle spacings.

The static BWIM algorithm is based on Moses' algorithm (Moses, 1979). It uses the equation:

$$M(x) = A_1 I[x] + A_2 I[x - L_1] + \dots + A_n I[x - L_{n-1}]$$

where:

$M(x)$ = Induced bending moment with first axle at position x ,

A_i = Weight of axle i ,

L_1, L_2, \dots, L_{n-1} = distances of axle numbers 2, 3, n respectively from axle No. 1,

$I[x]$ = Value of static influence line at position x .

By using a least squares minimisation procedure, the following matrix can be constructed (Dempsey 1997):

$$\begin{bmatrix} f_{11} & f_{21} & \cdots & f_{i1} \\ \vdots & \vdots & & \vdots \\ f_{1j} & f_{2j} & \cdots & f_{ij} \end{bmatrix} \begin{bmatrix} A_1 \\ \vdots \\ A_n \end{bmatrix} = \begin{bmatrix} m_1 \\ \vdots \\ m_n \end{bmatrix}$$

or,

$$[F_{ij}] [A_j] = [M_j]$$

where:

$$f_{ij} = \sum_{k=1}^T I_i(t_k) I_j(t_k)$$

$$m_j = \sum_{k=1}^T M^M(t_k) I_j(t_k)$$

$I_i(t_k)$ = Influence line at scanning time t_k ,

$M^M(t_k)$ = Measured bending moment at scanning time t_k ,

The robustness of the algorithm for a particular case can be defined as the value of the determinate of the F matrix. The higher the value of the determinate the more robust the algorithm, as this gives a higher accuracy in the determination of the individual axles.

To examine the robustness of the algorithm, bridge spans of 16 m and 32 m being traversed by a theoretical two-axle vehicle with axle spacings of 4 m and 2 m were considered.

16m Long Simply Supported Bridge Being Traversed by Two Axle System

The theoretical 16 m long bridge was simply supported with a concrete beam and slab construction. It was 8.3 m wide and was constructed from a 160 mm thick concrete bridge deck supported by 9 'Y1' Beams of depth 700 mm, giving a value of $3.5 \times 10^{11} \text{ mm}^4$ for the second moment of area and a Z value of $0.823 \times 10^9 \text{ mm}^3$ to the bottom fibre.

The strain induced in the bridge was calculated at 5 discrete positions. The F matrix was constructed and the determinate calculated for both axle spacings:

$$\begin{array}{ll} 4 \text{ m axle spacing:} & \det = 3.797 \times 10^{-14} \\ 2 \text{ m axle spacing:} & \det = 1.105 \times 10^{-14} \end{array}$$

It is important to note that, with both axle spacings, it was assumed that the scanning frequency of the system was the same, i.e., both trucks were recorded in 5 discrete positions. As can be seen, the value of the determinate of the matrix for the 2 m axle spacing crossing the bridge is lower than in the case of the 4 m spacing. This will result in a loss of accuracy in determining the individual axle weights of the truck.

32 m Long Simply Supported Bridge being Traversed by Two Axle system

The 32 m bridge was modelled with the same construction as the 16 m bridge above except that 9 'Y8' beams were used instead of the 'Y1's. The beams had a depth of 1400 mm; this resulted in the bridge having a value for the second moment of area of $1.823 \times 10^{12} \text{ mm}^4$ and a value of Z to the bottom fibre of $2.255 \times 10^9 \text{ mm}^3$. Again the F matrix of the B-WIM algorithm was constructed for

both the 4m and 2m axle spacing. The scanning frequency of the system remained the same as that of the 16 m bridge, but because the bridge is longer, recordings of strain were made with the truck at 9 discrete positions. These results are:

$$4 \text{ m axle spacing: } \det = 1.623 \times 10^{-14}$$

$$2 \text{ m axle spacing: } \det = 0.423 \times 10^{-14}$$

As for the 16m bridge, the determinate of the F matrix is lower for the 2 m axle spacing than for the 4m axle spacing. Figure 33 shows a comparison of the determinates for each of the bridges and axle spacings.

From Figure 33 it can be seen that, as the span of the bridge increases or the vehicle axle spacing decreases, the robustness of the B-WIM algorithm decreases. The algorithm is found to be more robust for the 4 m axle spacing crossing the 32 m bridge than for the 2 m axle spacing traversing the 16 m bridge. Therefore doubling both the bridge span and the axle spacing gives a more robust algorithm.

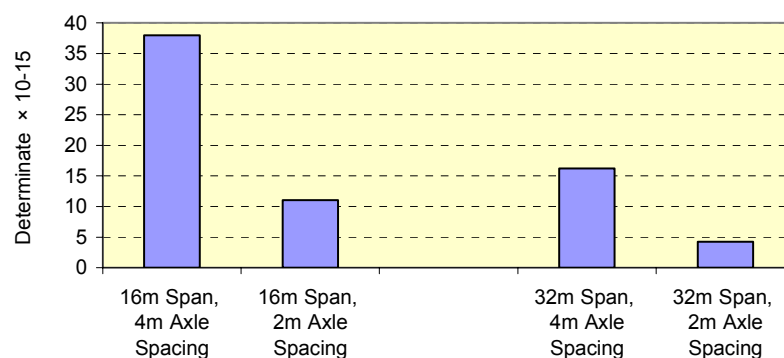


Figure 33: Comparison of determinates for various bridge span lengths and axle spacings

It was found that, for a system with the same scanning frequency, the algorithm is more robust for shorter span bridges being traversed by large axle spacings. Clearly, axle spacing is a function of the traffic and outside the control of the B-WIM algorithm. However, it is useful to note that shorter bridges tend to give a more robust algorithm than longer ones. This can be understood qualitatively by considering that, as the span of the bridge increases, the algorithm's ability to distinguish the weights of the individual axles is lessened because the vehicle tends to act more like a point load. On shorter bridges the gross vehicle weight of the vehicle is similar in accuracy to that on longer span bridges because the gross vehicle weight is not affected by this phenomenon.

6.3.2 The Basis of a Combined Algorithm

A combined B-WIM algorithm is one which combines data from a pavement WIM system with strain data taken from a B-WIM system with the objective of increasing the accuracy overall. The standard B-WIM algorithm is based on the least squares minimisation procedure described in the previous section. The combined bridge weigh in motion system works in much the same manner except that it uses additional information obtained from the pavement sensors in the form of instan-

taneous dynamic axle weights. The algorithm applied to a two axle truck is considered here. The objective function for the combined system can be expressed as:

$$Obj = \frac{\lambda_1}{T} \sum_{k=1}^T [M(t_k) - M^M(t_k)]^2 + \frac{\lambda_2}{2} (A_1 - R_1^*(t^*))^2 + \frac{\lambda_2}{2} (A_2 - R_2^\gamma(t^\gamma))^2$$

where:

A_1 & A_2 = weight of axles 1 and 2 respectively,

R_1^* & R_2^γ = Forces applied by the first and second axles respectively as they are measured crossing the pavement sensors at times t^* and t^γ respectively,

λ_1, λ_2 = Weighting factors dictating balance between pavement and bridge data ($\lambda_1 = 1, \lambda_2 = 0$ gives a pure B-WIM system while $\lambda_1 = 0, \lambda_2 = 1$ gives a pure pavement WIM system, $\lambda_1 + \lambda_2 = 1$)

This objective function is minimised with respect to A_1 and A_2 and, after some rearrangement, the following equation is obtained:

$$\begin{bmatrix} \frac{\lambda_1}{T} \sum_{k=1}^T I_1(t_k)I_2(t_k) + \frac{\lambda_2}{2} & \frac{\lambda_1}{T} \sum_{k=1}^T I_2(t_k)I_1(t_k) \\ \frac{\lambda_1}{T} \sum_{k=1}^T I_1(t_k)I_2(t_k) & \frac{\lambda_1}{T} \sum_{k=1}^T I_2(t_k)I_2(t_k) + \frac{\lambda_2}{2} \end{bmatrix} \begin{bmatrix} A_1 \\ A_2 \end{bmatrix} = \begin{bmatrix} \frac{\lambda_1}{T} \sum_{k=1}^T M^*(t_k)I_1(t_k) + \frac{\lambda_2}{2} R_1^*(t^*) \\ \frac{\lambda_1}{T} \sum_{k=1}^T M^*(t_k)I_2(t_k) + \frac{\lambda_2}{2} R_2^\gamma(t^\gamma) \end{bmatrix} \quad (15)$$

By solving the above equation for A_1 and A_2 , the axle weights and thus the gross vehicle weight of the vehicle can be determined.

Testing Of Combined Algorithm

The algorithm was theoretically examined by generating simulated dynamic axle forces for the pavement system and bending moment influence responses for the B-WIM system. A 10 m long simply supported bridge with a Span to Depth ratio of 1/20 was considered. The vehicle was a 12 tonne two-axle truck having an axle spacing of 8 m. In order to examine the feasibility of the combined algorithm, a statistical study was carried out. The BWIM system utilised one simulated bending moment sensor placed at mid-span. This involved the algorithm being run 200 times. Each time it was supplied with two randomly varying dynamic axle forces and one randomly varying bending moment influence line. The mean and 80% confidence interval for the errors were determined for various values of λ_1 and λ_2 . The variation in the data was set so that both the standard B-WIM system (when $\lambda_1 = 1$) and the pavement WIM system (when $\lambda_2 = 1$) had an accuracy class of B(10).

Figure 34 shows the mean accuracy and 80% confidence intervals for the error in Gross Vehicle Weight for various values of λ_1 and λ_2 .

From Figure 34 the mean error of the system varies by a small percentage as the values of λ_1 and λ_2 change. However, what is important to note is that, when the value of λ_1 is in the range of 0.4 to 0.6, the band width of the confidence interval is smaller giving a higher expected level of accuracy

in vehicle weight. This gives an increased performance over the pavement WIM system or BWIM system individually. The accuracy class of the GVW determination is increased from a class B(10) to a class B+(7). Figure 35 (a) and (b) show the mean and confidence intervals for the errors in the weights of the first and second axes of the vehicle respectively.

Again for the individual axle weights, with a value for λ_1 in the range of 0.4 to 0.6, the algorithm performs better than the other two algorithms (pavement and bridge) individually. The increase in accuracy class is again from B(10) to B+(7) for individual axles.

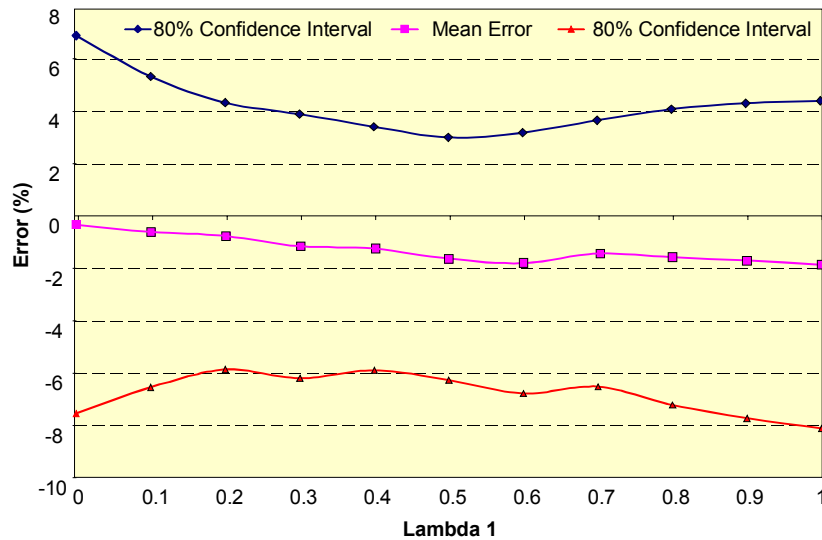
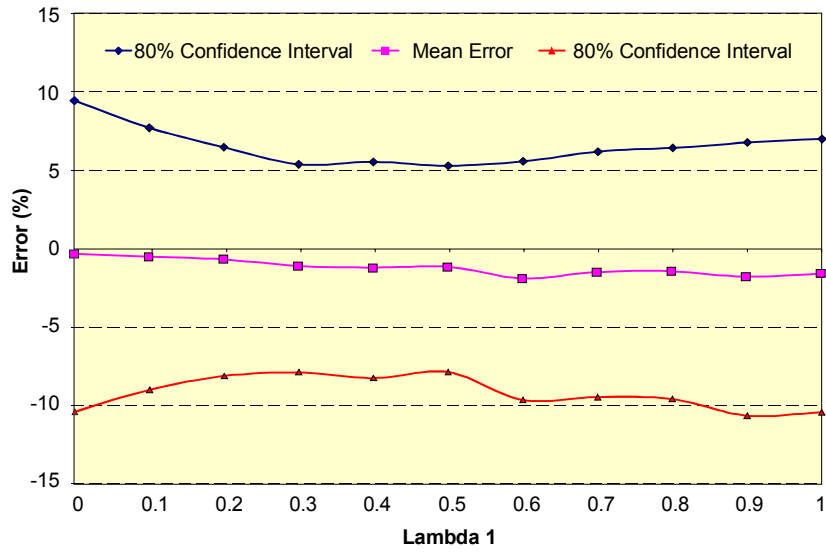


Figure 34: Errors in GVW for Combined Bridge Weigh-In-Motion System

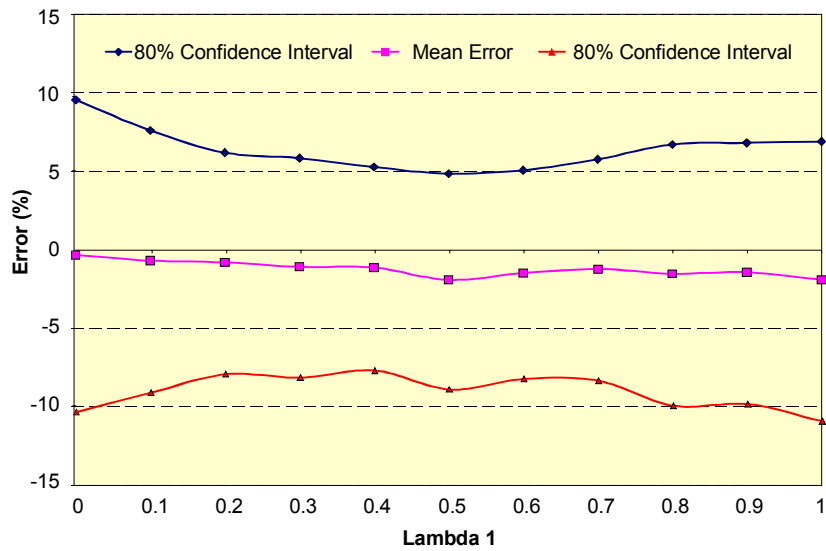
In conclusion, a combined bridge Weigh-In-Motion algorithm was examined to determine its feasibility. It was found that the algorithm had the potential to perform better than either bridge or pavement systems acting alone, giving greater accuracy in determining individual and gross vehicle weights.

6.4 The Development of a Dynamic Bridge WIM Algorithm

Pavement WIM systems measure an instantaneous force for the time the tyre is supported on the WIM sensor. This time depends on the sensor width and vehicle speed and only a small portion of the tyre oscillation is recorded. The deviations above or below the static value could be well in excess of 30% on a pavement in good condition. If a WIM system is able to measure the load for a full period of the lowest frequency, the problem of dynamic oscillation would be overcome. The only existing WIM system capable of achieving this uninterrupted record is a B-WIM system. B-WIM systems measure truck forces continuously as the truck travels on the bridge. As the bridge length increases, the period of measurement increases and lower frequency components of the force can be successfully detected. This is simply not possible in pavement strip sensors due to the very short period of measurement. Therefore, if truck mass is negligible compared to bridge mass, truck dynamic effects on measurements are naturally reduced by the bridge inertia.



(a) Errors in Axle 1



(b) Errors in Axle 2

Figure 35: Individual Axle Errors for Combined WIM System

The traditional B-WIM approaches have limitations when the dynamic behaviour of the bridge-truck structural system does not follow a periodical oscillating pattern around the static response. These dynamic sources of inaccuracy are related to the excitation of the dynamic wheel forces by

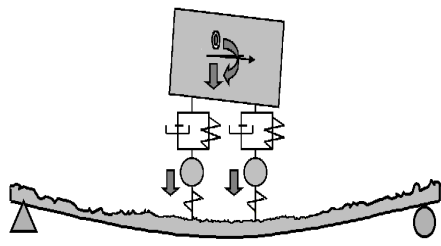
the bridge support or a bump in the approach (Lutzenberger & Baumgärtner 1999), measurements with a small number of natural periods of vibration (Peters 1984), bridges with low first natural frequencies, or the occurrence of a significant dynamic amplification. For bridges with high natural frequencies, low-pass filtering of the signal can be used to remove the effects of bridge vibration. However, this was found in the Lulea B-WIM tests (see workpackage 3.1 and Chapter 8) to have an adverse effect on accuracy, particularly for individual axles. In these tests, a very low 4 Hz hardware filter removed not only dynamics and noise, but frequency components of the static response. A more reasonable filter could have improved results. When bridges have a low natural frequency, filtering such a dynamic component could inadvertently remove a significant part of the static response.

All the approaches to date calculate the weights in the time domain, this is, strain measurements from each scan are compared to corresponding theoretical values. In this section, an alternative dynamic bridge WIM system is presented based on a frequency spectrum approach (González & O'Brien 1998). This spectral approach utilises the frequency components of the strain signal and requires no prior knowledge of the influence line. The frequency domain representation of the signal, although entirely equivalent to the time domain representation, facilitates the suppression of high frequency effects. This system was calibrated in a totally experimental way, without any theoretical reference to the structural behaviour.

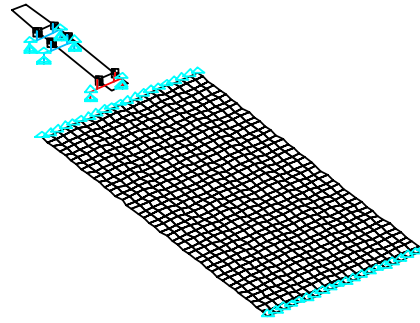
Other research has focused on the development of dynamic algorithms in the time domain (DB-WIM). These ones try to correct the deviation from the static value that bridge and truck dynamics could introduce in the measured strain (Dempsey et al 1998, O'Connor 1987). Most of these procedures yield a unique average load as a result of using the whole strain record at one longitudinal sensor location. This assumption could induce significant errors due to the actually varying applied load. Kealy and O'Brien extended the traditional static algorithm based on one sensor location to the use of several sensors along the length of the bridge (section 6.2). This approach has the advantage of providing the complete distribution of varying axle forces as the truck traverses the bridge and appears to reduce the effect of truck bouncing and rocking motions overall. However, it does not address the issue of bridge vibration which can result in significant errors for bridges with low natural frequencies. A dynamic multi-sensor algorithm was developed in WP1.2 to overcome this problem (González et al. 1999). This algorithm compares the measured strain to the theoretical total strain instead of the static component (given by influence lines). The equations of the total strain are made up of static and dynamic components. They can be derived from the mechanical characteristics of the bridge and the variables representing its general dynamic behaviour: natural frequencies, mode shapes and damping.

6.4.1 Theoretical Testing

Theoretical bridge-truck interaction models are used to generate strains at different locations along the bridge that allow the feasibility of the different dynamic algorithms to be assessed. Road surface irregularities are idealised as a stochastic process and generated from power spectral density functions as suggested by ISO. The DB-WIM algorithm is tested theoretically with a planar numerical model (Frýba 1972) as shown in Figure 36(a). Other truck configurations are modelled using finite element techniques (Cifuentes 1989, Baumgärtner 1998) for further testing, as shown in Figure 36(b). The finite element solution requires the introduction of a LaGrange multiplier technique to simulate the interaction between bridge and truck models.



(a) Numerical approach



(b) Finite element approach

Figure 36: Theoretical Bridge-Truck Dynamic Interaction Models

6.4.2 Spectral Algorithm

According to the linearity and the time-shifting properties of Fourier transforms of digital signals, the total spectrum of the bridge response to a calibration truck can be expressed as:

$$\overline{H}_y(f) = \overline{H}_x(f)[A_1 + A_2 e^{(-jfn_1)} + \dots + A_i e^{(-jfn_{i-1})} + \dots + A_r e^{(-jfn_{r-1})}] \quad (16)$$

where:

$\overline{H}_y(f)$ = Spectrum of total strain.

$\overline{H}_x(f)$ = Spectrum of the strain response due to a moving *unit* load.

A_i : = Weight of axle “ i ”.

j : = Imaginary number, i.e., $\sqrt{-1}$.

r : = Number of axles.

n_i : = Number of readings between the first axle and the axle “ $(i+1)$ ”.

f : = Frequency, as “ $f=2\pi k/N$ ”, where “ k (0,1,2,..)” is the k^{th} harmonic of the sample.

N : = Number of strain readings induced by a vehicle crossing the bridge.

As bridge frequencies and spectral leakage due to their components take place for relatively high frequencies, it is possible to assume for the lowest frequencies:

$$\overline{H}_y(f) \approx \overline{H}_m(f) \quad (17)$$

where $\overline{H}_m(f)$ is the spectrum of the measured strain. Substituting Equation (17) in Equation (16), the spectrum corresponding to the pass of a single unit load can be obtained for the lowest frequencies as shown in Equation (18):

$$\overline{H}_x(f) = \overline{H}_m(f) / [A_1 + A_2 e^{(-jfn_1)} + \dots + A_i e^{(-jfn_{i-1})} + \dots + A_r e^{(-jfn_{r-1})}] \quad (18)$$

Very low speeds of the calibration truck allow for the collection of a lot of readings, and a good definition of low frequency components. A variety of speeds are necessary to evaluate the magnitude component of the fundamental harmonics for different sizes of the sample. Therefore, the scanning frequency should be quite high to reduce spectral leakage due to non-harmonic compo-

nents. Some dispersion in spectra calculated through Equation (18) will occur due to truck dynamics.

Once the spectrum of the bridge response due to a unit load is known, axle weights can be calculated by minimising an error function defined as the sum of squares of differences between the expected spectrum and the measured one, as follows:

$$\sum_{f=0}^{f_c} [\overline{H}_x(f) \sum_{i=1}^r (A_i e^{-jfn_{i-1}}) - \overline{H}_m(f)]^2 = 0 \quad (19)$$

where “ f_c ” is the limiting frequency at which spectra are compared. The spectrum $\overline{H}_x(f)$, taken as reference, must be the one corresponding to the speed of the traffic event being analysed. This spectrum can be calculated through inverse transform and interpolation from the calibration spectra obtained using Equation (18).

The error function is minimised by differentiating with respect to the weight of the k^{th} axle, A_k , which leads to the following expression:

$$\sum_{f=0}^{f_c} [\sum_{i=1}^r [A_i e^{-j2fn_{i-1}} \overline{H}_x(f)] e^{-jfn_{k-1}} \overline{H}_x(f)] = \sum_{f=0}^{f_c} [\overline{H}_m(f) \overline{H}_x(f) e^{-jfn_{k-1}}] \quad (20)$$

In matrix form, the axle weights are given by:

$$\{A\}_{rx1} = [H]_{rxr}^{-1} \{M\}_{rx1} \quad (21)$$

where the elements of the matrix of coefficients $[H]$ are given by Equation (22) and the vector of independent terms $\{M\}$ by Equation (23).

$$[H]_{ik} = \sum_{f=0}^{f_c} [e^{-jf(n_{i-1}+n_{k-1})} \overline{H}_x^2(f)] \quad (22)$$

$$\{M_k\} = \sum_{f=0}^{f_c} [\overline{H}_m(f) \overline{H}_x(f) e^{-jfn_{k-1}}] \quad (23)$$

Spectra $\overline{H}(f)$ are composed of real and imaginary parts (or magnitude and phase). Axle weights are obtained from Equation (21) using complex arithmetic. Some further details are given by Gonzalez and OBrien (1998).

However, the spectra are limited by the time the load is on the bridge and low frequency components could not be defined accurately in every case. Accordingly, while effective for vehicles with a low number of axles, this frequency domain approach failed to accurately predict the axle weights for trucks with a high number of axles.

If the bridge response is mainly static, an automatic procedure for the determination of the experimental influence line in the frequency domain can be successfully derived from this spectral algorithm. So, the spectrum of the influence line is obtained by calculating the unit contribution of all readings to a given frequency (Equation (18)). The influence line can be obtained in the time domain through the inverse transform of this unit spectrum. The limitations of a direct calculation in the time domain or the inconvenience of an experimental adjustment, point by point, are overcome in this way.

6.4.3 Dynamic Multi-sensor Bridge WIM Algorithm (González et al. 1999)

A dynamic multi-sensor system is based on the accurate determination of the theoretical strain response due to a moving constant load at different bridge locations. This is obtained by a) experimental determination of the natural frequencies and damping of the bridge; b) calculation of the mode shapes based on the bridge geometry, and c) adjustment of the unit response curves to give a best fit to the static values of the calibration vehicle. Each sensor location can be calibrated differently.

If there are a number of sensors, m , greater than or equal to the number of axles n , it is possible to minimise the error function defined in Equation (24):

$$f = \sum_{k=1}^{k=m} (\varepsilon_{kt} - \varepsilon_{km})^2 \text{ at each instant "t"} \quad (24)$$

where ε_{kt} is the theoretical total strain due to the applied load at location k and ε_{km} is the corresponding measured strain.

The total strain response ε_{kt} from a bridge due to a truck crossing can be modelled with a dynamic model based on constant loads. The total theoretical strain $\varepsilon_t(t)$ at a certain location can be approximated as a function of the applied axle weights and the total (static + dynamic) strain response due to a unit moving load as follows:

$$\varepsilon_t(t) = \sum_{i=1}^n A_i \varepsilon_{i1}(t) \quad (25)$$

where A_i is the weight of axle i , and $\varepsilon_{i1}(t)$ is the contribution to the total strain response of a unit load at the location of axle i . Figure 37 shows the influence line for the bending moment at midspan versus the corresponding total strain response used in this new approach for a 20 m bridge of natural frequency 4 Hz. This is the total strain corresponds to a moving load travelling at 20 m/s. Unlike the static component, the total strain for a given load depends on its speed, so there is a different curve taken as reference for each speed.

The assumption of linearity and superposition involved in this formulation has been proven to match more realistic approaches (Dempsey & Brady 1999), even though the dynamic problem is non-linear. The theoretical model is also generated with constant loads, so interaction between bridge and truck masses is neglected. This simplification allows a calculation in real time and a significant improvement in accuracy compared to the static algorithm based on the influence line. A more sophisticated model such as a quarter car could be considered instead of constant loads, but the difference in accuracy might not be justifiable due to the introduction of new unknown parameters.

Figure 38 illustrates the quality of the adjustment obtained by the dynamic algorithm in comparison to the real strains. The total measured strain and the real static strain are obtained from numerical simulations (Figure 36(a)). Another curve represents the adjustment obtained by using equation (25) if considering constant loads. The dynamic BWIM system will be more accurate, the closer its adjustment is to the total strain. The same figure shows the quality of the adjustment obtained by a static algorithm as proposed by Moses in comparison to the real static strain. In this case, it is possible to notice how the static approach overestimates the weight of both axles when trying to adjust the static answer to the total strain (the real static strain is unknown a priori).

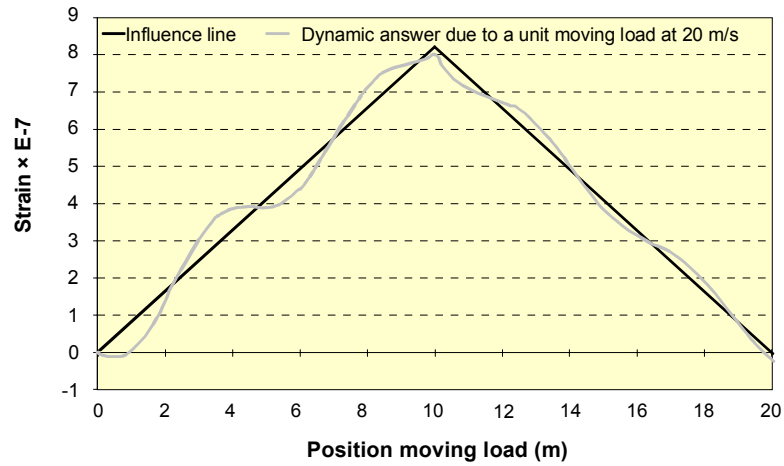


Figure 37: Influence line versus Dynamic unit response at midspan

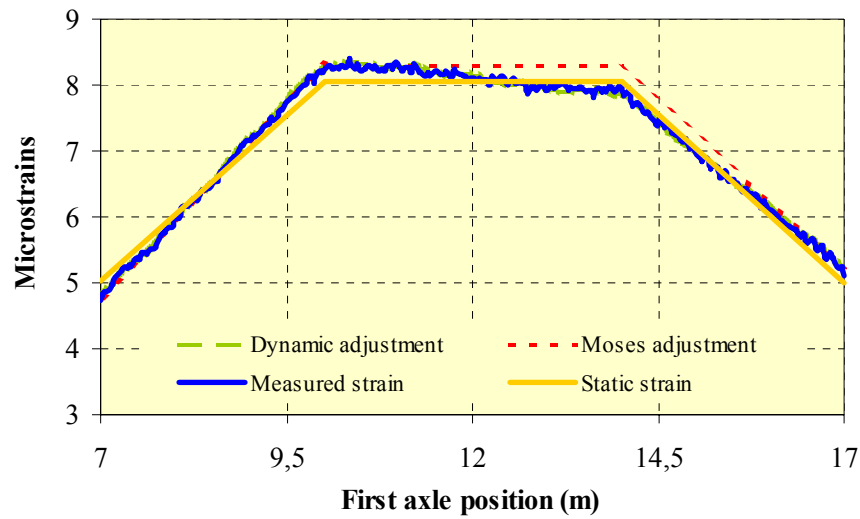


Figure 38: Strain induced by a 2-axle vehicle and adjustment by static and DB-WIM algorithms

By combining Equations (24) and (25), we get:

$$f = \sum_{k=1}^{k=m} (\epsilon_{k1}A_1 + \epsilon_{k2}A_2 + \dots + \epsilon_{kn}A_n - \epsilon_{mk})^2 \text{ at each instant "t"} \quad (26)$$

Differentiating Equation 26 with respect to the axle weight and setting it equal to zero gives:

$$\frac{df}{dA_i} = 2 \sum_{k=1}^{k=m} (\epsilon_{k1}A_1 + \epsilon_{k2}A_2 + \dots + \epsilon_{kn}A_n - \epsilon_{mk}) \epsilon_{ki} = 0 \quad (27)$$

which can be expressed in matrix form as:

$$\begin{bmatrix} \sum_{k=1}^{k=m} \mathcal{E}_{k1} \mathcal{E}_{k1} & \sum_{k=1}^{k=m} \mathcal{E}_{k2} \mathcal{E}_{k1} & \dots & \sum_{k=1}^{k=m} \mathcal{E}_{kn} \mathcal{E}_{k1} \\ \sum_{k=1}^{k=m} \mathcal{E}_{k1} \mathcal{E}_{k2} & \sum_{k=1}^{k=m} \mathcal{E}_{k2} \mathcal{E}_{k2} & \dots & \sum_{k=1}^{k=m} \mathcal{E}_{kn} \mathcal{E}_{k2} \\ \dots & \dots & \dots & \dots \\ \sum_{k=1}^{k=m} \mathcal{E}_{k1} \mathcal{E}_{kn} & \sum_{k=1}^{k=m} \mathcal{E}_{k2} \mathcal{E}_{kn} & \dots & \sum_{k=1}^{k=m} \mathcal{E}_{kn} \mathcal{E}_{kn} \end{bmatrix} \begin{Bmatrix} A_1 \\ A_2 \\ \dots \\ A_n \end{Bmatrix} = \begin{Bmatrix} \sum_{k=1}^{k=m} \mathcal{E}_{mk} \mathcal{E}_{k1} \\ \sum_{k=1}^{k=m} \mathcal{E}_{mk} \mathcal{E}_{k2} \\ \dots \\ \sum_{k=1}^{k=m} \mathcal{E}_{mk} \mathcal{E}_{kn} \end{Bmatrix} \quad (28)$$

Finally, weights can be calculated from equation (29):

$$\{A\}_{nx1} = [\mathcal{E}_1]_{nxn}^{-1} * \{\mathcal{E}_m\}_{nx1} \quad (29)$$

The matrix components for the last equation are defined in Equation (28). If the number of strain sensor locations is high enough, Equation (29) provides a solution through most of the bridge. There are certain critical areas: i.e., at the start and end of the bridge, where the small strains induce rounding errors (these areas should not be considered in calculations). If $|\mathcal{E}_1|$ is null for a combination of sensors, it will be necessary to choose a different location. The static value can be obtained from the root mean square of the calculated instantaneous axle forces.

Figure 39 shows the value of the determinant $|\mathcal{E}_1|$ at each instant for a 4-axle truck on a 20 m simply supported bridge with sensors spaced every 2 m. The importance of the determinant as an indicator of potential accuracy, is presented in section 6.2 (see also Kealy & O'Brien 1998). It can be seen in the figure that the magnitude of the determinant is similar for the dynamic and static cases. The limit on the number of axles that a solution can be found for, is overcome with the use of a high number of sensors and the least squares fitting technique introduced here. Unlike the 'static' determinant, the 'dynamic' determinant is not symmetric.

Figure 40 shows the differences between the representation of the axle load history obtained by the two existing multi-sensor B-WIM algorithms in the case of the front axle of a moving 2-axle vehicle. The multi-sensor systems are not able to reproduce the instantaneous applied axle force accu-

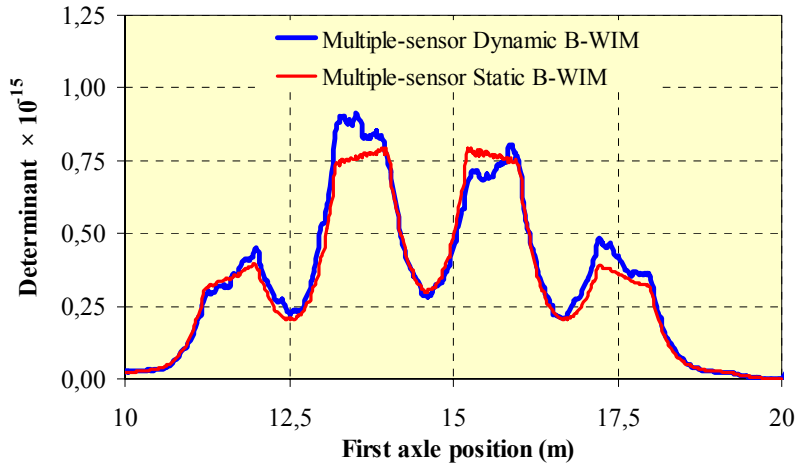


Figure 39: Values of determinant $|\mathcal{E}_1|$ for each vehicle position

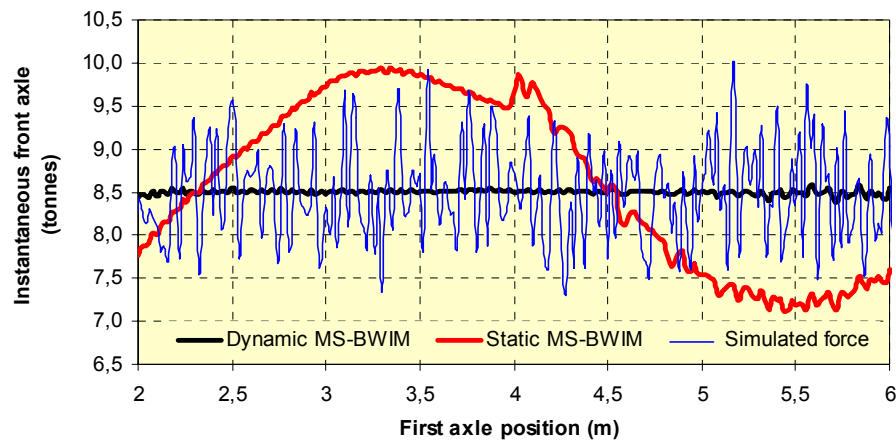


Figure 40: Applied axle load calculated by 2 different multi-sensor approaches using a least squares fitting technique at each instant

rately, but the dynamic system gives results around the real static weight of 8.5 tonnes along most of the bridge length.

The accuracy of B-WIM algorithms is sensitive to changes of some truck mechanical characteristics as compared to the ones used during calibration. The bridge modelled is a simply supported 20 m single span with a first natural frequency of 4.26 Hz and 1% damping. A 2-axle body vehicle is modelled numerically to analyse the influence of truck parameters during calibration. The features of the calibration truck taken as reference are: $5 \times 10^4 \text{ kg} \times \text{m}^2$ body inertia, 10 000 kg body mass equally distributed between axles, 4 m axle spacing, travelling at 20 m/s, and each axle has the following characteristics: 1000 kg axle mass, 7000 N×s/m suspension damping, 80 000 N/m suspension stiffness and 700 000 N/m tyre stiffness. The road conditions are good. Some of the parameters that can vary are distribution of load between axles, axle spacing and tyre stiffness. Their influence is studied by modifying the original value by a percentage while leaving the rest of the vehicle properties unaltered. The performance of the dynamic multi-sensor Bridge WIM algorithm is compared to a static approach (Moses, 1979) for each simulation (Figure 36(a)). The gross vehicle weight is the same in every case. Figure 41(a) and (b) give the maximum relative error in weights for both the static and the new algorithms due to differences in the axle spacing and the position of the centroid of the body mass. Both algorithms are very accurate when there is only a change in axle spacing of the calibration truck. While the static algorithm gets less accurate when both axles are very closely spaced (tandem configurations), the new algorithm achieves the same degree of performance. When the body weight distribution between axles changes, the dynamic algorithm is generally more accurate and shows a smaller standard deviation. In the same way, the influence on accuracy of a difference in tyre stiffness is illustrated in Figure 41(c). A significant error appears for a decrease of 25% in the tyre stiffness as a result of a lower axle hop frequency. This very low frequency results in an average value far from the static one. Figure 41(d) represents the applied load against axle position for this case. The inaccuracy is a consequence of the reduced number of strain readings available due to bridge length and speed. This limitation in readings makes it difficult to distinguish the static component from the dynamic low frequency components of the varying force. However, the 0.2 Hz frequency of this example is only a theoretical case, not a realistic one. In practice, these truck frequencies will be around 2 Hz, which corresponds to an in-

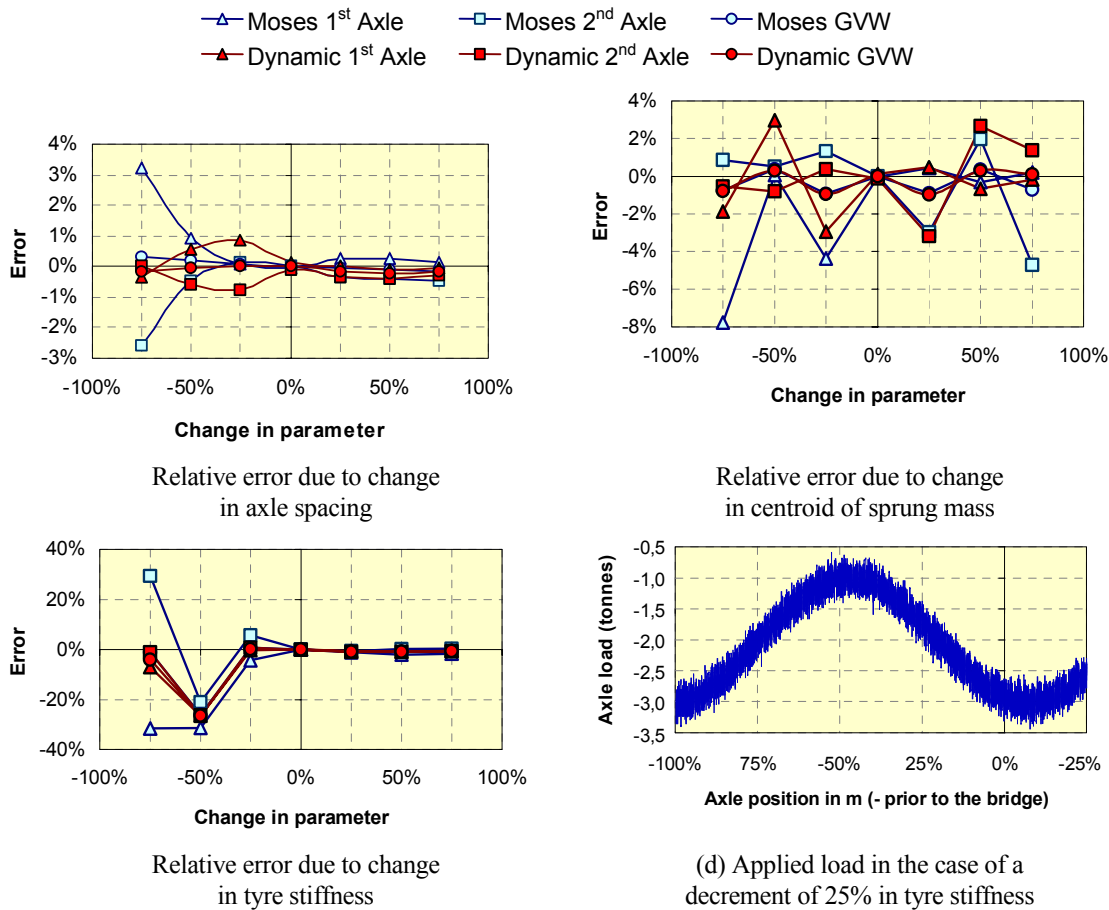


Figure 41: Effect on accuracy of the change of vehicle mechanics

crease of the tyre stiffness in the graphic. For these cases, the performance of both algorithms is good.

Two and three-axle finite element truck models (Figure 36(b)) with front axle and rear single axle or tandems were used for further testing (individual axles of axle group spaced at 1.2 m). The redistribution of load between these closely spaced axles is important, and the calculation of their individual weights is usually problematic (except for shorter integral bridges, where axle from a group criteria has been found in some experiments to be in the same accuracy class as the other criteria). Accuracy in the estimation of static weights by the static and dynamic algorithms is given in Table 6. Simulated calibration takes place under Limited Reproducibility conditions. The set of 2 vehicles are simulated in fully loaded, half loaded and unloaded conditions at two different speed levels, 20 and 25 m/s. In practice, the standard deviations would be expected to be greater than the ones shown in the table due to errors in the estimation of axle spacing, speed or variations in the truck initial conditions and transverse location.

The results show an improvement in the estimation of axle weights and a significantly reduced standard deviation when applying the multi-sensor algorithm.

Table 6: Accuracy Classification

Sample size	GVW		Group of axles		Single axle		Axle in a group	
	12		6		18		12	
Algorithm	static	dyn.	static	dyn.	static	dyn.	static	dyn.
mean (%)	0.027	0.122	3.952	0.494	-3.432	-0.212	-0.884	-3.124
Stand. Dev. (%)	0.698	0.693	0.672	1.682	5.409	1.493	25.63	14.012
π_0 (%)	89.16	89.16	85	85	89.64	89.64	86.16	86.16
δ (%)	5	5	7	7	20	8	> 70	40
δ_{\min} (%)	2	2.6	6.8	5.9	16.9	4.2	73	39.8
π (%)	99.96	99.96	88.96	92.31	95.4	99.85	< 86.1	86.5
Accuracy Class	A(5)	A(5)	A(5)	A(5)	C(15)	A(5)	>E(50)	E(40)

The errors in GVW obtained by the static approach are slightly less than for the dynamic approach. However, the static algorithm cannot estimate individual axle weights as accurately as the dynamic algorithm. The reason for the poor results obtained for axles in a group in Table 6 are related to the difficulty of distinguishing the effects of individual closely-spaced axles in bridge measurements for such a bridge (it would be expected to be better in shorter bridges).

6.4.4 Dynamic Bridge WIM Algorithm based on one sensor location

Applying the simultaneous dynamic equations at different sensor locations gives a very similar instantaneous value along the bridge as was shown in Figure 40. It seems therefore reasonable to hypothesise that a single sensor could achieve a similar accuracy. The difference from Moses's approach would be the use of the dynamic response due to a unit load instead of the influence line.

The formulation for this DB-WIM Algorithm is derived by minimising an error function defined by the squared difference between measured and theoretical strains. The error function is:

$$\Psi = \sum_{t=1}^{no_records} (\varepsilon_m(t) - \varepsilon_t(t))^2 \quad (30)$$

where $\varepsilon_m(t)$ is measured strain. $\varepsilon_t(t)$ is the total theoretical strain at a certain instant t derived in (25).

By substituting equation (25) into equation (30), it is found that:

$$\Psi = \sum_{t=1}^{no_records} (\varepsilon_m(t) - \sum_{i=1}^{no_axles} A_i \varepsilon_{i1}(t))^2 \quad (31)$$

Ψ is minimised by differentiating and setting to zero:

$$\frac{\partial \Psi}{\partial A_i} = 0 \quad (32)$$

which gives:

$$\sum_{t=1}^{no_records} [\varepsilon_m(t) - \sum_{i=1}^{no_axles} A_i \varepsilon_{i1}(t)] \varepsilon_{i1}(t) = 0 \quad (33)$$

Re-arranging equation (33) gives:

$$\sum_{t=1}^{no_records} \left[\sum_{i=1}^{no_axles} A_i \varepsilon_{i1}(t) \right] \varepsilon_{i1}(t) = \sum_{t=1}^{no_records} \varepsilon_m(t) \varepsilon_{i1}(t) \quad (34)$$

or, in matrix form:

$$[T]\{A\} = \{M\} \quad (35)$$

where $[T]$ is a matrix whose elements only depend on the total answer due to a unit load, axle spacings and speed:

$$[T]_{ij} = \sum_{t=1}^{no_records} \varepsilon_{i1}(t) \varepsilon_{j1}(t) \quad (36)$$

$\{A\}$ is a column vector composed of the unknown axle weights, and $\{M\}$ is a column vector that depends on the measured strain as well as the total answer due to a unit load, axle spacing and speed:

$$\{M\} = \sum_{t=1}^{no_records} \varepsilon_m(t) \varepsilon_{i1}(t) \quad (37)$$

Finally, axle weights are calculated as:

$$\{A\} = [T]^{-1} \{M\} \quad (38)$$

Gross Vehicle Weight (GVW) is obtained by summing the individual axle weights:

$$GVW = \sum_{i=1}^{no_axles} A_i \quad (39)$$

This formulation implies:

- Truck dynamics are removed through least squares fitting of all the readings along the bridge. The value that is obtained should be very close to the static answer.
- Bridge mass/inertia is taken into account in the formulation. No filtering techniques that rely on a sufficient number of vibration periods for a safe removal of bridge dynamics are necessary.

A two-axle vehicle model has been used to test this system based on one longitudinal position. The vehicle has been crossed over the bridge at 3 different speeds (15, 20 and 25 m/s) and 3 different loading conditions (empty, half and fully loaded). Road conditions are assumed to be good. The bridge has been modelled as a simply supported single span with a length of 32 m, 5.2% damping, and first natural frequency 3.58 Hz. The mechanical characteristics of the structure correspond to a real bridge in Slovenia. The accuracy class for GVW is A(5) and B(10) for the criteria of Gross Vehicle Weight and Single Axle respectively. The same accuracy class has been obtained by the static or the new dynamic Bridge WIM algorithm. This is due to the bridge length and first natural frequency, that allows for a sufficient number of natural periods of vibration to take place, so that re-

moval of dynamics by the traditional static approach is effective enough. (Note that accuracy classes obtained from simulations are not comparable to field results due to sources of error not accounted for in the simulations)

The dynamic algorithm based on one longitudinal location was tested in a long span bridge in Belleville (France) during the Continental Motorway Test. The bridge is a continuous two-span bridge of about 50 m per span (1.33 and 2 Hz are the first two natural frequencies). The section is made of a concrete slab and steel box. Longitudinal bending was measured at midspan of the first span and an accuracy class B(10) was obtained for gross weight in full repeatability conditions. Individual axle weights could not be estimated accurately as the vehicle acts as a whole concentrated load on such a long bridge. However, transverse bending of the concrete slab is more important and localised for this bridge than longitudinal bending of the steel box (more similar to a beam response), and its application in B-WIM systems could lead to more accurate results. A two-dimensional algorithm that allows for transverse position of the truck appears to be necessary if transverse bending is to be used for weight calculations in the near future.

Theoretical simulations have been carried out with different bridge finite element models (Figure 36(b)) (González 2001). Two- and three-axle trucks with front axle and rear single axle or tandem were used in the tests (individual axles of group spaced at 1.2 m). The set of two vehicles were crossed over the bridge with three loading conditions at three different speed levels and 'good' road conditions. The performance of three algorithms is compared in Table 7: a static algorithm based on one longitudinal location, DB-WIM as defined in this section, and a static multiple-sensor B-WIM algorithm. This table summarises accuracy results based on longitudinal strain and finite element simulations under limited reproducibility conditions. Other algorithms such as the spectral approach described in Section 6.4.2 or the dynamic version of the multiple-sensor B-WIM algorithm in Section 6.4.3, have not been considered. It was found that the first algorithm did not give good results when having more than two axles on a bridge. Compared to the dynamic multiple-sensor B-WIM algorithm, the static version of the multiple sensor system was preferred because the static B-WIM algorithm has generally been more accurate than DB-WIM and it involves fewer parameters (both one-sensor and multiple-sensor algorithms are based on the same equations).

A 30 m beam model (3.33 Hz first natural frequency) was used to analyse the influence of road profile and truck suspension on B-WIM accuracy. The system was calibrated with a two-axle linear sprung vehicle and tested with a four-axle non-linear sprung vehicle (11 degrees of freedom). Air and steel suspensions on both smooth and rough pavements were considered. In smooth road conditions, static multiple-sensor B-WIM achieved the most accurate overall class B+(7) (corresponding to the criterion of individual axle weights). The traditional static B-WIM had the same accuracy class, A(5), for gross vehicle weight as multiple-sensor B-WIM, but it failed to predict individual axle weights accurately (E(45)). The 30 m span length makes it difficult to identify individual axles from strain at only one location, and multiple-sensor B-WIM derives a more accurate value from the load history. DB-WIM was the most inaccurate system regardless of the criterion adopted. The performance of DB-WIM improves when considering air suspensions, but it cannot cater effectively for different dynamic behaviours. DB-WIM approximates the total strain with a particular dynamic model (i.e., based on moving constant loads). If this approximation is not good, then an averaging of all dynamics, as carried out in the static algorithm, gives better results.

In conclusion, the dynamic excitation of the bridge can produce very important errors. The level of this excitation will depend on the truck mechanical characteristics and the conditions of the road prior to and on the bridge. Rough road profiles result in very poor results for any existing B-WIM

algorithm. Weights of lorries with steel suspensions are estimated less accurately than those with air suspensions, as they are not as heavily damped. It has also been seen that the traditional static B-WIM algorithm generally achieves reasonable results in gross vehicle weight regardless of the accuracy in individual axle weights. The implementation of a static B-WIM algorithm is easier than a dynamic B-WIM algorithm. DB-WIM can only be justified in bridges with a smooth road profile, low natural frequencies and a high bridge dynamic component (e.g., if the bridge is too short and the strain response does not exhibit a sufficient number of dynamic oscillations to compensate for each other). A DB-WIM might also give a more accurate result when the total response is strongly influenced by speed (e.g., the maximum bridge response occurs for some pseudo-frequencies of the vehicle and a simple dynamic model can allow for this variation in the strain response better than a static approach). However, it is necessary to check that the dynamic bridge model approximates the measured strain well. A number of truck configurations representative of the traffic should be employed to ensure that the assumptions of the model are correct. This is a tedious task and it does not guarantee better accuracy in every case (see Table 7). For instance, in bridge responses with very high dynamics (i.e., ‘poor’ road profile), the estimation of gross vehicle weight by the traditional static algorithm (averaging the effect of dynamics) might result in greater accuracy than the DB-WIM attempt to model the total strain dynamically (as this match will be extremely difficult).

Table 7: Accuracy results for different bridge finite element models

Bridge type	Criterion	Algorithms based on one longitudinal location at midspan		Static Multi-Sensor
		Static	Dynamic	
Isotropic slab, 16 m long, 4.51 Hz (1 st natural frequency)	Single axle	C(15)	C(15)	A(5)
	Group of axles	B+(7)	B+(7)	A(5)
	Gross weight	A(5)	A(5)	A(5)
	Overall	C(15)	C(15)	A(5)
Two span isotropic slab, 18.5 m each span, 4.18 Hz (1 st nat. f.)	Single axle	D+(20)	B(10)	A(5)
	Group of axles	B+(7)	A(5)	A(5)
	Gross weight	A(5)	A(5)	A(5)
	Overall	D+(20)	B(10)	A(5)
Slab with edge cantilever, 20 m long, 4.80 Hz (1 st nat. f.)	Single axle	B(10)	C(15)	A(5)
	Group of axles	A(5)	A(5)	A(5)
	Gross weight	A(5)	A(5)	A(5)
	Overall	B(10)	C(15)	A(5)
Voided slab deck, 25 m long, 3.80 Hz (1 st natural frequency)	Single axle	D(25)	C(15)	C(15)
	Group of axles	C(15)	B+(7)	D+(20)
	Gross weight	A(5)	A(5)	C(15)
	Overall	D(25)	C(15)	D+(20)
Beam and slab, 20 m long, 6.13 Hz (1 st natural frequency)	Single axle	B+(7)	C(15)	A(5)
	Group of axles	A(5)	C(15)	A(5)
	Gross weight	A(5)	C(15)	A(5)
	Overall	B+(7)	C(15)	A(5)
Two span Cellular, 31 m each span, 2.95 Hz (1 st natural frequency)	Single axle	C(15)	B+(7)	C(15)
	Group of axles	B+(7)	A(5)	D(25)
	Gross weight	A(5)	A(5)	C(15)
	Overall	C(15)	B+(7)	D(25)

Accordingly, a static B-WIM algorithm is generally recommended (more accurate in bridges with relatively high natural frequency and low dynamics). If a high level of accuracy is required, a static multiple-sensor B-WIM algorithm can improve accuracy in individual axle weights over a single-sensor algorithm very significantly. However, there is still a need to analyse the number and location of sensors that guarantee a better instantaneous solution. If the bridge has a long span, multiple-sensor B-WIM might require an excessive number of sensors and other possibilities such as the measurement of transverse bending should be considered.

7. DURABILITY: FREE OF AXLE DETECTOR SYSTEMS

Since the development of bridge weigh-in-motion (B-WIM) systems in the early 1980's (Moses, 1979), axle detectors have traditionally provided information about velocity, axle spacing and category of the vehicle as it crosses the bridge. As they are the only part of the equipment directly exposed to traffic, this made them the element of the equipment most prone to deterioration. The idea of using a B-WIM system without any axle detectors was first considered by LCPC, France in response to requirements of the Chambre du Commerce du Havre concerning the Pont de Normandie. The thickness of the pavement on this bridge is quite thin. Therefore, in order to ensure and maintain the waterproofing of the deck, no axle detectors were allowed on the road surface. In response to this problem, the idea of 'Free of Axle Detector' (FAD) B-WIM system was considered whereby strain gauges underneath the bridge structure would be used for axle detection as well as weight calculation. Initial studies by Dempsey et al. (1998a) showed the feasibility of FAD systems for orthotropic decks. Žnidarič et al. (1999a) examined the use of short slab bridges for FAD B-WIM measurements. If successfully applied to a wider range of bridges, such approaches could considerably increase the durability of WIM systems, particularly in harsh climates. Theoretical models (dynamic truck interaction) were also developed to examine the feasibility of extending FAD systems to a wide range of bridge types.

7.1 Review of Bridge WIM Instrumentation - Strain Measurements and Axle Detection

Regardless of the type used, all B-WIM systems use an existing instrumented bridge or culvert from the road network. Main members of the structure are instrumented and strains are measured to provide information about its behaviour under moving vehicles. Most of the existing systems require axle or vehicle detectors on the pavement close to the bridge to provide vehicle type, velocity and axle spacings. Axle detectors in existing B-WIM systems can be either *removable*, such as tape switches, road hoses or similar pneumatic sensors, or *permanent* piezo-ceramic or other similar built-in pavement sensors.

Two detectors in each lane provide velocity of each axle and thus the dimensions, velocity and axle configuration of the vehicle (Figure 42). Depending on the data processing software, they are placed before or on the bridge. In its permanent form the installation process is the same as for bar sensors in pavement installations.

Strains are measured either by strain gauges or reusable strain transducers (Figure 43) which are attached to the main structural elements. In the past, mid-spans have been traditionally used as they generally provide the highest strain values, which were then used for axle weight calculations. Recent studies, however, showed that other locations could provide adequate or even improved information about structural behaviour under traffic.

7.2 Bridges Appropriate for FAD B-WIM Instrumentation

Although there is no theoretical limit to the number of axles (vehicles), which can be on the bridge during the measurements, it has been shown that shorter spans have several advantages (Žnidarič et

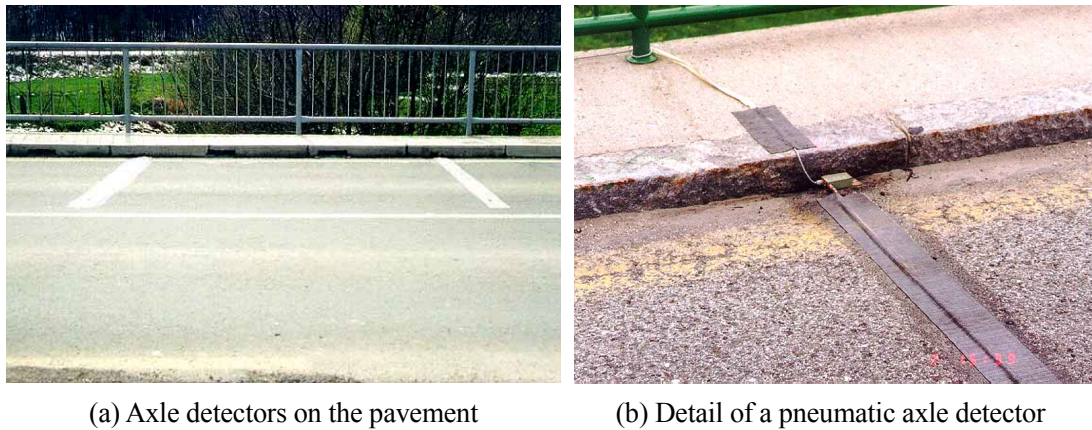


Figure 42: Existing B-WIM axle detection

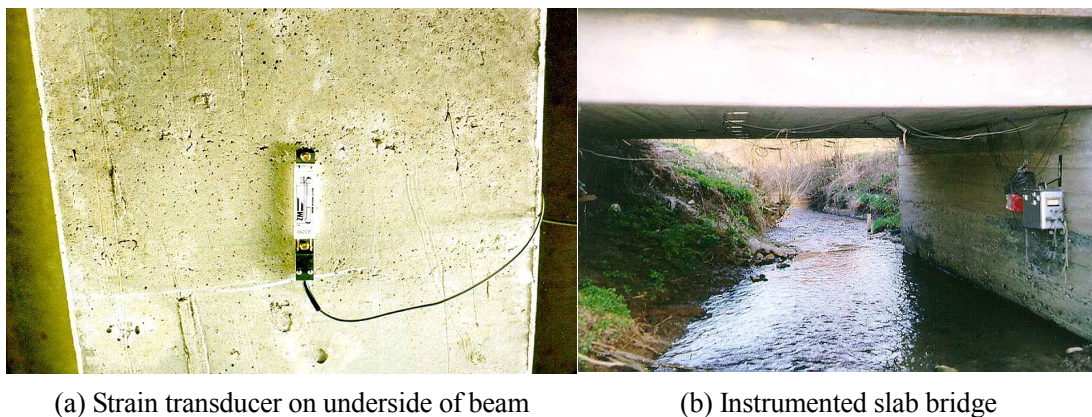


Figure 43: Existing B-WIM strain measurements

al., 1999a) over longer spans. One of them is that the contributions of individual, closely spaced axles are much easier to identify, which generally improves the accuracy of the measurements. Figure 4 (left) and (right) show typical strain responses from an 8 m long and 50 cm thick integral slab bridge and from a simply supported 32 m long beam bridge respectively. Both bridges were traversed by a 5-axle semi-trailer. For the first span, very sharp peaks for all, even closely spaced axles were recorded. For the latter bridge, all axle information was filtered from the response of the 4 times longer and much thicker superstructure. In addition, 4 Hz eigen-frequency of the bridge was excited and caused further noticeable difficulties in axle identification.

The general shape of the strain signals under the moving vehicle is defined by:

- the shape of the influence line (Figure 44),
- the ratio between the span length and the (short) axle spacings and
- the thickness of the instrumented superstructure.

Longer instrumented spans are more difficult to use for distinguishing individual axles. Even on thin superstructures the individual axle contributions in the total strain response are difficult to recognise when the ratio between the shortest axle spacing and the span exceeds 8.

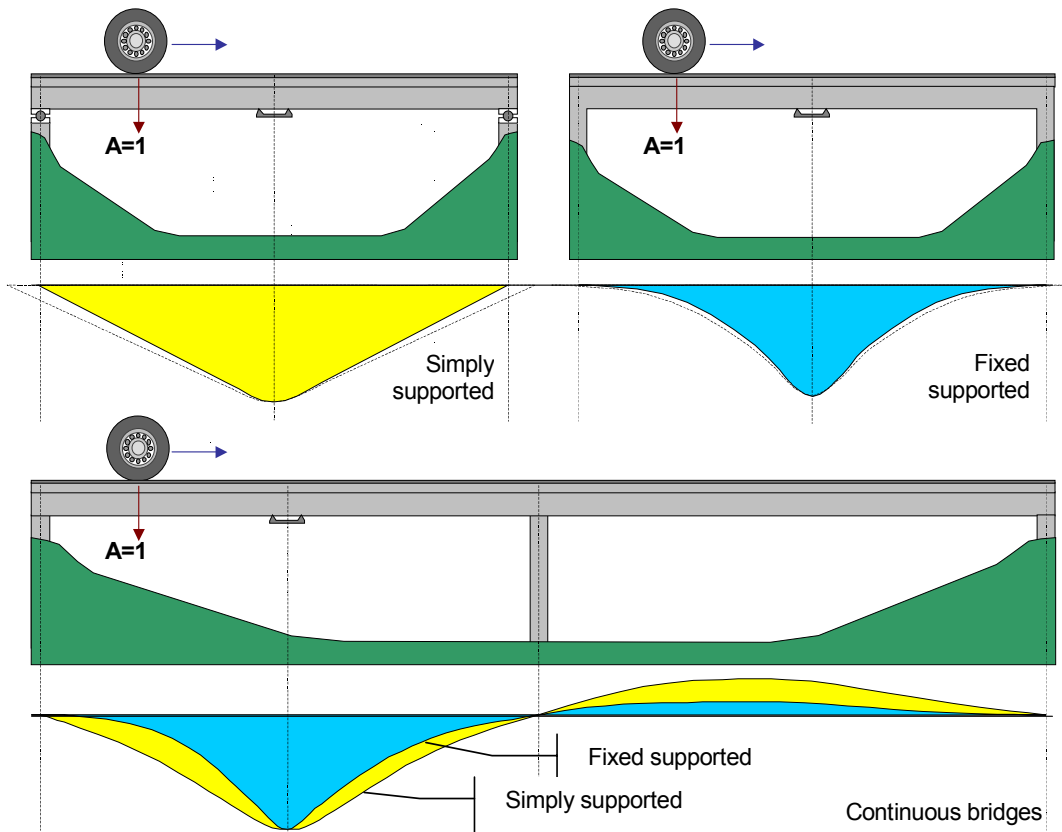


Figure 44: Influence lines for simply and fixed supported (integral) single-span bridge and for a 2-span bridge

Thickness of the superstructure is another extremely important parameter as it defines the sharpness of the peaks (to what extent the measured strain peaks are smoothed out, Figure 45). When the ratio between the width of a peak of the influence line, P_w , and its height, P_h , is more than 2, then the percentage of the closely spaced axes which can be identified, decreases rapidly. As can be seen from Figure 45, P_w and P_h depend on the shape of the influence line, the length of the span and the thickness of the superstructure.

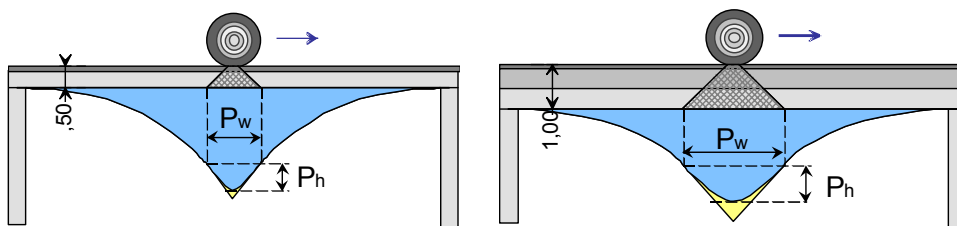


Figure 45: Influence of the superstructure thickness on the peak of the influence line

If bridge-vehicle interaction does not cause any dynamic problems, then the suitability of a span for FAD can be summarised by the FAD coefficient:

$$FAD = \frac{L \times H}{d_{min} \times f_i}$$

where L is the length of the span, H thickness of the superstructure, d_{min} minimal axle spacing and f_i influence line factor, defined according to Figure 46.

The first experiments showed that a span is appropriate for FAD measurements if the FAD coefficient is less than 2.

The effect of the superstructure thickness given a tandem axle spacing $d_{min}=15\%$ of the span length, is presented in Figure 47, (left). If thickness exceeds 5% of the span length, the strain peaks are clearly smoothed out. On the other hand, it is practically impossible to identify individual axes of such tandem on simply supported longitudinal members of the span (Figure 47, right) even when the thickness of the superstructure is only 5% of the span length.

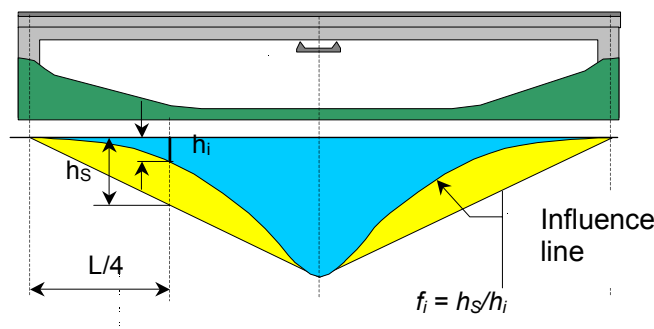


Figure 46: Definition of factor f_i

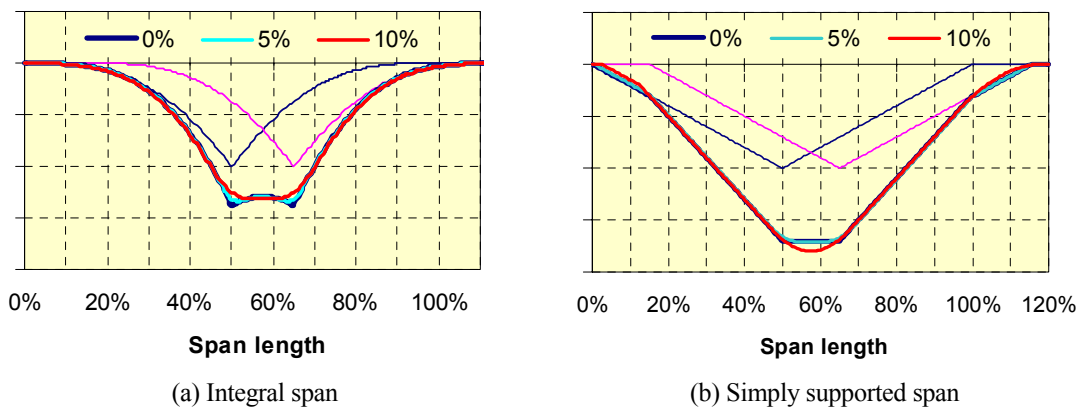


Figure 47: Responses of two bridge spans with 3 different superstructure thicknesses, expressed in percentage of the span length, to the passage of a tandem with axle spacing equal to 15% of the span length

Following the above rules, the good candidates for FAD B-WIM instrumentation are:

- short span, frame-type slab bridges (Figure 48, left) with typical f_i factor around 3 and FAD coefficient between 1 and 2 (the most common frame-type slab bridges are 6 to 12 m long concrete integral underpasses with thickness of the slab between 40 and 60 cm) and
- longer span bridges with thin slabs which is supported in the lateral direction by cross beams or stiffeners (orthotropic deck or similar bridges, Figure 48, right) with FAD coefficient below 0,5.

On the other hand, a 32 m long and 1.5 m thick simply supported beam bridge with a FAD coefficient of more than 40 does not match any of the above conditions and is clearly inappropriate for the FAD B-WIM measurements.



Figure 48: FAD installation on a short slab bridge (left) and instrumented section of the orthotropic deck bridge in Autreville (right)

7.3 Calculation of velocity and axle spacings

On bridges instrumented for FAD, the individual axles are generally easy to identify which makes velocity calculation a straightforward process. It generally requires calculating the time difference Δt between two first axle peaks from the strain records measured at two locations along the bridge. While at least two sections between the crossbeams are instrumented on the orthotropic deck bridges (Figure 49 (a)), short slab bridges are usually instrumented around $\frac{1}{4}$ and $\frac{3}{4}$ of the span (Figure 49 (b)). Time interval Δt is calculated either:

- by applying the identification algorithm which proved more efficient for the orthotropic deck bridges or
- by first defining the axle peaks from the signals and afterwards applying the same algorithm as with B-WIM systems with axle detectors.

7.3.1 Orthotropic FAD identification algorithm

Most orthotropic bridge decks consist of a steel plate (about 10 – 12 mm thick) supported by longitudinal stiffeners (normally trapezoidal in shape, but can vary from country to country). The longitudinal stiffeners are supported every 4-5 m in the longitudinal direction by transverse cross beams or diaphragm beams. Initial tests at the beginning of the *WAVE* project indicated that the sensitivity

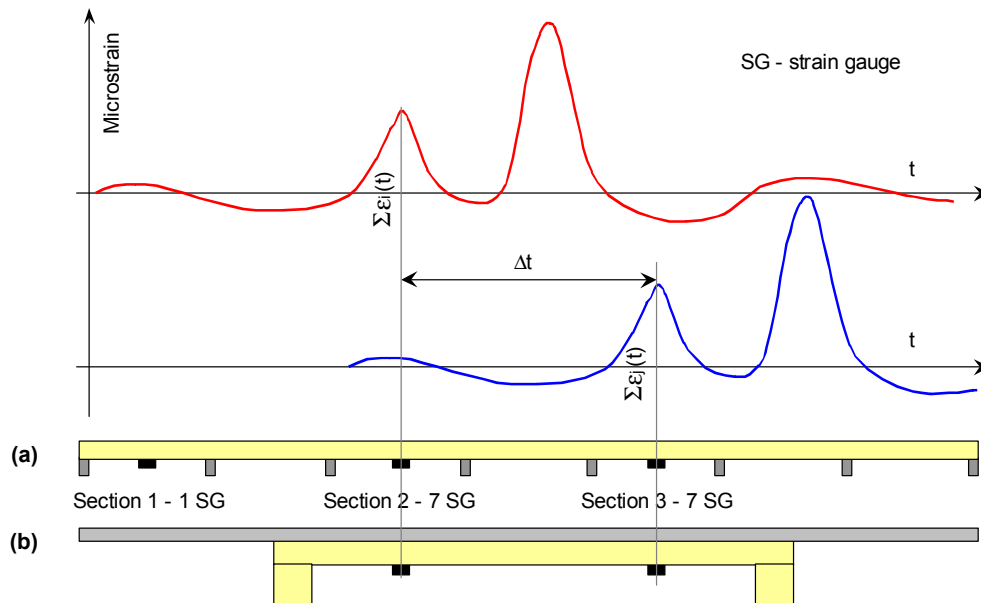


Figure 49: Schematic of (a) orthotropic deck and (b) short span slab bridge and response to passage of a 2-axle truck

of the orthotropic deck would make it possible to detect vehicle occurrences, number of axles, velocity and axle spacings solely from the measured strain recorded underneath the bridge. Therefore, an algorithm for the identification of trucks and the evaluation of number of axles, truck velocity and axle spacings was developed for orthotropic decks. The importance of the correct evaluation of velocity has been shown to be extremely important in B-WIM calculations (Dempsey, 1997; Žnidarič & Baumgärtner, 1998). Axle detectors on the road surface provided very accurate velocities but, as axle detectors are not allowed on the road surface for the orthotropic deck, the velocity has to be calculated directly from the strain gauges. This was achieved as follows: three sections were instrumented. The distance between the first and second and second and third instrumented sections was 9.24 m. The first section contained one strain gauge, which was placed on the stiffener located directly below the average right wheel path of trucks. The other two sections were instrumented more thoroughly with all 7 stiffeners in the slow lane being monitored.

The first part of the process was to accurately determine the velocity of the truck. The following optimisation procedure was used:

Find Δt , to minimise:

$$O(\Delta t) = \sum_{t=1}^T \left[\sum_{i=1}^G \varepsilon_i(t + \Delta t) - \sum_{j=1}^H \varepsilon_j(t) \right]^2$$

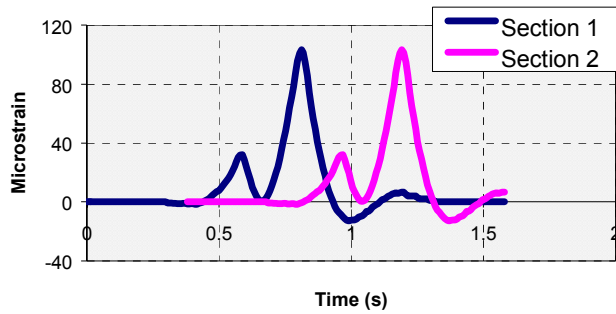
where:

- Δt = time taken for the truck to travel between the two instrumented sections,
- t = time,
- T = total time for the truck to cross the two-instrumented sections,
- G = number of instrumented stiffeners in section 1,

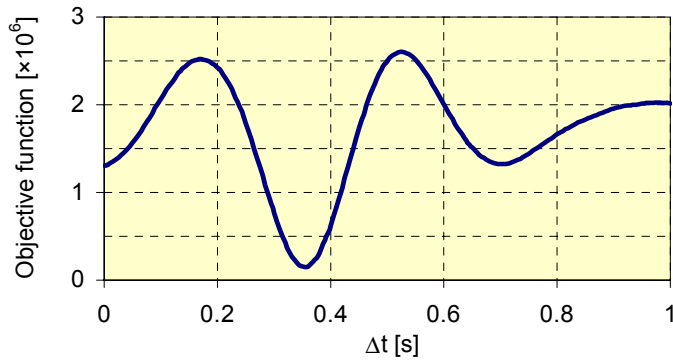
- H = number of instrumented stiffeners in section 2,
- $\varepsilon_i(t+\Delta t)$ = strain in the i^{th} gauge at time $t+\Delta t$,
- $\varepsilon_j(t)$ = strain in the j^{th} gauge at time t .

Figure 50(a) shows the measured response of the sum of the gauges in the two instrumented sections due to the passage of a 2-axle truck over an orthotropic bridge. Figure 50(b) illustrates the velocity objective function for various time shifts, Δt . It is evident that there is a clear and distinct global minimum of the objective function and, as the distance between the two-instrumented sections is known, the velocity can be readily calculated.

Once the velocity has been calculated, the next step is to identify the number of axles in the truck. Figure 48(right) shows the instrumentation of one section of the orthotropic deck. The response of this section to the passage of a 5-axle truck is shown in Figure 51. It is clear to see the response of the bridge to each of the truck axles (even individual axles within a tandem and tridem). Due to this sensitivity of the deck, it was possible to develop an algorithm to identify the necessary truck parameters. This algorithm for identifying axles peaks from the strain signals is outlined in Figure 52. The exact position of the maxima is located by finding the exact times that the first derivative of the strain changes from positive to negative. If the number of peaks identified at section 2 equals that of section 3 and the time between the peaks at both sections is similar to within a specified tolerance, then a vehicle event has been identified.



(a) Response of instrumented sections



(b) Evaluation of velocity objective function

Figure 50: Response of the sum of the gauges in the 2 instrumented sections due to the passage of a 3-axle truck

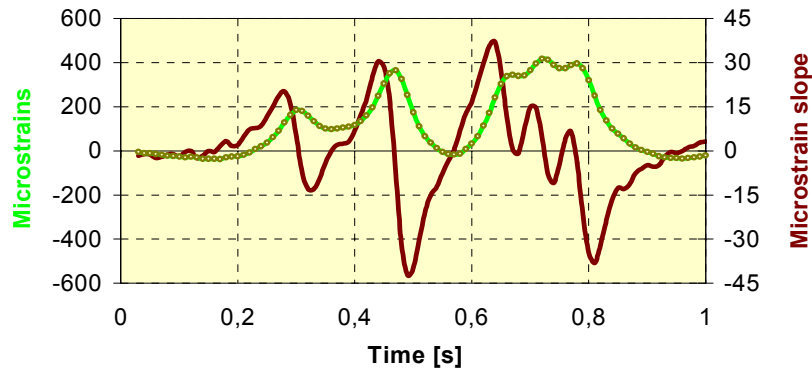


Figure 51: Response of one stiffener to the passage of a 5-axle truck

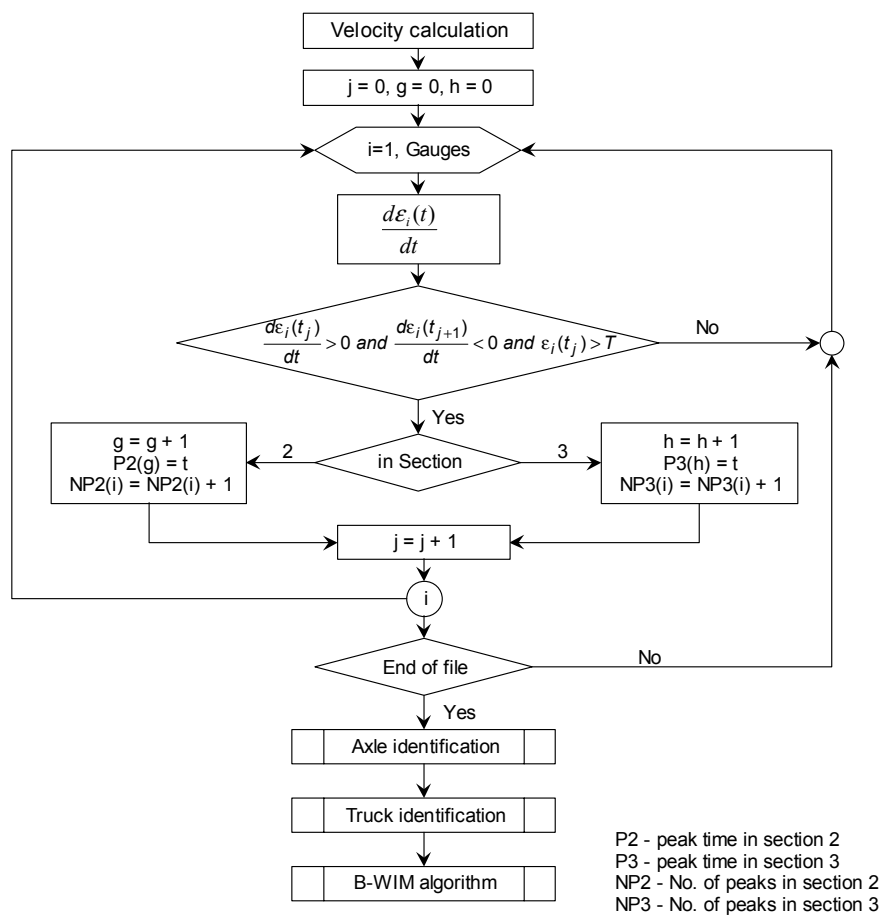


Figure 52: Axle peak identification algorithm for orthotropic deck B-WIM

7.4 Upgrade of the SiWIM Software for FAD

To provide automatic real-time axle detection based on measured strain signals from short slab bridges, a new module for the SiWIM software is under development. As in the orthotropic deck B-WIM algorithm described above, it searches for axles by permanently monitoring the amplitude of the strain signal, y_b , at every point t (Figure 53). For each of these points, axle checks are performed according to the flow chart in Figure 54. The following 5 parameters are needed:

- N - number of points in the averaging interval
- T - threshold level of the signal; values under this level are discarded in the calculation
- T_T - threshold level to differentiate between axles of trucks and those of cars
- D_T - required difference between $(P_t - P_{t-1})$ and $(P_t - P_{t+1})$ for trucks
- D_C - required difference between $(P_t - P_{t-1})$ and $(P_t - P_{t+1})$ for cars

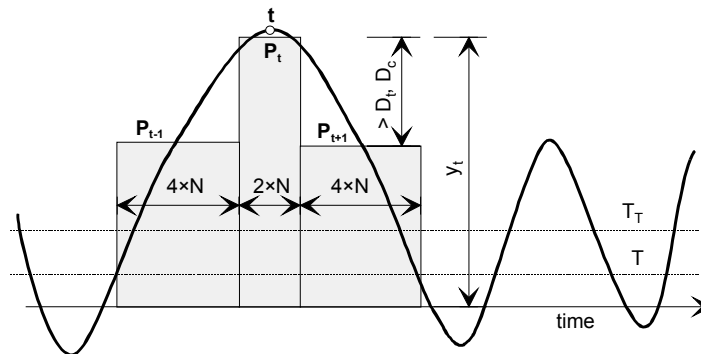


Figure 53: Values of P_t , P_{t-1} and P_{t+1} evaluated from the strain signal

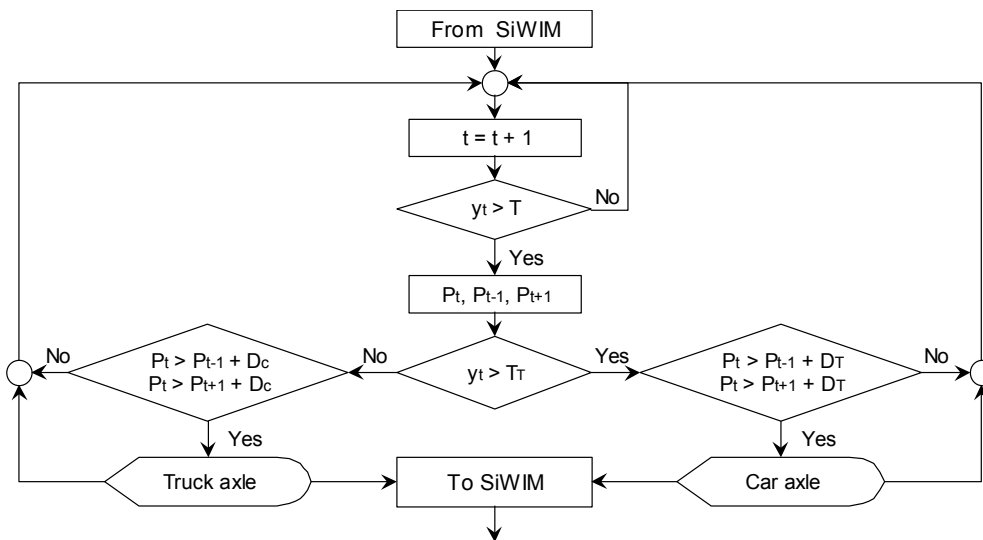


Figure 54: Flowchart outlining the FAD modulus in SiWIM software

An axle is defined based on the three average values:

$$P_t = \frac{1}{2 \times N} \times \sum_{i=t-N}^{t+N} y_i, \quad P_{t-1} = \frac{1}{4 \times N} \times \sum_{i=t-5 \times N}^{t-N}, \quad P_{t+1} = \frac{1}{4 \times N} \times \sum_{i=t+N}^{t+5 \times N} y_i$$

A typical screen display from the SiWIM software, implementing the FAD algorithm, is presented in Figure 55.

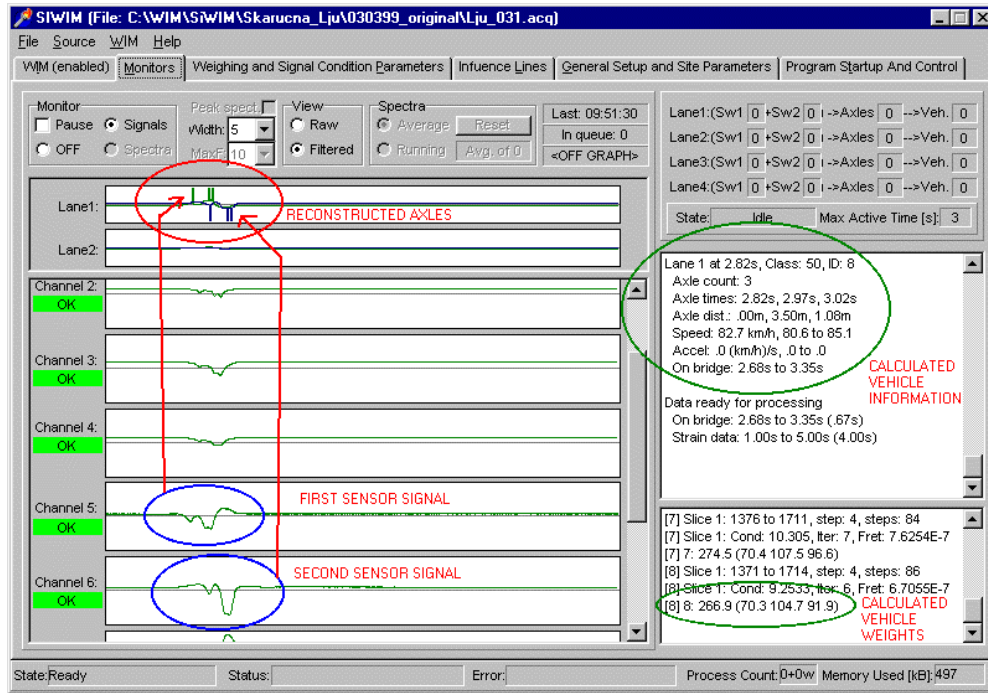


Figure 55: FAD implementation in the SiWIM software

8. TESTING THE ACCURACY OF B-WIM SYSTEMS

8.1 Orthotropic Bridge Weigh-in-Motion

8.1.1 Instrumentation and Experimentation

The Autreville bridge over the Moselle river in eastern France on the A31 between Metz and Nancy was chosen as the bridge to develop and test the prototype B-WIM system for orthotropic decks. There were two reasons for this: (a) ease of accessibility for instrumentation and experiments and (b) its location close to the Continental Motorway Test (CMT) (Stanczyk & Jacob, 1999). (The CMT is a test of WIM systems carried out under the guidance of the European Commission, DG VII, COST – Co-Operation Science and Technology Transport programme, COST 323 ‘Weigh-in-Motion of Road Vehicles’). This consists of testing several marketed and commercially available pavement based WIM systems on the same stretch of motorway on the A31 in eastern France. Trucks were randomly stopped from the traffic flow and their static axle and gross vehicle weights were determined from portable axle scales. The WIM weights recorded as the truck passed the WIM systems were compared to the measured static weights in order to determine the accuracy of each system. This provided easy access to a large database of truck weights and characteristics, which was used to validate and classify the accuracy of the system in determining truck characteristics including axle and gross vehicle weights.

The Autreville bridge (Figure 56), on the A31 motorway, is approximately 10 km downstream of the CMT site. The bridge consists of three spans (74.5m, 92.5m and 64.75m). There are four lanes and two emergency lanes, which are carried by an orthotropic steel plate of approximately 30.5m in width. It is supported by longitudinal stiffeners, which are trapezoidal in shape at 600mm centres. The longitudinal stiffeners are supported every 4.62m by transverse cross beams, which span between the two main I-beams (3.8m in depth) of the bridge (Figure 58). During the project, the layout of bridge instrumentation was changed in order to improve the identification and weight calculation algorithms. The instrumentation consisted of strain gauges, which were placed in the longitudinal direction on the bottom of the longitudinal stiffeners (Figure 57 and Figure 58). The final configuration consisted of three instrumented sections. The first section consisted of one strain gauge which was used as a warning or alert sensor to initiate the recording of strain in the other two instrumented sections. The second and third sections were used to identify vehicles, calculate number of axles, truck velocities, axle spacings, axle and gross vehicle weights and are, therefore, instrumented more thoroughly. For both of these sections, a strain gauge was placed on each of the seven stiffeners under the slow lane. Figure 57 and Figure 58 illustrate the details of these two instrumented sections.

The experimental test programme was divided into two different stages. The first consisted of a series of tests to determine the feasibility of using orthotropic decks as WIM sites. This included initial tests with three different truck configurations, determination of experimental transverse and longitudinal influence lines using trucks of known weight, tests with an instrumented truck and the study of dynamic effects induced in the bridge by the passage of two different trucks at a range of velocities. These tests were also used to aid the development of the algorithms and to test them.



Figure 56: Autreville bridge in eastern France

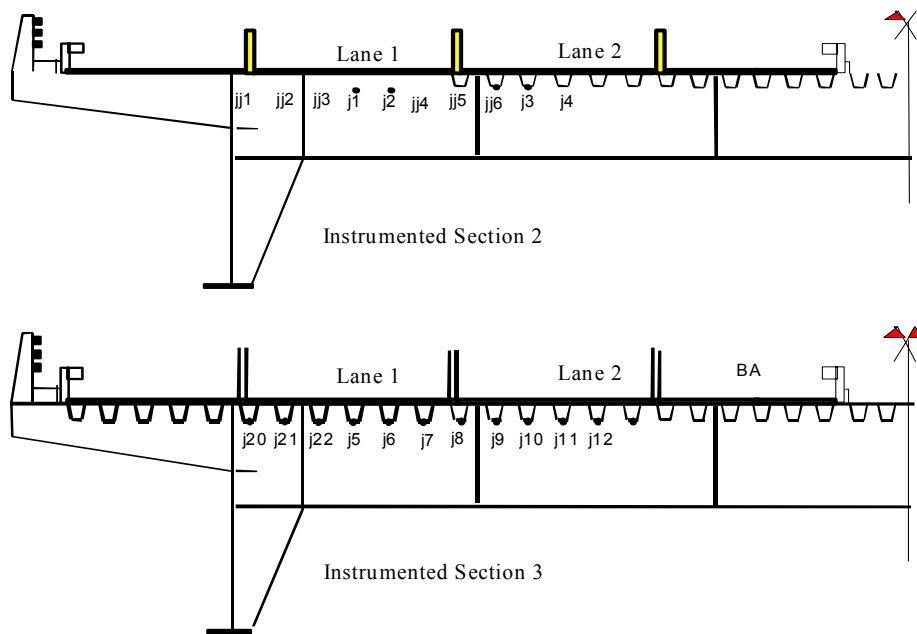


Figure 57: Schematic of instrumented sections 2 and 3



Figure 58: Details of transverse cross beams supporting the longitudinal stiffeners and instrumentation

The second series of tests was conducted within the framework of the COST 323 CMT programme, in which trucks were stopped from normal traffic and their vehicle registration, number of axles, axle spacings, axle weights, tyre types and suspension types were all recorded. As the trucks passed the bridge, they were identified and the strains in the instrumented sections were recorded. These strains were then passed through the weight calculation algorithm and a comparison made between the WIM weights and the static reference weights. Table 8 gives a more detailed outline of the experimental test programme.

Table 8: Experimental Programme on Autreville Bridge

Date	Type of Test	Number of Trucks
Nov-96	Controlled Test (Initial Test)	3 (4 passes each)
Apr-97	Controlled Test (Transverse Location Effects)	1 (12 passes)
Apr-97	Static Weighing of Random Trucks (CMT)	2
Aug-97	Static Weighing of Random Trucks (CMT)	16
Mar-98	Controlled (Static and Dynamic Effects)	2 (31 passes each)
Mar-98	Static Weighing of Random Trucks (CMT)	13
Jun-98	VTT Instrumented Truck	1 (5 passes)
Aug-98	Static Weighing of Random Trucks (CMT)	28
Mar-98	Static Weighing of Random Trucks (CMT)	7
Mar-98	Controlled Test (Multiple Presences)	2 (8 passes each)

8.1.2 Results and Accuracy Classes

In order to verify the proposed identification algorithm described above, it was tested on some experimental data collected in August 1997 and July 1998. Seventeen trucks of different configurations and axle weights were stopped from the traffic flow. They were weighed statically axle by axle at a static weighing station just before the Obron test site (Continental Motorway Test). The axle spacing, width of wheelbase and type of wheels (twin, single or wide based) were recorded and a photograph of each truck was also taken. As these trucks approached the bridge, they were identified from the traffic flow and the strains in the two instrumented sections were recorded as the trucks crossed the bridge. The transverse position of the trucks and the velocity of the truck was also determined using an infra-red transmitter and receiver.

The FAD algorithm failed to identify only one of the forty-four trucks. The truck which was not identified, had two different sets of unloaded closely spaced axles. However, this truck was identified correctly when it was initially assumed to be a 6-axle truck in the identification algorithm. The strain records for each of these trucks were passed through the algorithm described above. The output velocity was compared to the value of the velocity which was measured by the infra-red system, the axle spacings were compared to those values which were measured at the weighing station, and the WIM axle and gross vehicle weights were compared to the static axle weights. Figure 59 illustrates the accuracy of the calculated WIM weights with respect to the static weights. The accuracy of the calculated velocities was found to be within the accuracy tolerance of $\pm 5\%$. The errors in the calculated axle spacings were also found to be within the upper and lower bound limit require-

ments for the axle spacing parameter as described in section 6.1.4. Figure 59 and Table 9 show the accuracy classes obtained according to the COST 323 specification. The accuracy class obtained for each of the categories was found to be D+(20). This means that, for approximately 95% (the exact figure depends on the test conditions) of the trucks considered in the sample, the accuracy of the calculated gross vehicle weights is $\pm 20\%$.

As already mentioned, it was found that the variation in transverse locations of the trucks within lanes had a significant effect on the amplitude of the bridge response. This led to the development of the optimisation algorithm based on a two-dimensional bridge model, which allows for the different responses of the stiffeners depending on their position relative to the transverse location of the truck. This effect of the transverse location on the accuracy of the calculated axle and gross vehicle weights was due to the extreme sensitivity of the orthotropic deck and the stiffening effect of the main I-beams of the bridge on the longitudinal stiffeners closest to it. This effect was negated by using the optimisation algorithm based on the 2-dimensional bridge model (Figure 60(b)). This resulted in an improvement in the accuracy class from D+(20) (Table 9) where the 1-D bridge model was used, to C(15) (Table 9) where the 2-D bridge model was used in the optimisation algorithm.

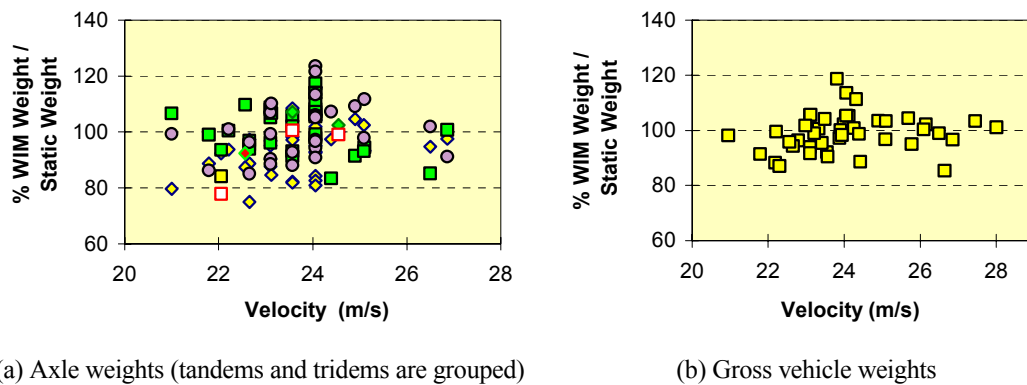


Figure 59: Results from optimisation and identification algorithm

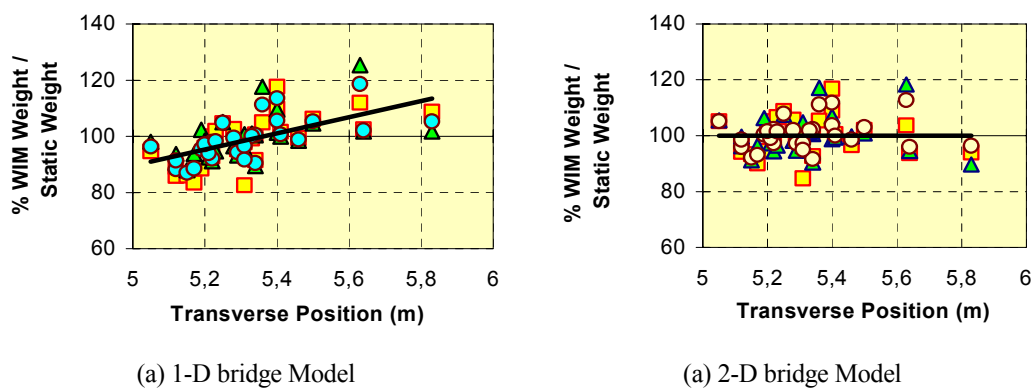


Figure 60: Comparison of accuracy for gross vehicle weights calculated from optimisation algorithms

Table 9: Accuracy classification according to COST 323 specification

Criterion	Number	Mean (%)	St.dev. (%)	π_0 (%)	Class	δ (%)	δ_{\min} (%)	π (%)	Class retained
Single axle	89	3.79	10.10	92.6	D+(20)	25	21.6	96.4	D+(20)
Group of axles	44	0.5	10.12	91.0	D+(20)	23	20.7	94.4	
Gross weight	44	1.12	7.61	91.0	D+(20)	20	15.7	97.4	

Table 10: Accuracy classification according to COST 323 specification (optimisation algorithm based on 2-D bridge model)

Criterion	Number	Mean (%)	St.dev. (%)	π_0 (%)	Class	δ (%)	δ_{\min} (%)	π (%)	Class retained
Single axle	55	0.79	8.95	91.6	C(15)	20	18.3	91.6	C(15)
Group of axles	27	0.17	8.22	89.1	C(15)	18	16.9	89.1	
Gross weight	28	0.55	5.55	89.3	C(15)	15	11.5	89.3	

8.2 Tests in Lulea, Sweden

A series of tests were carried out at a site adjacent to the COST 323 *Cold Environment Test* near Lulea, Sweden. This was part of Workpackage 3.1 (Cold Climates) and full details are given in that report. A brief summary is given here for comparison with other B-WIM results.

The bridge selected for instrumentation is at the Southern end of the test site at Alean. It is a two-span integral bridge with two equal spans of 14.6 m and is straight in plan. The bridge deck has a mid-span depth of 550mm and is solid in cross-section. Traffic is carried by one lane in each direction with no central median.

On site, eight mechanical strain amplifiers were bolted to the centre of the soffit of the bridge under the southbound carriageway of the first (North) span. Pneumatic tubes were fixed across the southbound lane, one before the bridge and the second immediately at the end of the first span with a recorded distance between them.

As the data collection was not automatic, the Bridge WIM system only participated when Trinity College or University College Dublin staff were present, namely, in June 1997 (1st Summer), March 1998 (Winter) and June 1998 (2nd Summer). In all three cases, the system was re-installed and re-calibrated. Data from strain transducers was recorded and stored by TCD/UCD staff as the post-weighted trucks passed over the bridge. The resulting raw data was subsequently post-processed.

Repeated runs of two calibration trucks provided by the Swedish National Roads Administration were used to calibrate the system for each of the tests. Once calibration was carried out, there was no further adjustment of the mechanical strain amplifiers for the remaining period of the tests. Traffic control was not used during these passes.

The first Summer test was performed from 10th to 12th of June 1997. However only data from Wednesday 11th and Thursday 12th was recorded due to problems with the data acquisition system on June 10th. The Winter test was performed from 11th to 13th March 1998. The second Summer test was performed on the 15th and 16th June 1998. A 4 Hz analogue filter was utilised in the data acqui-

sition for the 1st Summer and the Winter tests. It will be shown that this resulted in a loss of definition in the bridge response and therefore, virtually unfiltered data was used for the 2nd Summer test.

The data was processed independently in ZAG and TCD/UCD using different Bridge WIM algorithms. The algorithm developed by ZAG is known as SiWIM (described in section 5) while that developed in Trinity College Dublin and University College Dublin will be referred to as DuWIM.

8.2.1 TCD/UCD Results (DuWIM)

The DuWIM B-WIM algorithm is based on the principles outlined by Moses (1979). It consists of finding the values of axle weights that minimise the objective function,

$$O = \sum_{i=1}^K \{\varepsilon_A^M(x_i) - \varepsilon_A(x_i)\}^2$$

where:

$\varepsilon_A(x_i)$ = theoretical strain at A when the first axle is at a distance x from the start of the bridge,

K = number of scans while the truck is on the bridge,

$\varepsilon_A^M(x_i)$ = measured strain when the first axle is at a distance x_i from the start of the bridge

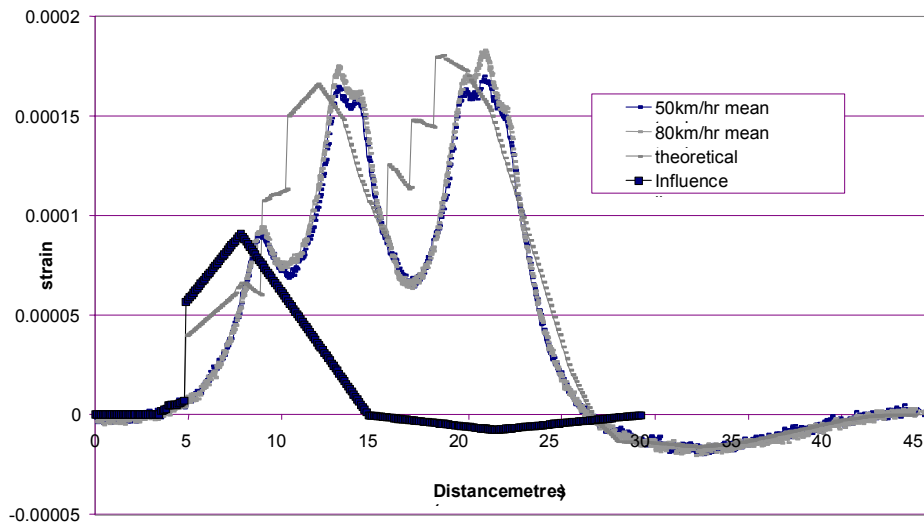
Individual axle weights are summed to determine the gross vehicle weight.

A unique feature of the DuWIM approach was a ‘point by point’ graphical method of manually deriving the influence line from the bridge response to the calibration truck. The process starts with a crude estimate of the influence line (consisting of a series of line segments) and the corresponding theoretical response of the bridge to the calibration truck. At this stage the match between experiment and theory is quite poor.

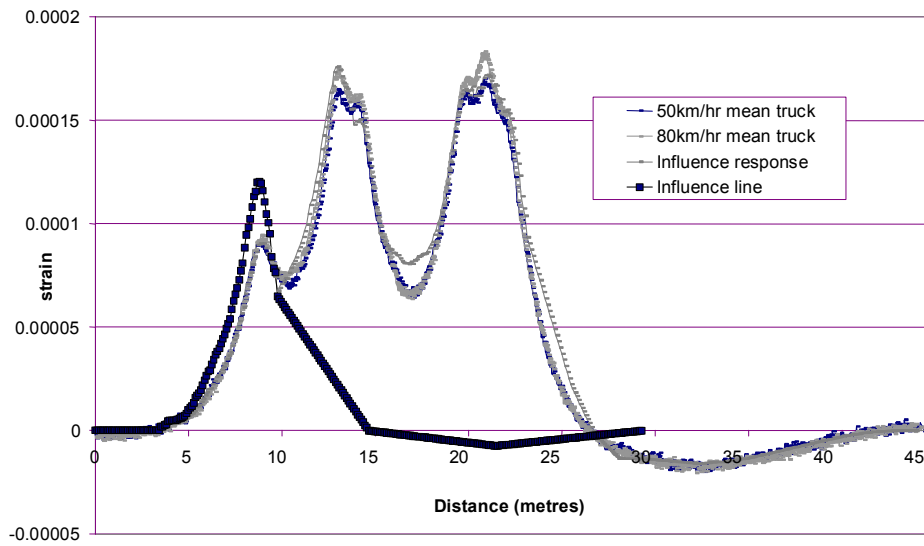
Adjustments are made to the influence line on the basis of a graphical comparison of theory and measurement in a spreadsheet. The first adjustment to the influence line is to multiply all the negative values (that is, the strain in one span due to a unit load in the other span) by a calibration factor. The calibration factor is adjusted until there is a match between the negative portion of the theoretical response and the negative portion of the calibration trucks.

The next step is to adjust the values in the positive part of the influence line. This is done on a ‘point by point’ basis. To start with, the first points at the start of the influence line should be adjusted as, for the first 4.2 m of the influence response, there is only one axle on the bridge (the distance between the first axle and the second is 4.2 m in this case). Hence, all these points should be adjusted first – Figure 61(a).

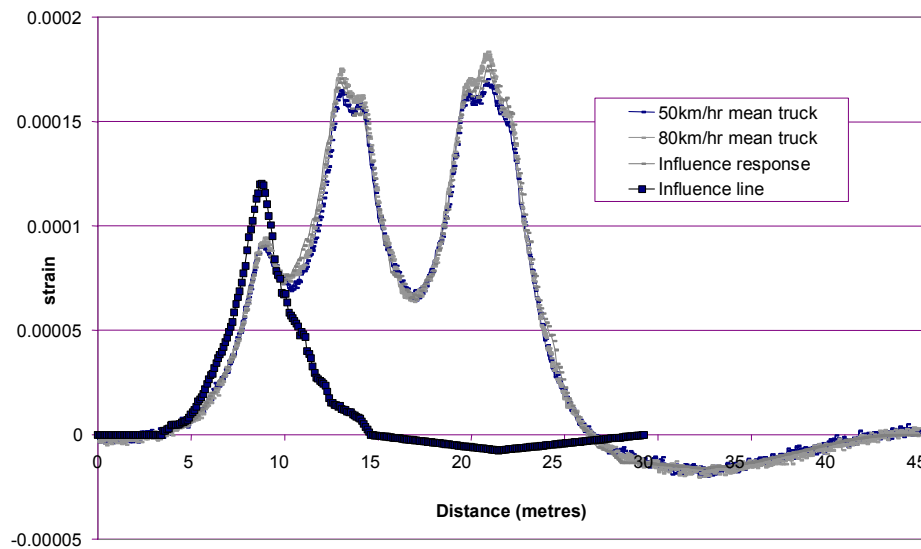
After 4.2 m, each change in the influence line affects two points (for a 2-axle calibration truck) in the theoretical response. However, the solution is easily identified graphically. The comparison at this stage is illustrated in Figure 61(b). The method is continued point by point until a good match has been made between the theoretical response and the complete calibration truck measurements – Figure 61(c). As can be seen from the figure, the agreement between the theoretical and measured responses is very close. This experimental influence line is now ready to be used in an analysis.



(a) Match when only 1 axle is on bridge



(b) Adjustment to middle portion of influence line



(c) Final influence line and match

Figure 61: Point by point process

Graphical results from the DuWIM algorithm for the 1st Summer test are presented in Figure 62. The data was analysed in accordance with the COST323 draft specification and the results are presented in Table 11. An accuracy class of C(15) was returned.

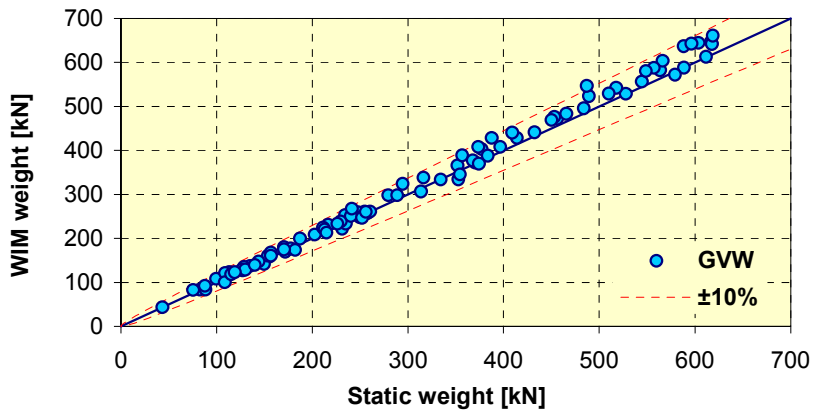
Table 11: Results of the first Summer Test

Criterion	Number	Mean (%)	St.dev. (%)	π_0 (%)	Class	δ (%)	δ_{\min} (%)	π (%)	Class retained
Single axle	156	-0,25	8,43	93,5	C(15)	20	17,0	97,2	C(15)
Group of axles	162	2,09	5,93	93,5	B(10)	13	12,6	94,4	
Gross weight	95	1,49	4,01	92,8	B(10)	10	8,6	96,6	

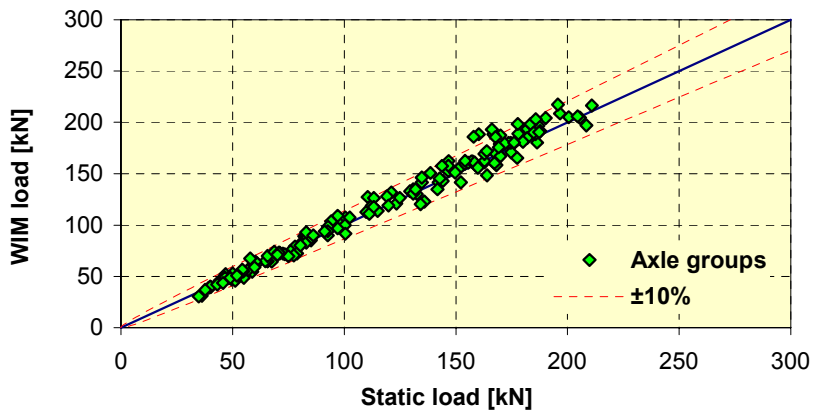
Graphical results from the Winter test are presented in Figure 63. The accuracy classification in accordance with the COST 323 draft specification are presented in Table 12. As for the 1st Summer test, an accuracy class of C(15) was returned.

Table 12: Results of the Winter Test

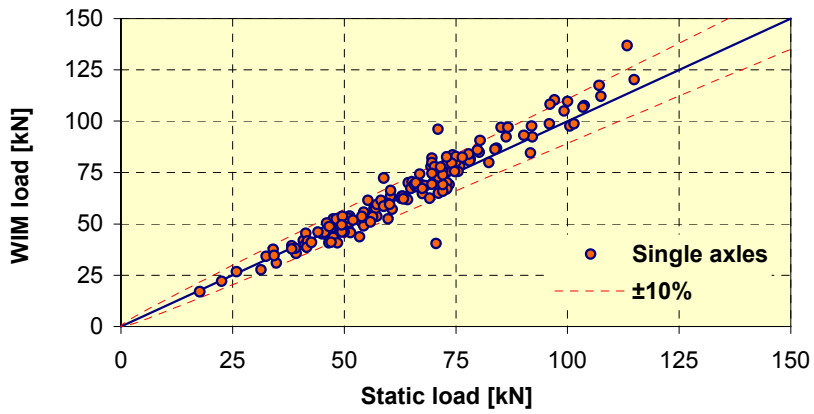
Criterion	Number	Mean (%)	St.dev. (%)	π_0 (%)	Class	δ (%)	δ_{\min} (%)	π (%)	Class retained
Single axle	164	-0,64	8,45	93,5	C(15)	20	17,1	97,1	C(15)
Group of axles	220	-1,77	8,40	93,8	C(15)	18	17,2	95,0	
Gross weight	116	-1,49	7,20	93,1	C(15)	15	14,8	93,5	



(a) Gross Vehicle Weights

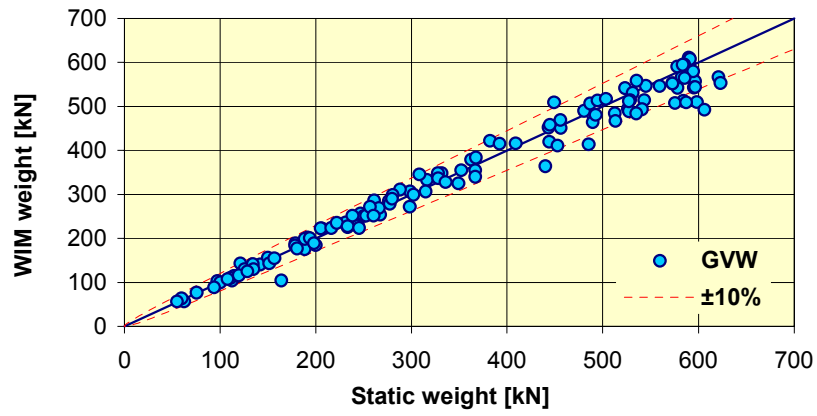


(b) Axle Groups

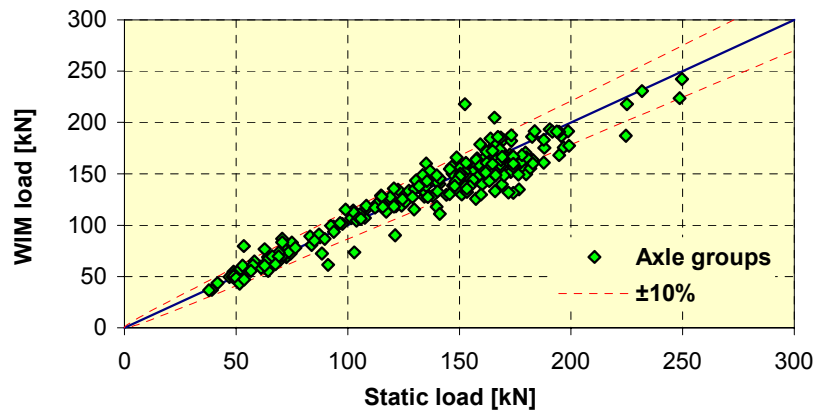


(c) Single Axles

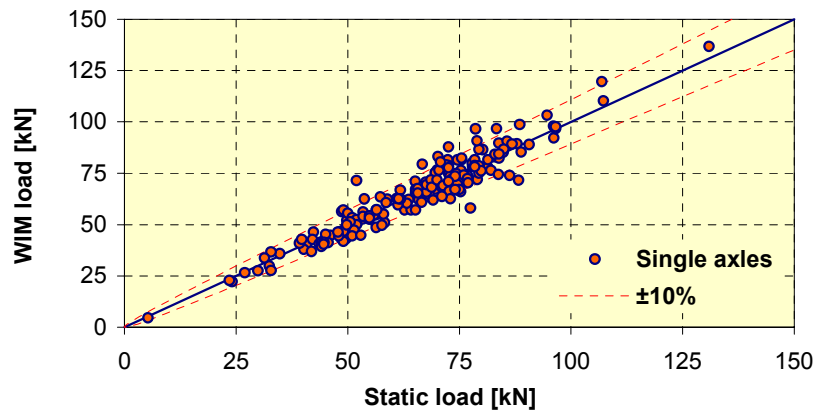
Figure 62: Graphs of WIM versus Static Weights for the 1st Summer Test; (a) Gross Vehicle Weights, (b) Axle Groups, (c) Single Axles



(a) Gross vehicle weights



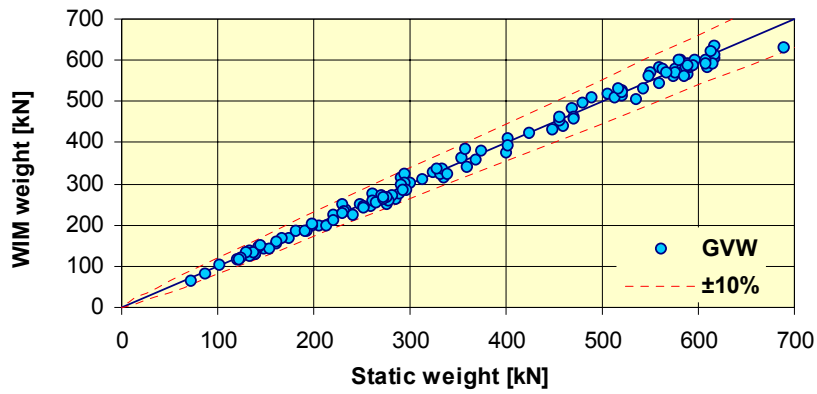
(b) Axle groups



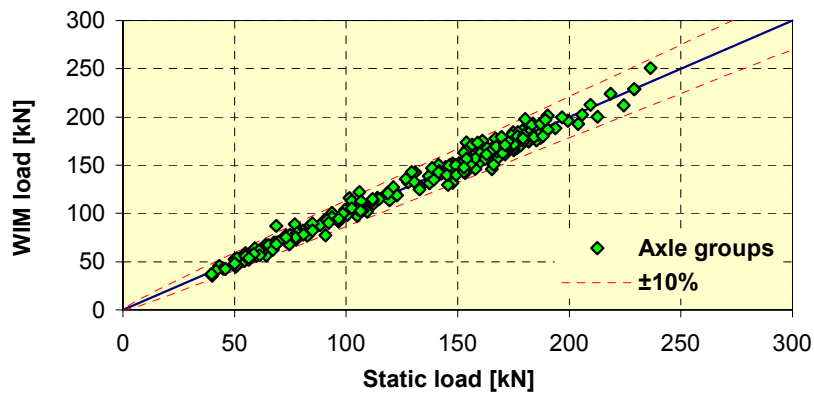
(c) Single axles

Figure 63: Graphs of WIM versus Static Weights for Winter Test; (a) Gross Vehicle Weights, (b) Axle groups, (c) Single axles

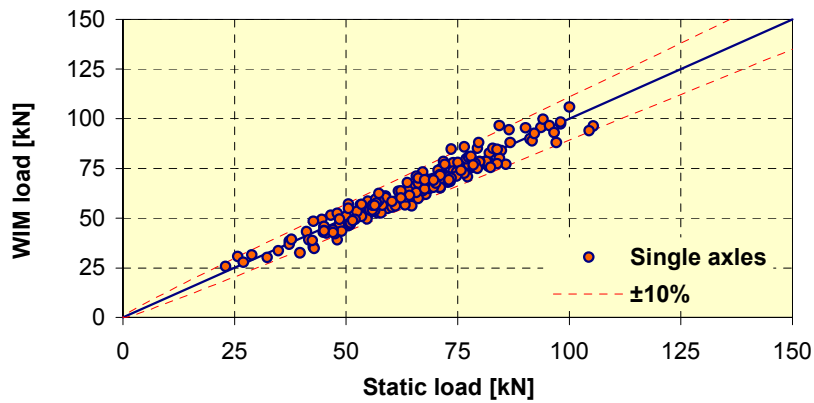
Graphical results from the 2nd Summer test are presented in Figure 64. The accuracy classification in accordance with the COST 323 draft specification is presented in Table 13. This time, without filtering, an accuracy class of B(10) was returned.



(a) Gross vehicle weights



(b) Axle groups



(c) Single axles

Figure 64: WIM versus static weight for 2nd Summer test; (a) Gross vehicle weight, (b) Group of axle weights, (c) Single axle weights

Table 13: Accuracy classification for 2nd Summer Test

Criterion	Number	Mean (%)	St.dev. (%)	π_0 (%)	Class	δ (%)	δ_{\min} (%)	π (%)	Class retained
Single axle	188	-1,31	7,27	93,7	B(10)	15	14,8	94,0	B(10)
Group of axles	239	-0,18	5,26	93,9	B(10)	13	10,6	98,0	
Gross weight	122	-0,88	3,72	93,1	B(10)	10	7,7	98,4	

8.2.2 ZAG Results (SiWIM)

Full details of the ZAG analysis of the Lulea tests are given in the report for WP3.1; a summary is provided here. Table 14 to Table 16 depict accuracy results from the random traffic measurements the 1st Summer, Winter and 2nd Summer tests respectively.

Table 14: Accuracy of the CET bridge WIM measurements from 1st Summer Test

Criterion	Number	Mean (%)	St.dev. (%)	π_0 (%)	Class	δ (%)	δ_{\min} (%)	π (%)	Class retained
Single axle	177	0,22	8,97	93,6	C(15)	20	18,1	96,1	C(15)
Group of axles	150	0,35	6,24	93,4	B(10)	13	12,6	94,3	
Gross weight	95	-0,60	5,49	92,8	C(15)	15	11,2	98,6	

Table 15: Accuracy of the CET bridge WIM measurements from Winter Test (with and without temperature compensation)

Type	Criterion	Number	Mean (%)	St.dev. (%)	π_0 (%)	Class	δ (%)	δ_{\min} (%)	π (%)	Class retained
Random traffic R2	Single axle	174	1,46	7,95	93,6	C(15)	20	16,2	97,9	C(15)
	Group of axles	214	-0,41	8,51	93,8	C(15)	18	17,1	95,1	
	Gross weight	114	0,11	5,75	93,0	C(15)	15	11,6	98,3	
Random traffic Temp.	Single axle	174	0,67	7,69	93,6	C(15)	20	15,5	98,4	C(15)
	Group of axles	214	-1,13	7,90	93,8	C(15)	18	16,0	96,5	
	Gross weight	114	-0,61	5,11	93,0	C(15)	15	10,4	99,3	

For the second Summer test, the results of the random traffic did not give satisfactory results initially. The main reasons observed were several miss-matches of the trucks weighed on B-WIM system and on the static scales and absence of air temperature data. Results before and after adjustments are presented in Table 16. SiWIM results for all three periods are presented in Figures 66 to 68.

Table 16: Accuracy of the CET bridge WIM measurements from June 1998, (I)

Type	Criterion	Number	Mean (%)	St.dev. (%)	π_0 (%)	Class	δ (%)	δ_{\min} (%)	π (%)	Class retained
Random traffic R2	Single axle	225	-1,48	13,50	93,8	D(25)	30	27,3	96,1	D(25)
	Group of axles	232	-3,05	11,73	93,9	D(25)	28	24,3	97,0	
	Gross weight	125	-2,26	8,76	93,2	D+(20)	20	18,2	95,7	
Random Traffic Adj.	Single axle	187	0,75	6,42	93,7	B(10)	15	13,0	96,9	B(10)
	Group of axles	191	-0,86	5,75	93,7	B(10)	13	11,7	96,2	
	Gross weight	104	-0,03	2,83	92,9	B+(7)	7	5,7	97,5	

8.2.3 Integral slab bridge

The 9° skewed integral bridge (Figure 65), with a 60 cm thick and 10.00 m long slab, is a typical underpass located on Slovenian motorways. Four strain transducers were installed to acquire data for the SiWIM algorithm. Unfortunately, only channel 2 was properly amplified and consequently, all results were calculated from *strains from one transducer only*. The pavement was moderately smooth, with no obvious bump before the bridge. A low-speed WIM station was in operation 1.6 kilometres from the site, providing reference weights to test the accuracy in full reproducibility conditions (COST 323, 1997b).

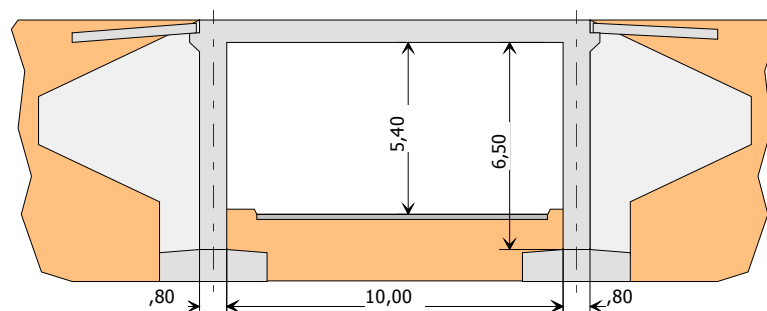
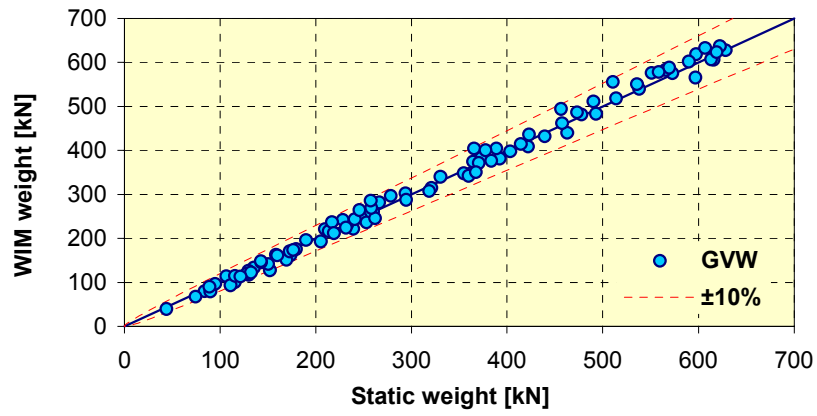


Figure 65: Side elevation of an integral slab bridge

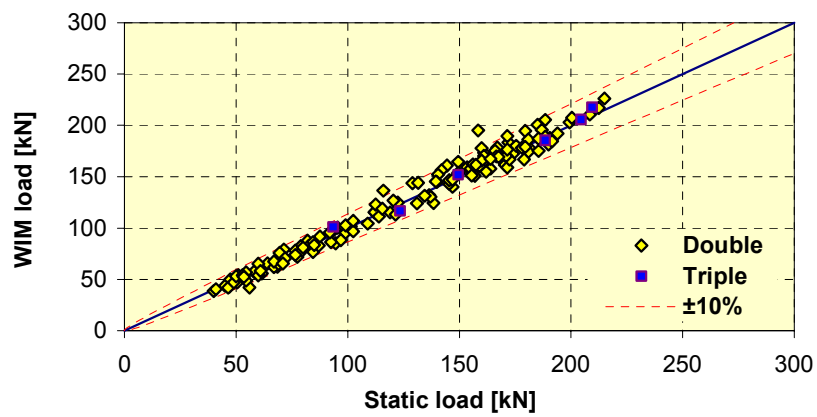
8.3 Slab bridges

In WP1.2, several different types of short slab bridge, previously considered as only conditionally acceptable for bridge WIM, were instrumented. Such structures have two important advantages: they are often the most common type of the bridge available and they are usually very easy to instrument. The SiWIM[®] software, described in section 5, was used for the analyses.

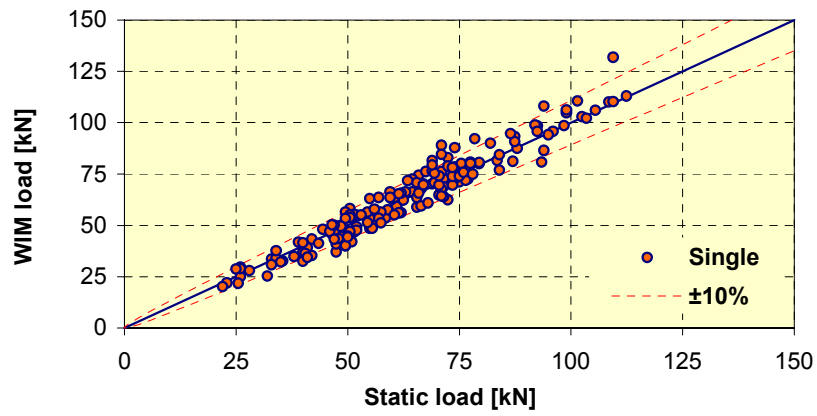
Several types of analysis were applied and the most characteristic results are collected in Table 17. The different types of analysis comprise:



(a) Gross vehicle weights

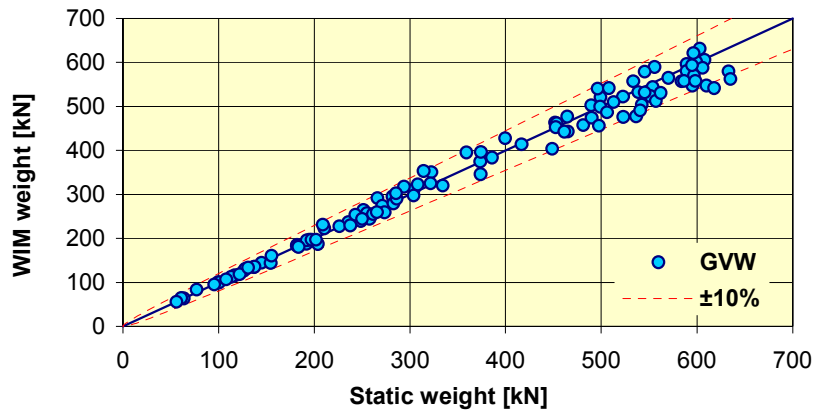


(b) Axle group loads

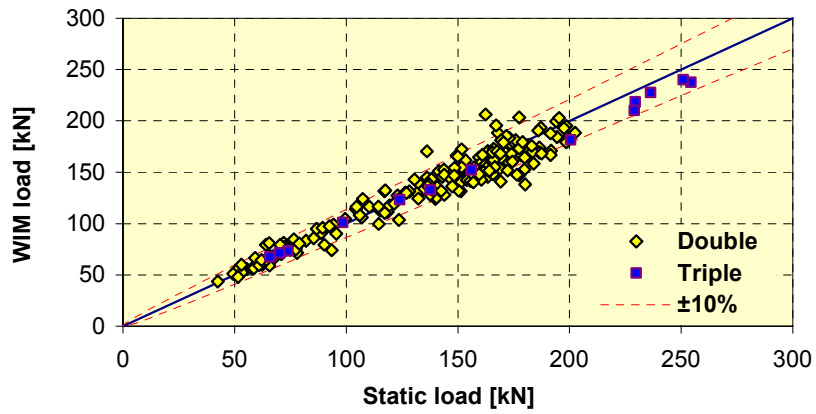


(c) Single axles

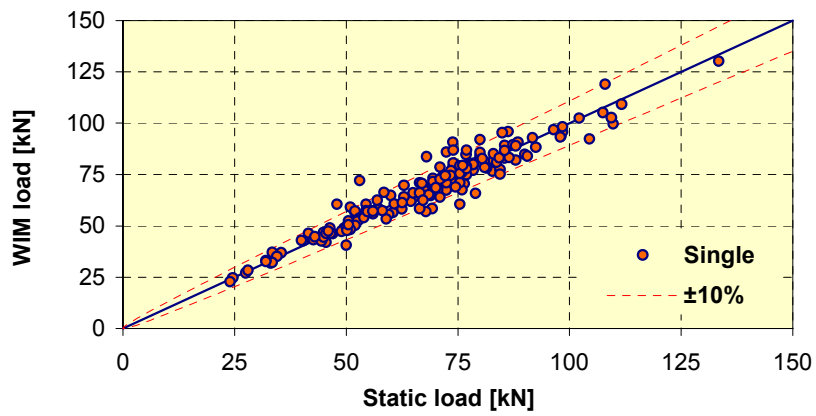
Figure 66: SiWIM results for Luleå – 1st Summer Test



Gross vehicle weights

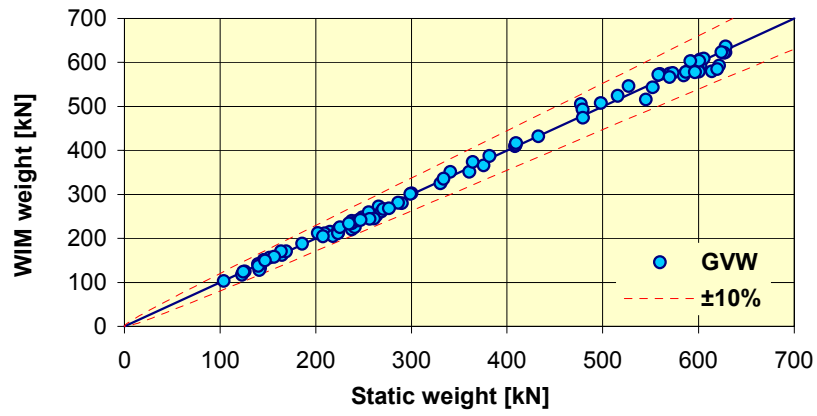


(b) Axle groups

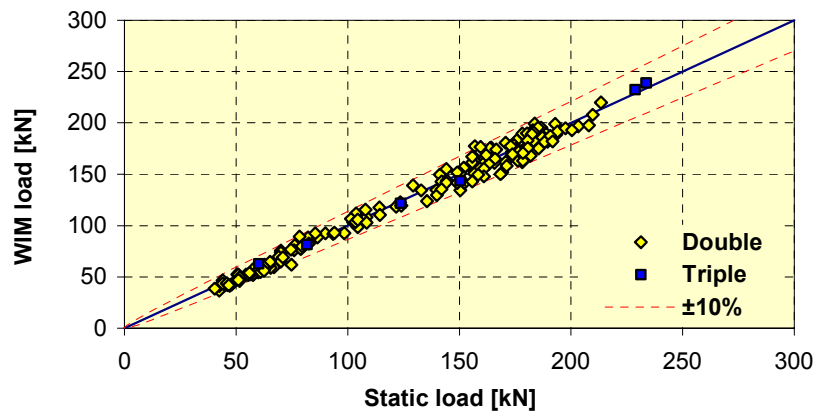


(c) Single axles

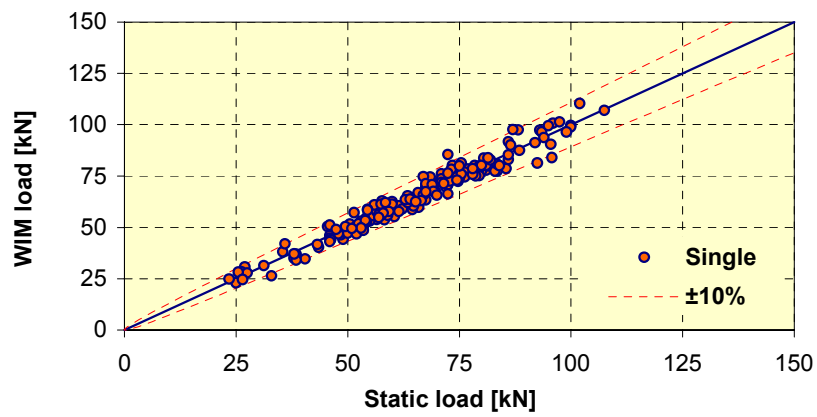
Figure 67: SiWIM results for Luleå – Winter Test



Gross vehicle weights



Axle groups



(c) Single axles

Figure 68: SiWIM results for Luleå – 2nd Summer Test

- I. Theoretical influence line for single fixed supported span was used. Calibration factor for all vehicles was obtained from the first five 5-axle semi-trailers.
- II. As above except the theoretical influence line was replaced by the experimental one.
- III. As above but 2 calibration factors were used: one for all semi-trailers based on the first five 5-axle semi-trailers and the other for all the rest based on the first five 2-axle rigid trucks (Method II calibration).
- IV. Optimisation of results, based on minimisation of error between measured and calculated strains, was added to adjust the vehicle's velocity and to fine-tune the axle loads.
- V. In addition, for all vehicles except for two-axle trucks, 4% of load from the first axle was re-distributed to all other axles (Method III calibration, Figure 69).

Table 17: Accuracy results from the integral slab bridge obtained by the SiWIM system, (R2, I)

Analysis	Criterion	Number	Mean (%)	St.dev. (%)	π_0 (%)	Class	δ (%)	δ_{\min} (%)	π (%)	Class retained
I	Single axle	59	3,29	12,62	91,8	D(25)	30	26,3	95,5	D(25)
	Group of axles	16	-0,95	5,25	85,8	B(10)	13	11,0	92,5	
	Gross weight	30	2,27	6,44	89,6	C(15)	15	13,8	92,6	
II	Single axle	60	2,71	9,81	91,8	D+(20)	25	20,5	96,9	D+(20)
	Group of axles	18	-1,05	4,26	86,7	B+(7)	10	9,0	91,1	
	Gross weight	31	1,59	5,48	89,8	C(15)	15	11,6	97,1	
III	Single axle	60	0,88	9,74	91,8	C(15)	20	19,8	92,1	C(15)
	Group of axles	18	-1,92	3,70	86,7	B+(7)	10	8,4	93,8	
	Gross weight	31	-0,25	5,08	89,8	C(15)	15	10,4	98,5	
IV	Single axle	60	1,41	7,59	91,8	C(15)	20	15,6	97,7	C(15)
	Group of axles	18	-2,40	4,16	86,7	B+(7)	10	9,6	88,8	
	Gross weight	31	-0,09	4,63	89,8	B(10)	10	9,5	91,7	
V	Single axle	60	-0,14	6,93	91,8	B(10)	15	14,1	93,8	B(10)
	Group of axles	18	0,84	5,11	86,7	B(10)	13	10,7	94,1	
	Gross weight	31	0,03	4,62	89,8	B(10)	10	9,5	91,8	

Table 17 indicates how some additional tools, which were not available in the older B-WIM systems, have improved the results and increased the overall accuracy class up to B(10).

8.3.1 Two-span integral slab bridges, skewed 7° and 26°

To investigate the influence of skew on accuracy, simultaneous measurements of two almost identical 2-span integral slab bridges were made. Both structures are parts of a longer bridge over the Mura river in north-eastern Slovenia. The only major difference between the two structures is the skew which is 7° for the structure on the left bank and 26° for the one on the right bank of the river (Figure 70).

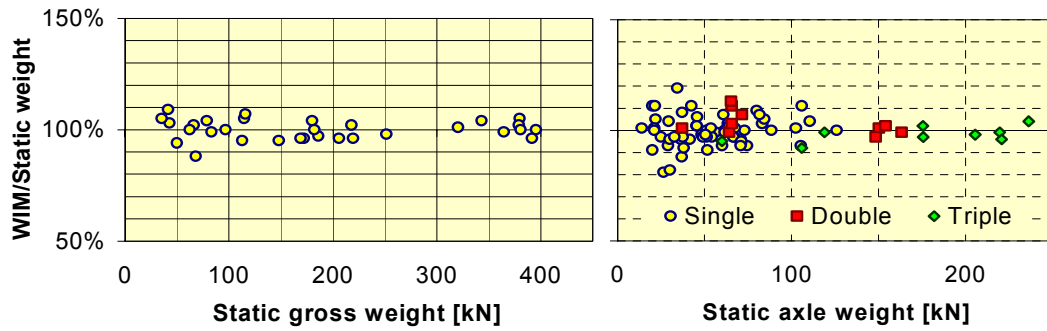


Figure 69: Results of Type V analysis of the full reproducibility test on the slab bridge

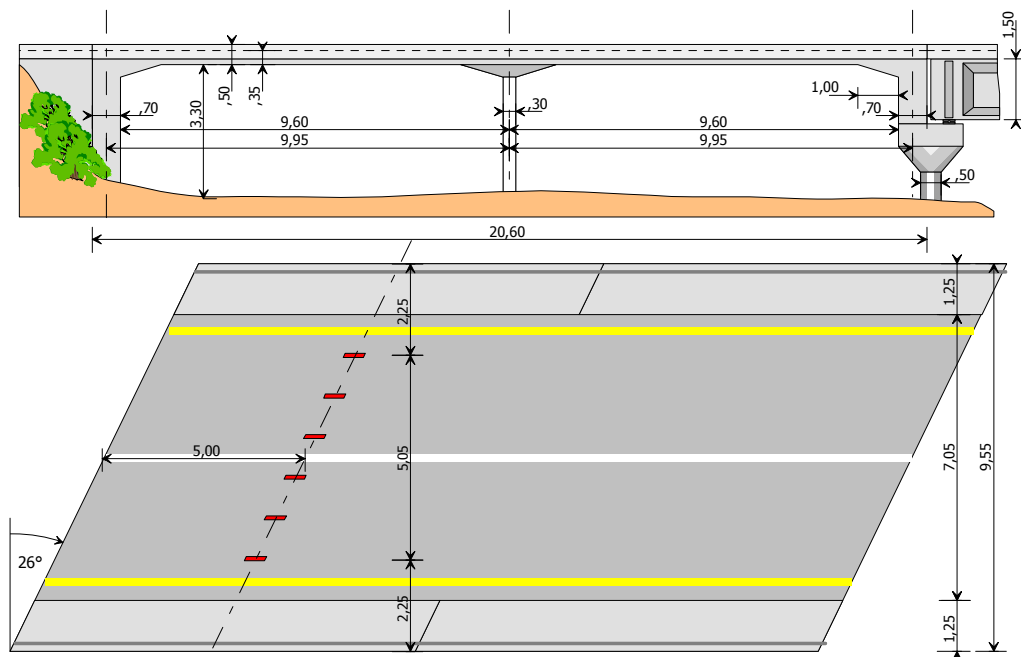


Figure 70: Two span integral slab bridge with a skew of 26°

Calibration was made with a fully loaded and an empty 3-axle rigid truck. A weigh bridge scale from a nearby quarry was used to obtain static reference weights for trucks loaded with gravel. Those vehicles which represented the majority of fully loaded trucks crossing the bridge, were used as a sample of heavy traffic. Measurements were performed simultaneously on both bridges. Results are presented in Table 18.

As the scale was located on the left bank of the river, traffic was measured only in one direction. It must be noted that all trucks were rigid and heavily loaded (only two were inside the legal limits) which had a beneficial influence on the accuracy of results. All the single axles were steering axles

and have in most cases represented less than 20% of the GVW. As the static reference weights for the first axles could be obtained only by subtracting the static axle load of the rear tandem from the GVW, the accuracy of single axles is two classes below the other two criteria. However, high single axle bias indicates that calibration by axle rank could improve the single axle results. Generally it can be concluded that accuracy of the results from the skewed bridge is only slightly lower than that from the straight one, which implies that carefully instrumented and calibrated skewed bridges can provide satisfactory results.

Table 18: Accuracy results of traffic on skewed and straight 2-span slab bridges (R2, I)

Bridge	Criterion	Number	Mean (%)	St.dev. (%)	π_0 (%)	Class	δ (%)	δ_{\min} (%)	π (%)	Class retained
Skewed Dir. 1	Single axle	27	7,29	9,26	89,1	D+(20)	25	22,9	92,7	D+(20)
	Group of axles	37	2,20	4,24	90,4	B+(7)	10	9,5	92,2	
	Gross weight	32	2,84	3,53	89,9	B(10)	10	8,8	94,6	
Straight Dir. 1	Single axle	31	5,24	8,32	89,8	C(15)	20	19,4	90,9	C(15)
	Group of axles	33	-0,84	4,77	90,0	B+(7)	10	9,9	90,4	
	Gross weight	32	0,43	3,17	89,9	B+(7)	7	6,5	92,3	

8.3.2 Integral slab bridge with a span of 8 m and a bump

To investigate the influence of surface roughness and evenness, another integral slab bridge with the span of 8 m has been instrumented. The major difference from the bridge in Figure 65 was a bump on this bridge, which caused considerable bouncing of all vehicles passing it.

Two pre-weighed vehicles, a 3-axle rigid truck and a 5-axle semi-trailer, were used for calibration. Both were driven fully loaded and empty. Results in Table 19 show that, when using all measured vehicles, accuracy is much lower than on smooth bridges. While the GVW accuracy remains very good, the dynamic interaction causes considerable load distribution of *light single axles and axle groups*. However, if all axles below 20 kN are not taken into account (as stated in the COST 323 Specification), the overall accuracy increases considerably. Again, large bias of single axles and groups of axles, indicates that calibration by axle rank could further improve the results.

Table 19: Accuracy results on an 8 m integral span slab bridge with a bump, (r2, I, k=0.8)

Bridge	Criterion	Number	Mean (%)	St.dev. (%)	π_0 (%)	Class	δ (%)	δ_{\min} (%)	π (%)	Class retained
VA 023	Single axle	52	-6,22	7,86	96,20	D(25)	30	28,40	97,32	E(40)
	Group of axles	32	6,94	11,85	95,40	E(40)	43	40,28	96,84	
	Gross weight	34	0,00	3,23	95,50	B(10)	10	9,82	95,92	
VA 023 > 20 kN	Single axle	40	-4,61	5,23	95,80	C(15)	20	19,49	96,41	C(15)
	Group of axles	26	1,53	4,61	95,00	C(15)	18	14,74	98,50	
	Gross weight	28	0,00	3,12	95,20	B(10)	10	9,58	96,18	

8.3.3 Culvert-type bridge

The next structure investigated was a very old, culvert-type bridge with a span of only 3 m (Figure 71). As the structure is very short, it was hoped that it could be suitable for FAD (free-of-axle-detection) bridge WIM measurements. However, the 1.25 m thick superstructure filtered out many peaks of the closely spaced axles which made axle detection with the present, simple algorithm, very difficult. To evaluate all pre-weighted vehicle crossings, it was necessary to reinsert some of the missing axles manually. A 3-axle rigid truck and a 5-axle semi-trailer, both fully loaded and empty, were used for calibration and several runs with two different velocities were done.

Despite the fact that this bridge is, in almost every criterion, unsuitable for WIM measurements, an accuracy class D+ was achieved (Table 20).

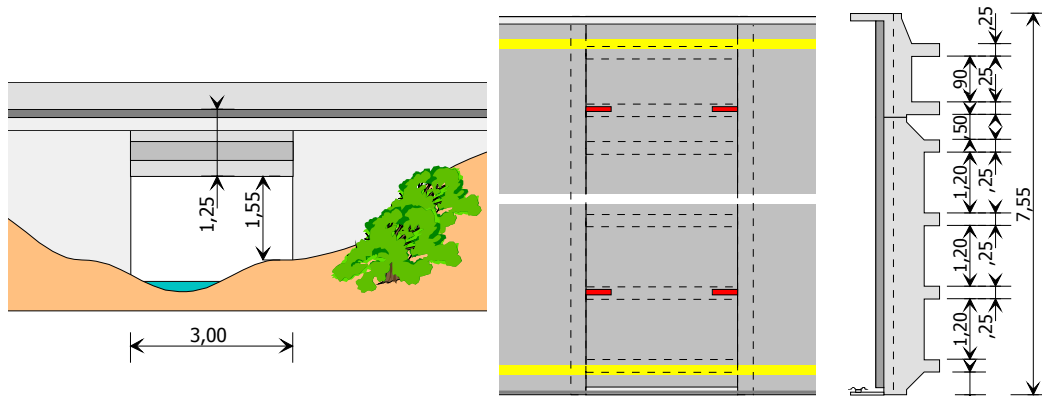


Figure 71: Culvert-type bridge

Table 20: Accuracy results of the culvert-type bridge, (r_2 , I, $k=0,8$)

Type	Criterion	Number	Mean (%)	St.dev. (%)	π_0 (%)	Class	δ (%)	δ_{min} (%)	π (%)	Class retained
Calibration (r_2)	Single axle	24	-1,14	6,80	94,80	D+(20)	25	21,21	97,96	D+(20)
	Group of axles	35	-0,17	6,25	95,50	D+(20)	23	18,95	98,63	
	Gross weight	24	0,00	5,62	94,80	D+(20)	20	17,35	97,65	

8.3.4 Conclusion for Slab Bridges

A typical integral slab bridge with average evenness of the pavement showed that careful selection of the influence line and higher methods of calibration can result in an overall accuracy class of B(10).

A similar bridge with poor evenness (with a heavy bump over the span) was instrumented to estimate the influence of vehicle dynamics on the accuracy of the results. When the axles below 20 kN were not taken into account, an overall accuracy class of C(15) was achieved which was only one class lower than on a similar bridge with smooth pavement. This indicates that evenness of the pavement is important, but even poor pavement can provide acceptable results.

Results obtained on two almost identical bridges with different skew showed little difference in accuracy between the 26° skewed bridge and the 7° skewed one. Thus, carefully calibrated skewed bridges can be used for B-WIM measurements.

The Cold Environment Test (CET) was a major test involving a large sample from random traffic that was carried out under strictly controlled conditions. In the 2nd Summer Test for which unfiltered data was used, B(10) accuracy was achieved from two independently developed B-WIM algorithms. CET test results also show that the accuracy and functioning of the B-WIM system successful in a range of different environmental conditions including extreme cold.

These experiments also revealed the importance of precise static axle weighing, which can significantly influence overall accuracy of the results, particularly when performance of high quality WIM systems is being evaluated.

It can be concluded, that a great variety of short span slab bridges, which are easy to find and instrument, can be used for bridge WIM measurements. If the influence line is selected carefully and if enough attention is paid to the calibration procedure and its results, even uneven pavement and high skew of the bridge will probably provide reasonably accurate results. On the other hand, accuracy class B(10) or better is achievable on straight spans with smooth pavement over them, regardless of the ambient temperatures.

Some more work is needed to define bridge WIM behaviour under long term measurements in the full environmental reproducibility conditions and to further develop higher methods of calibration and self-calibration.

9. CONCLUSIONS, RECOMMENDATIONS AND FUTURE NEEDS

Bridges instrumented for weigh-in-motion measurements are still quite rare around Europe, despite being well represented in Australia and in some other countries. As bridges are much longer than pavement WIM sensors, they have considerable potential for accuracy. In addition, the same strain records can be used for bridge monitoring and as indicators of structural damage by fatigue. Research from WP1.2 reveals that major difficulties observed with B-WIM systems in the past (limited selection of appropriate bridges, lower accuracy of results than expected etc.) can be avoided when using new and updated algorithms and more powerful computers and data-acquisition systems. The accuracy of the recent results is most encouraging; B-WIM systems have been shown to have accuracy easily comparable to other types of WIM system.

In addition, several advantages of B-WIM systems have been identified or confirmed. Firstly, B-WIM systems require limited activity on the pavement which improves the durability of the equipment and reduces traffic delays during installation and maintenance. This is of particular importance in cold climates. Also, first successful attempts have been made on some bridges to replace the axle detectors with appropriate strain readings from under the structure. When fully developed, this should further improve durability of B-WIM systems. Secondly, installation of a B-WIM system is fast, easy and the system is completely portable. Thirdly, off-scale weighing is eliminated as B-WIM systems weigh the complete vehicle. Lastly, the evenness of the pavement has less influence on the accuracy of weighing than with pavement WIM systems.

On the other hand, some difficulties have not been entirely solved yet. One of them is the presence of more than one heavy vehicle on the bridge at the time of weighing which, at the moment, is not catered for by the algorithms. However, if short bridges are instrumented, the probability of such events is very low. The second one is that, despite a greatly extended selection of bridges, some road sections may still not have an appropriate bridge for B-WIM measurements. Users who do not have an appropriate background in bridge engineering, may also experience some difficulties understanding the calibration process, although this is no longer a problem when experimental influence lines are used, as was the case for the 'point-by-point' calibration procedure adopted for the Lulea tests.

It seems likely that further progress will be made in B-WIM on several fronts. The SiWIM system is likely to be fully commercialised and its open architecture will be of great benefit for other developers of B-WIM algorithms. The principle of commercial B-WIM is gaining widespread acceptance, particularly for orthotropic bridges and for cold climate regions. The developments in FAD - Free of Axle Detector systems - are most promising and will provide a very strong reason for using B-WIM in preference to pavement WIM in some circumstances. These are in their infancy and there are many potential improvements in accuracy and in the range of bridge types to which it can successfully be applied. It seems inevitable that FAD will be accompanied by the widespread adoption of optimisation techniques as pioneered for orthotropic B-WIM. This will eventually overcome the reductions in accuracy that might be anticipated with FAD. Other methods to improve accuracy will emerge which may involve dynamic algorithms and/or combinations of bridge and pavement WIM for the first class A accuracy systems. It seems beyond doubt that the future prospects for B-WIM are bright indeed.

10. REFERENCES AND BIBLIOGRAPHY

- Baumgärtner, W. (1998), 'Bridge-truck interaction: simulation, measurements and load identification', *5th International Symposium on Heavy Vehicle Weights and Dimensions*, Maroochydore, Australia, March/April.
- Bignonnet, A., Carracilli, J. & Jacob, B. (1990) 'Comportement en fatigue des ponts metalliques application aux dalles orthotropes en acier' Rapport final, Commission des Comunautes Europeennes, recherche CECA No. 7210 KD/317 (1986-1989) LCPC - IRISD.
- Cifuentes, A.O. (1989), "Dynamic response of a beam excited by a moving mass", *Finite Elements in Analysis and Design 5*, Elsevier Science Publishers B.V., Amsterdam, pp. 237-246.
- COST 323 (1997a), *Collection and analysis of requirements as regards weighing vehicles in motion*, EUCO-COST/323/2E/97, EC/DGVII COST Transport Secretariat, Brussels, January, 1997, 64 pp.
- COST 323 (1997b), European Specification on Weigh-in-Motion of Road Vehicles, Draft 2.2, EUCO-COST/323/6/97, June.
- Costain Dow Mac Limited, 'Bridge Beams - Standard Details', Revised march 1989.
- Dempsey, A.T., O'Brien, E.J. and O'Connor, J.M. (1995), 'A Bridge Weigh-In-Motion System for the Determination of Gross Vehicle Weights' in Post Proceedings of First European Conference on Weigh-In-Motion of Road Vehicles, eds. B. Jacob et al., ETH, Zürich, pp. 239-249.
- Dempsey, A.T., Kealy, N.J., O'Brien, E.J. and Hartnett, M.A., (1996), 'Improvements in the accuracy of weigh-in-motion systems', NATDAQ 96 - *Proceedings of National Traffic Data Acquisition Conference*, Alliance for Transportation Research, Albuquerque, New Mexico.
- Dempsey, A.T. (1997), 'The accuracy of bridge weigh-in-motion systems', Ph.D. thesis, Trinity College Dublin, Ireland.
- Dempsey, A.T., Jacob, A.T. and Carracilli, J., (1998a), 'The use of instrumented orthotropic bridges for determining vehicle weights, dimensions and parameters', *Proceedings of the 5th International Symposium on Heavy Vehicles Weights and Dimensions*, Australian Road Research Board, Brisbane, Australia.
- Dempsey, A.T., Žnidarič, A. and O'Brien, E.J. (1998b), 'Development of a Dynamic Bridge Weigh-In-Motion Algorithm' in *Proceedings of the 5th International Symposium on Heavy Vehicles Weights and Dimensions*, Maroochydore, Australia.
- Dempsey, A.T. and Brady, S.P. (1999), 'Verification of Assumptions in the Dynamic Multiple Sensor Bridge Weigh-In-Motion Algorithm – The Effect of Superposition of Moving Constant Loads on Simply Supported Beams', Departmental Report 1999-01, Department of Civil Engineering, University College Dublin.
- Dempsey, A., Jacob, B. and Carracilli, J. (1999), 'Orthotropic Bridge WIM for determining Axle and Gross Vehicle Weights', in *Proceedings of the Final Symposium of the project WAVE*, Ed. B. Jacob, Hermes Science Publications, Paris, France, 227-238.

- Frýba, L. (1972), *Vibration of solids and structures under moving loads*, Noordhoff International Publishing, Groningen, The Netherlands.
- González, A.(2001), *Development of Accurate Methods of Weighing Trucks in Motion*, Ph.D. Thesis, Trinity College Dublin, Ireland.
- González, A and O'Brien, E.J. (1998), 'The Development of a Dynamic Bridge Weigh-In-Motion Algorithm' in *Pre-Proceedings of Second European Conference on Weigh-In-Motion of Road Vehicles*, eds. E.J. O'Brien & B. Jacob, JAE, Lisbon, pp. 445-453.
- González, A, Brady, S. and O'Brien, E.J. (1999), 'A Dynamic Multi-Sensor Bridge Weigh-In-Motion Algorithm', in *Proceedings of the Final Symposium of the project WAVE*, Ed. B. Jacob, Hermes Science Publications, Paris, France, 209-217.
- Jacob, B.A. (1994), 'European Research Activity COST 323 - Weigh-in-Motion of Road Vehicles', *Proceedings of NATDAC'94*, Rocky Hill, Connecticut, 18-22 Sept..
- Jacob, B.A. and O'Brien, E.J. (1996), 'WAVE - A European Research Project on Weigh-in-Motion', *National Traffic Data Acquisition Conference (NATDAQ '96)*, Vol. II, ed. G. Knoebel, Alliance for Transportation Research, Albuquerque, New Mexico, 659-668.
- Kealy,N.J.,(1997) 'The development of a multiple sensor location bridge weigh-in-motion system', M.Sc. thesis, Trinity College Dublin, Ireland.
- Kealy, N.J., O'Brien, E.J. (1998), 'The development of a multi-sensor bridge weigh-in-motion system', *5th International Symposium on Heavy Vehicle Weights and Dimensions*, Maroochydore, Australia, March/April, pp. 222-235.
- Lutzenberger, S., Dinkel, J. and Baumgärtner, W. (1998), 'PRISIM – Ein Softwaremodul zur Simulation der dynamischen Interaktion zweier relativ zueinander bewegter Finite Element Strukturen', MacNeal-Schwendler Anwenderkonferenz Kloster Andechs.
- Lutzenberger, S. and Baumgärtner, W. (1999), 'Interaction of an Instrumented Truck crossing Belleville Bridge', in *Proceedings of the Final Symposium of the project WAVE*, Ed. B. Jacob, Hermes Science Publications, Paris, France, 239-240.
- Moses, F. (1979), 'Weigh-in-Motion System Using Instrumented Bridges', *Transportation Engineering Journal*, ASCE, **105**, TE3, 233-249.
- O'Brien, E.J., Žnidarič, A. and Dempsey, A.T., (1996) 'Comparison of two independently developed bridge WIM systems', *Engineering Foundation Conference Vehicle-Infrastructure Interaction IV*, San Diego, California.
- O'Brien, E., Dempsey, A., Žnidarič, A. and Baumgärtner, W. (1999), 'High-Accuracy Bridge-WIM Systems and future Applications', in *Proceedings of the Final Symposium of the project WAVE*, Ed. B. Jacob, Hermes Science Publications, Paris, France, 45-54.
- O'Connor, C. and Chan, T.H.T. (1987), 'Dynamic Wheel Loads from Bridge Strains', *Journal of Structural Engineering*, ASCE, Vol. **114**, No. 8, August, 1703 – 1723.
- Penka, E. (1997), 'Fahrzeug – Brückeninteraktion: Verbundbrücke Belleville', Diplomarbeit Nr. 85, L.f. Baumechanik, TU München.
- Peters, R.J.,(1984) 'AXWAY - A system to obtain vehicle axle weights', *Proceedings 12th Australian Road Research Board Conference*, **12**, 1, 17-29.
- Peters, R.J. (1986), 'CULWAY - an Unmanned and Undetectable Highway Speed Vehicle Weighing System', in *Proc. 13th AARB Conference*, Australian Road Research Board, **13**, 6.

-
- Rao, S.S. (1984), *Optimization: Theory and Applications*, 2nd Edition, John Wiley & Sons.
 - Snyder, R. (1992), 'Field Trials of Low-Cost Bridge Weigh-In-Motion', *Publication FHWA-SA-92-014*, Washington DC.
 - Stanczyk, D. and Jacob, B. (1999), 'European test of WIM systems: CMT on the A31 motorway', in Post-Proceedings of the 2nd European Conference on WIM, eds. E.O'Brien & B. Jacob, Lisbon, Sept 14-16, COST323, Luxembourg, 51-62.
 - Žnidarič, A., Žnidarič, J. and Terčelj, S., (1991), 'Determination of the true traffic load in the process of safety assessment of existing bridges', in *Proceedings of the 12th Congress of Structural Engineers of Slovenia*, 241-246 (in Slovenian).
 - Žnidarič, A., O'Brien, E.J. and Jacob, B.A. (1996), 'Live Load Assessment - European WIM Activities' in *Diagnosis of Concrete Structures*, Proceedings of the 2nd RILEM International Conference, Strbske Pleso, Slovak Republic, Oct. 1996, 289-294.
 - Žnidarič, A. and Baumgärtner, W. (1998), 'Bridge Weigh-In-Motion Systems – An Overview', in *Pre-proceedings of the 2nd European Conference on Weigh-In-Motion*, eds. E.J. O'Brien & B. Jacob, Lisbon, Portugal, 139-152.
 - Žnidarič, A., Lavrič, I. and Kalin, J. (1998), 'Extension of Bridge WIM Systems to Slab Bridges', in *Pre-Proceedings of 2nd European Conference on Weigh-In-Motion*, eds. E.J. O'Brien & B. Jacob, Lisbon, Portugal, 263-272.
 - Žnidarič, A., Dempsey, A., Lavrič, I., Baumgärtner, W. (1999a), "Bridge WIM systems without axle detectors", in *Proceedings of the Final Symposium of the project WAVE*, Ed. B. Jacob, Hermes Science Publications, Paris, France, 101-110.
 - Žnidarič, A., Lavrič, I. and Kalin, J. (1999b), 'Bridge WIM Measurements on Short Slab Bridges', in *Proceedings of the Final Symposium of the project WAVE*, Ed. B. Jacob, Hermes Science Publications, Paris, France, 217-226.

Printing of this report has been financially supported by:



Cestel d.o.o.

Traffic Engineering and Telecommunications
Puhova ulica 2
SI-1000 Ljubljana
Slovenia

Tel.: +386 1 568 17 19

Fax.: +386 1 568 60 99

E-mail: info@cestel.si

URL: www.cestel.si

Main activities:

- static weighing (gross weights and axle loads)
- measurements of vehicles dimensions (length, height, width)
- weigh-in-motion measurements
- development of bridge weigh-in-motion systems
- service, repair and calibration of axle weighing scales
- service and repair of traffic signalling equipment